DEVELOPMENT OF A CONTROL SYSTEM FOR GAS CONCENTRATION AND TEMPERATURE IN AN ANIMAL PREFERENCE CHAMBER

BY

RYAN M. JOHNSON

THESIS

Submitted in partial fulfillment of the requirements
for the degree of Master of Science of Agricultural and Biological Engineering
in the Graduate College of the
University of Illinois at Urbana-Champaign, 2013

Urbana, Illinois

Adviser:

Assistant Professor Angela Green

ABSTRACT

An enhancement of the environmental control capabilities was planned and executed for an Environmental Preference Chamber (EPC) used for animal behavior testing. A fuzzy logic controller (FLC) was designed and built to control distinct ammonia concentration levels independently in each of the EPC's four compartments. The FLC was written in MATLAB and utilized in tandem with custom software created in a visual-based programming language. The control software compared NH_3 measurements from an infrared photo-acoustic gas analyzer to user-defined setpoints for each compartment, and input the difference to the FLC. The FLC computedan incremental change to the voltage signal used to adjust four Mass Flow Controllers, changing the volumetric flow rate of supplied NH_3 to each compartment. Average (± standard deviation) NH_3 concentrations were: 1.8 ± 0.8ppm, 10.2 ± 0.5ppm, 20.1 ± 0.8ppm, and 40.5 ± 1.3ppm for setpoint concentrations of 0, 10, 20, and 40ppm, in each of the four compartments, respectively. Approximately 90 minutes were required for all compartments to be within 5% of their setpoint concentration when starting from fresh air conditions.

An expansion of the heating capacity of each compartment of the Environmental Preference Chamber was performed by increasing the installed heat capacity of in-line electrical resistance coils from 200W to 600W. The maximum temperature rise increased from 5.7±0.5°C to 15.1±0.6°C, with a time constant, τ, of 1.3±0.1 h. The 600W heating capacity achieved 95% of a 1°C and 3°C positive temperature step response in 12.3±2.3 min and 24.0±3.3 min, respectively. This was faster than the original 200W heating system, which achieved 95% of a 1°C and 3°C positive temperature step response in 18.0±2.8 min

and 51.9±12.8 min, respectively. The setpoint overshoot of the new 600W heating system was 1.5±0.4°C and 0.9±0.1°C for 1°C and 3°C, respectively. This overshoot was greater than for the original 200W heating system, which showed a 0.4±0.1°C overshoot for the +1°C step response and a negligibly small overshoot for the 3°C. Cooling to room temperature was achieved using supply fans. First-order step response time constants, τ, for 1°C and 3°C negative step responses to ambient air temperature were 39.0±3.4 min and 26±1.4 min, respectively.

The discrete On/Off temperature controller did not noticeably impact the performance of the fuzzy logic gas concentration controller when operating simultaneously. Four distinct ammoniated environments were created while the temperature controller was set to maximum temperature rise. The ammonia concentrations experienced minor perturbations during temperature rise, but the gas concentration controller quickly corrected these. The exhaust fan created noise in the Temp/Rh sensors, affecting the temperature control by dampening any oscillations when achieving a setpoint of 27°C (temperature increase of +5°C above ambient air temperature). No meaningful difference was observed in the gas concentration controller performance when simultaneously maintaining a temperature setpoint.

Acknowledgements

I would like to extend thanks to all of the people who helped and supported my work through this project. To all of the faculty, graduate students and undergraduate assistants in the AWES Lab who helped me run wires, hold ladders, calibrate sensors, take videos, burn up resistors, accidentally breathe in a lot of ammonia, and build all sorts of "stuff" that contributed to the development of this system. Special thanks to Yijie Xiong, Jingwei Su, and John Cloud who helped complete a lot of the "grunt" work.

Thanks to Professor Angela Green and Professor Richard Gates, who patiently guided me towards solutions when I had no idea what I was doing. I first walked into the ABE department as a Civil Engineering Undergraduate who knew nothing about animals, instrumentation or control systems. Thank you for providing this opportunity to work in the lab and become a better engineer. Also thanks to Tatiana Sales-Lust who modeled for me how to be an effective Graduate Student when I first arrived at the ABE department.

Of course, special thanks to my friends and family for their moral support throughout this project. They were a strong voice of reason during the evenings when my brain did not feel like functioning anymore.

And finally, thanks to God for providing the health, stability and opportunities that have led to this educational experience. He was my rock during this thesis project and gave me reason to never be anxious for what lie ahead.

Table of Contents

1. Introduction

1.1 Animal Preference Testing

Animal Welfare – Why perform preference testing?

For meat, milk, and egg production, animals are commonly raised in large indoor facilities, which require engineering and management for environmental control. Animals will produce heat and moisture and facilitate the production of dust and gases over time. When large numbers of animals are raised together indoors, this heat, moisture and pollutant production require well-designed heating and ventilation systems in order to ensure acceptable indoor environmental quality [DeShazer et al., 2009].

Animal productivity and environmental conditions have been directly correlated with their environment by many studies. For example, a severe decrease in egg production, feed intake and overall bird weight was observed in laying hens at ammonia (NH_3) concentrations at or above 100ppm [Charles, 1966; Deaton, 1982]. Swine were found to reduce feed intake up to 30% at NH_3 levels at or above 100ppm as well as experiencing inflammation in their respiratory tract [Drummond, 1980].

Many agencies recommend NH_3 exposure limits for humans due to its detrimental effects on health. The National Institute for Occupational Safety and Health (NIOSH) recommends a time-averaged exposure limit of 25ppm NH_3 over an 8-h period and 35ppm over 15 minutes, while the Occupational Safety and Health Administration (OSHA) recommends a 50ppm average NH_3 concentration exposure limit over an 8-h period [NIOSH, 2011]. The

United Egg Producers [2010] recommend that NH_3 concentrations should be less than 10ppm in poultry houses, and should rarely exceed 25ppm. Colina et al. [2000] also recommends a 25ppm exposure limit for swine production facilities.

Animal housing facilities have reported atmospheric dust and ammonia levels higher than these guidelines. Green et al. [2009] observed a mean NH_3 concentration of 46ppm in floor-raised laying hen facilities in the winter, with a maximum observed concentration of 89ppm. Redwine et al. [2002] observed that even under well-ventilated conditions, many commercial broiler houses could reach NH_3 concentrations upwards of 50ppm. Popescuo et al. [2010] measured NH_3 concentrations between 40-100ppm in select swine production facilities. Seasonal conditions are known to contribute to these high atmospheric ammonia conditions. For example, ventilation is typically reduced in the winter in order to decrease the heating load but this results in higher levels of air contaminants.

Animal welfare can be better understood by performing animal behavior tests. These tests are devised to "ask" animals what scenarios are most preferable to them [Dawkins, 2006]. There is ongoing discussion about the theory and usefulness of animal behavior tests in regards to measuring the animal's personal "preference" [Bruzzone and Corley, 2011; Duncan, 1978; Jensen and Pederson, 2008; Kirkden and Pajor, 2006]. Behavioral studies have been implemented to quantify behavioral changes due to important production factors such as flooring [Hudson et al., 1993; Hughes, 1976], social familiarity [Lindberg and Nicol, 1996; Nicol, 1986] and temperature [Alsam and Wathes, 1991].

The behavioral study of animal aversion to ammonia is of interest due to the aforementioned variability of ventilation control in animal housing. Jones et al. [1996] built an eight-compartment preference chamber for studying animal aversion to ammonia, used with broiler hens [Kristenson et al., 2000; Jones et al., 2005], laying hens [Wathes et al., 2002], and pigs [Jones et al., 1996]. Green and Xin [2008] developed a four-compartment environmental preference test chamber for the study of laying hen response to ammonia concentration. Both of these preference chambers successfully created distinct environments by adjusting the ammonia concentrations of each compartment in discrete, nominal increments. These designs were able to achieve different nominal ammonia concentrations with sufficient accuracy such that they could produce distinct physiological and behavioral responses from the test animals.

Environmental Preference Chamber

A four-compartment environmental preference chamber (EPC) with continuous control of temperature and gas concentration was developed at the University of Illinois Environmental Research Laboratory, Urbana-Champaign, and behavioral preference studies with laying hens commenced in 2010 [Sales et al., 2013; Sales, 2012]. The EPC consisted of four interconnected test compartments capable of housing small animals (poultry, piglets, etc.), which are used to perform animal preference tests. Indoor environmental variables, including temperature and ammonia concentration were independently controllable for each compartment, allowing distinctly different environments. Animals were able to travel between each compartment through clear acrylic tunnels equipped with swinging doors, allowing both an obstruction to reduce

infiltration of air between chambers as well as a separation of spaces that requires animals to make an active choice to travel from one compartment to another. Distinct environments were created in each compartment by independently conditioning the air in each of the four supply air ducts. Atmospheric ammonia concentration control was accomplished by supplying an external source of ammonia gas to each compartment through a mass flow controller *(GFC17, NH3 0-500ml-min^{-1}, Aalborg, Orangeburg, NY, USA).* The volumetric flow rate was adjusted by conditioning a voltage signal through four different sets of resistors placed in series. The number of resistors was manually chosen by the user in order to achieve nominal NH_3 concentrations of 0, 10, 20 and 40 ppm. An electronic relay board *(USB-ERB24, Measurement Computing, Norton, MA, USA)* controlled by the computer completed the circuit corresponding to the desired nominal NH_3 concentration. Temperature control was accomplished by triggering ON/OFF axial heaters with the electronic relay board. Further detail of this control scheme is outlined in APPENDIX A. A 2D schematic of the chamber is seen in Figure 1.1 below. RFID sensors and security cameras were installed in each chamber to monitor and quantify the location of each test animal. All environmental control equipment, including heaters, fans, and mass flow controllers, were controlled by a computer operating a custom program written in visual-based software (LabVIEW 8.2.1, National Instruments, Austin, TX, USA). All other environmental variables and stimuli such as space geometry, lighting, and accessibility of feed and water are uniform in all four compartments.

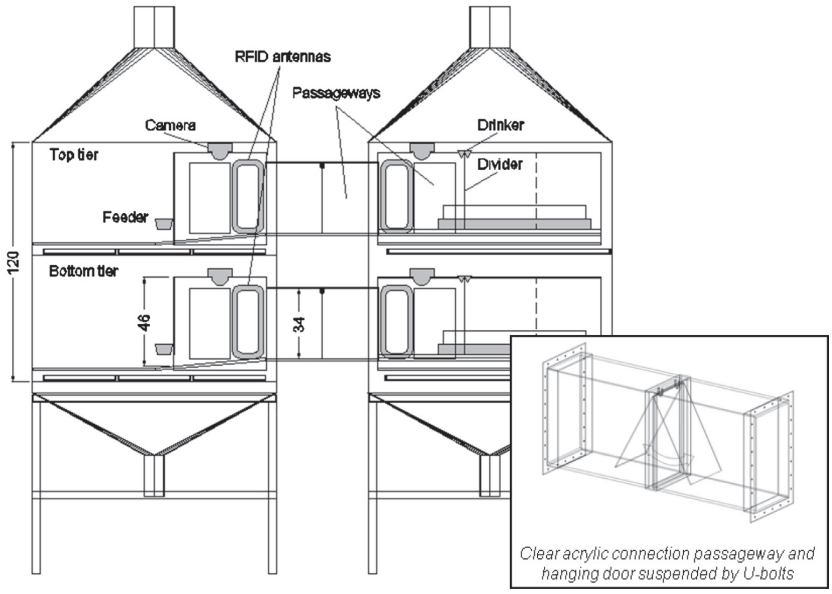

Figure 1.1: Schematic of the Environmental Preference Chamber (EPC). The EPC has two separated tiers, which allows two groups of animals to be tested simultaneously. Displayed with permission from G.T. Sales.

The EPC was commissioned for animal testing and began operation in 2011 [Sales et al.,, 2013]. After commissioning, the EPC was used in a study to quantify the environmental preference of laying hens to distinct NH_3 concentrations of 0, 10, 20 and 40ppm [Sales, 2012]. The EPC's design was sufficient for this experiment, but it was not equipped to create any other additional distinct environments. An expansion of its environmental control was desired; specifically, the development of improved gas concentration control and capability to achieve a higher temperature for heat-stress tests.

1.2 Techniques for Environmental Control

Techniques for Gas Concentration Control

Gases such as ammonia, hydrogen sulfide, carbon dioxide, and methane are generated during animal metabolism and waste storage in swine and poultry facilities [Heber et al., 2006]. The primary technique for controlling the concentration of an atmospheric gas considered in this study is to simulate the gas generation process by adding gas from an externally supplied source, such as a pressurized gas tank. In order to have effective control of the gas concentration, the ability to reliably measure it is also required. Gas sensors that are able to measure gas concentration reliably and consistently over an extended period of time are most preferred for environmental control. A gas concentration control scheme may be accomplished by linking the known, controllable volumetric flow rate of the supplied gas to the measured gas concentration within the animal chamber.

Atmospheric ammonia is an important environmental factor in environmental control due to physiological effects of excessive exposure to ammonia. Ammonia is a gas that naturally volatilizes from livestock waste. Ammonia emissions are quite variable depending on factors such as animal housing types, activity level, feeding times and waste handling systems [Anderson, 2003; Bunton et al., 2007]. Ni and Heber [2001] provided a comprehensive review of the current technology used to sample and measure atmospheric ammonia in animal facilities. They characterize ammonia measurement devices according to analytical methods (wet or dry), sensitivity, delivery of measurements results (direct or indirect readout), type of sensor use (single or multiple), method of sample air delivery, response time and cost. Some of these measurement techniques, such as gas tubes or

standardized wet chemistry methods are relatively inexpensive and accessible but come at the cost of being single use, lower sensitivity and non-practical for automated laboratory application. Other techniques such as FTIR spectroscopy, and photo-acoustic spectroscopy provide multiple reuses at high sensitivity and reliability, but at a higher cost. A reliable, multiple-reuse ammonia sensor is required for continuous control of ammonia concentration. The sensor should be able to interface with a computer to autonomously feed its measurements to the controller.

Techniques for Temperature Control

Heating is the addition of sensible heat into a space for the purpose of increasing or maintaining space temperature, or for replacing energy lost to colder surroundings. Heat that is added solely to increase or maintain temperature is known as sensible heat [ASHRAE, 2001]. Sensible heat may be added to the air by any number of techniques including direct radiation, convective heat coils, or the direct addition of heated air [McQuiston et al., 2005].

Convective heating coils typically function by warming intake air through a heat exchanger and blowing it into the conditioned space, diffusing and mixing the warmed air into the existing cooler air. A heating coil can be created by running hot water through thin piping or by electrical resistance. When this heating system is integrated into the ventilation duct, it is known as an all-air system. With a well-designed duct system, this technique allows flexibility in heating different zones of a building to varying capacities [McQuiston et al., 2005].

As opposed to sensible heating, sensible cooling is the removal of heat from a space for the purpose of lowering the existing dry-bulb temperature or for removing energy gained by surroundings so that a desired temperature may be maintained. Many buildings rely on either room or central air conditioning systems for their cooling needs when natural cooling is not possible. Both of these systems run ambient air past a chilled coil to reduce the temperature. As air cools down, its ability to retain moisture decreases until the dew point is achieved and condensation occurs. To account for this, the air is sometimes cooled below the desired temperature to condense the unwanted moisture and then reheated such that the relative humidity stays within comfortable limits. [McQuiston et al., 2005].

1.3 Control Schemes for Animal Housing

Stable environmental control of densely populated animal houses can be a very difficult task since the presence of animals affects the interior temperature and humidity nonlinearly, potentially resulting in long time constants to control system response. [Daskalov, 2006]. This is due to the internal sensible and latent heat loads generated from the presence of animals through respiration, metabolism, waste generation, and other means [DeShazer et al., 2009]. These changes in temperature and humidity, and the relationship between the two, become more profound in densely populated animal housing facilities than in more sparsely populated buildings, such as office or residential spaces. [McQuiston et al., 2005]. The effect of animal presence on interior environmental conditions is substantially lessened in most laboratory testing scenarios, but their contribution should be considered nonetheless.

Several control schemes may be implemented for temperature, moisture and gas concentration control. Examples from the literature were compared for their practicality and application priorities (i.e., control performance, energy savings, economics, ease of installation, etc.) [Zhang and Barber, 1995; Jones et al., 1996; Sales, 2012; Kolokotsa et al., 2009; Lute and van Paassen, 1995; Åström, 2002; Zhong, 2006; Wernhoff, 2012; Gates et al., 2001; Petriu, 2001; Gao, et al., 2000; Soyguder et al., 2009; Belohlavek and Klir, 2011]. The control schemes explored were: staged and discrete control systems, model-based control systems, PID control systems and Fuzzy Logic control systems.

Staged and Discrete Control Systems

In most animal production buildings, temperature is thermostatically controlled with a simple on/off controller. When the thermostat measures an ambient temperature lower than the locally defined setpoint it triggers the heating unit ON. When the temperature setpoint has been achieved, the heating unit is triggered OFF. As Zhang and Barber [1995] explain, the on/off controller for temperature control can also be paired with ventilation fans in stages depending on the sensible heat load and ventilation rate required to maintain fresh air conditions. Different stages of heating, ventilation rate and other controlled variables may be triggered ON and OFF as the need arises or scheduled beforehand. This control scheme is straightforward to implement in animal housing operations due to most already having a discrete number of heaters and fans. Such control is not always optimal but it is sufficient for achieving a setpoint with stability. As buildings size increases, there tends to be a larger number of ventilation stages in operation. This increased stage capacity requires either a larger acceptable deviation from the temperature setpoint or smaller

temperature differential stages [Gates et al., 2001]. To prevent excessive switching of ventilation loads, these discrete control stages can be linked to PID or fuzzy control schemes for further control optimization [Chao et al., 2000], both discussed later in this section. Such discrete controllers can also be digitally controlled through models. Chao and Gates [1996] used a state-based model was used to control two-staged ventilation in a greenhouse environment. Chao et al., [1995] created a thermal model to inform the staged ventilation in a broiler house.

Discrete, staged control systems have also been applied to control atmospheric gas concentrations in the laboratory setting. Jones et al. [1996] and Sales [2012] utilized discrete, staged control schemes to control ammonia concentration in their environmental preference chambers. Ammonia was supplied to each compartment in discrete increments, each equivalent to raising the NH_3 concentration of a compartment by about 10ppm. However, the "control" of these systems in particular was fully proctored by manual input. No programmed logic schemes were used to autonomously adjust the supply of ammonia in the compartments to maintain a setpoint. The loads of the discretized increments required tuning prior to use in animal behavior testing.

Model-Based Control Systems

Model-based control schemes utilize theoretical models in tandem with real, measured conditions to estimate an optimized response for environmental control. Model-based control schemes are not limited to any one specific control algorithm. In this context they refer to any control scheme that is augmented with theoretically derived relationships

within the system. Known data concerning weather patterns, the production cycle of animals, and the structure itself can be implemented into environmental control scheme [Bridges and Gates, 2009]. Kolokotsa et al. [2009] developed a predictive model in conjunction with a Building Energy Management System that utilized known theoretical relationships between controllable variables in an office environment (i.e., ventilation rate, temperature, relative humidity, illuminance, CO_2 concentration, etc.) and fixed variables (building envelope insulation, outdoor temperature, solar radiation, etc.). That model-based predictive controller compared the expected results of different control scenarios to make optimal control decisions for the building's lighting, automated windows and shading, and air condition system. It was able to anticipate changes to the outdoor temperature at night and even take into account the current weather conditions. Lute and van Paassen [1995] developed a linear-predictive model to control an HVAC system based on outdoor conditions. The model analyzed the heat balance of a building with regard to solar radiation and window and awning positions. Gates et al. [1996] developed a model to approximate the environmental control in a broiler facility. By accepting inputs of bird weight and number and house data such as the R-value, indoor and outdoor temperatures and relative humidity, the model estimated the ventilation rate and supplemental heat required to maintain desired environmental conditions. Chao et al. [1998] created a knowledge-based model to provide the thermal control of a greenhouse for single-stem rose production. This model negotiated the costs of its environmental control strategy using knowledge of the rose stem health, solar radiation, and the daytime and nighttime temperatures. Model-based control schemes can also be used replace the need for

expensive sensors in critical environments, such as those with high humidity [Sigrimis et al., 2000].

PID Control Systems

Proportional-Integral-Derivative (PID) controllers are a control loop feedback mechanism commonly used in industrial control systems as presented by Åström [2002]. A PID control controller conditions an output signal (control action) such that there is minimal error between a system response variable and a user-defined setpoint. This is accomplished in three parts: 1) the "Proportional" component, understood as the present error, 2) the "Integral" component, understood as the past error, and 3) the "Derivative" component, understood as the future error. A typical PID controller output is expanded from Åström's work as the following equation:

$$u(t) = K_p e(t) + K_i \int_0^t e(\tau)d\tau + K_d \frac{d}{dt} e(t)$$

where,

$e(t) =$ Error between the measured variable and the setpoint

$K_p =$ Proportional gain constant

$K_i =$ Integral gain constant

$K_d =$ Derivative gain constant

$t =$ Present time

$\tau =$ Time of integration

PID is used in a majority of closed-loop industrial processes and has been commonly applied in HVAC design throughout the 20th century [Zhong, 2006]. It can be used to continuously control air dampers, variable speed fans, chillers or heaters. Tuning the PID controller can be difficult for those who are not familiar with control theory or the system under control, but when tuned properly a building system can achieve and maintain a setpoint condition nearly optimally, that is, using minimal time or energy resources. In recent years, extensive research has also been made to develop techniques to optimize HVAC PID systems for energy savings [Wernhoff, 2012].

Fuzzy Logic Control Systems

Fuzzy Logic Control (FLC) is a generalized form of classical logic that allows the input of approximate or ambiguous ("fuzzy") data and outputs a crisp response [Belohlavek and Klir, 2011]. FLC accomplishes this by interpreting its input in multiple "fuzzy" truth states. In the formal logic used by conventional stage controllers, certain operating conditions are either TRUE or FALSE and the controller's response is then either TRUE or FALSE. Belohlavek and Klir explain how FLC differs by allowing multiple operating conditions to be simultaneously true with a certain "truth value" between 0 and 100%. This allows FLC to identify multiple subjective inputs simultaneously, such as "cold" and "hot", as the environmental conditions vary in magnitude. The implementation of mixing these subjective variables creates a tighter output response than a conventional stage controller [Gates et al., 2001].

FLC begins by mapping a "crisp" input value (i.e., temperature difference) against a set of logical stages, usually linguistic variables, in a process called "fuzzification". These stages represent subjective conditions (e.g., cold, warm, hot) that may have intersecting boundaries between one another. The intersection of stages allows the system to understand the current temperature as both "cold" and "warm", similar to how a sample of real-life observers would have varying reactions to their environment over a given temperature range [Belohlavek and Klir, 2011]. For example, in the basic "fuzzification" set observed in Figure 1.2, a temperature of 15°C could be interpreted as "50% Cold" AND "50% Warm" since the truth values of each state are both equal to 0.5

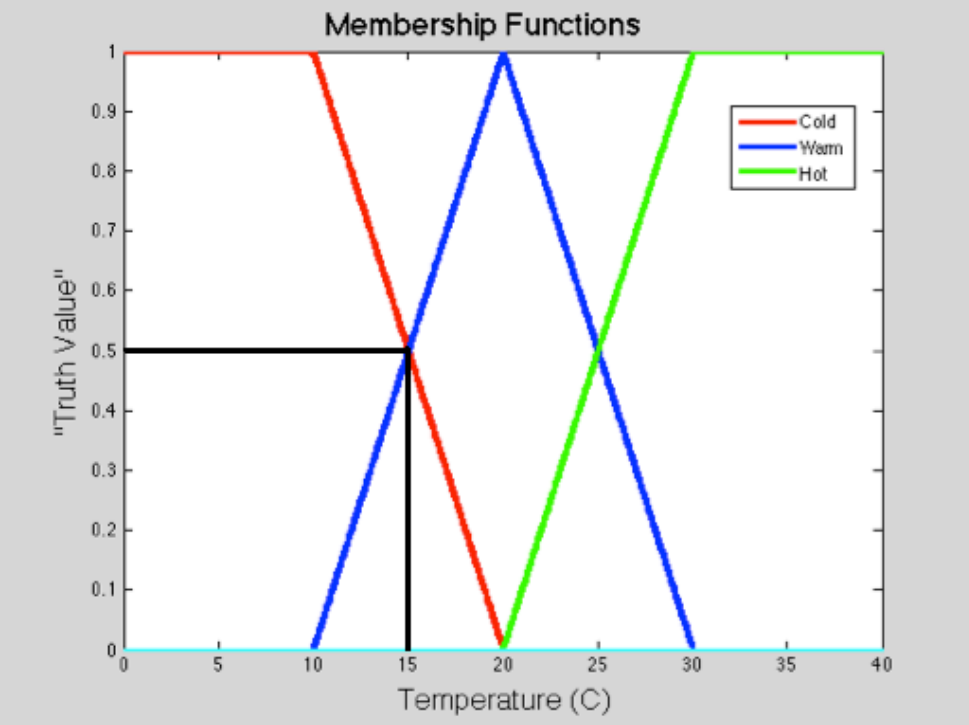

Figure 1.2: Example Fuzzification Set for a Temperature Control Response.
Each membership function is denoted a "Truth Value" on the y-axis. This enables otherwise independent logical stages to be simultaneously true. The Truth Values for "Cold" and "Warm" are both 0.5 at 15°C, as demonstrated by the black line.

Each stage is logically linked to a user-defined response similar to traditional logic controllers (e.g., IF "Cold" THEN "increase heat by 100W", and IF "Warm" THEN "increase heat by 0W"). Since multiple stages are observed simultaneously, the system must perform "defuzzification", where the final response output is the sum of all responses weighted according to how closely the input value fell into each stage [Petriu, 2001]. In the case of the previous example, the system response at 15°C could be interpreted as:

[Increase heat by 100W] * (0.5) AND [Increase heat by 0W] * (0.5)

RESULTS IN *[Increase heat by 50W]*

The user may define multiple outputs responses or even link multiple fuzzified inputs to a single output. This makes FLC very useful for programming Single-Input Multiple-Output (SIMO), Multiple-Input Single-Output (MISO) and Multiple-Input Multiple-Output (MIMO) control schemes. The control algorithm uses linear interpolation so the required computational power is low, even for very complex fuzzy sets. This makes FLC a useful alternative to classical analytical control theory for applications that are quite complex to model mathematically but are easier to explain qualitatively [Petriu, 2011].

Chao et al. [2000] developed an FLC to mimic the performance of conventional staged controllers (CSC) in agricultural facilities. The FLC was developed to easily adapt to existing CSC systems across broad range of installation sizes and control stages without any modifications. This FLC also allowed the user to trigger either of two priorities: control precision or energy savings. The performance of this FLC was improved over CSC when

applied to a greenhouse and broiler house, two environments with considerably different magnitudes of energy transfer and heating loads. This technique demonstrated that the addition of FLC could augment the performance of staged controllers in virtually any environmental control scenario. Further research was made by Gates et al. [2001] to identify which general building parameters are required to implement FLC on staged ventilation, such as building heat loss, dimensions, internal heat production, number of ventilation and heating stages, differential between stages, air density, and specific heat.

Gao et al. [2000] compared the performance of a FLC method to a commonly used PID control method for industrial temperature regulation. Using a simple self-tuning algorithm, FLC was able to outperform a PID controller in various systems with different setpoints, thermal masses, and time delays. This study did not necessarily prove that FLC is optimal over PID, but it provides a snapshot of the flexibility of FLC. FLC can be implemented in systems with complex and nonlinear dynamics that are difficult to model mathematically. Since FLC is designed from human experience, no mathematical model is required [Soyguder et al., 2009]

2. Objectives and Approach

2. 1 Objective Statement

The objectives of this study were to enhance the environmental control system of the Environmental Preference Chamber (EPC) at the University of Illinois in Urbana Champaign (UIUC) by:

1. Developing a control scheme to continuously control distinctly different atmospheric gas concentrations in each compartment simultaneously.
2. Expanding the temperature control scheme to attain higher maximum temperature.
3. Characterizing the performance of the gas concentration and temperature control schemes, independently and simultaneously.

2.2 Approach

Several design criteria were desired in the development of the gas concentration controller:

- *Ability to achieve any gas concentration setpoint along a continuous range* – the exact gas concentration setpoints of future animal behavior tests are still unknown. The ability for the user to define this setpoint along a continuous range (within the floating point precision of the control software) allows functionality despite this unknown.
- *Simultaneously achieves and maintains four distinct setpoints between the four compartments* – the experimental design of animal behavior tests requires that the environments of each compartment to be distinctly different. Simultaneous control

of the compartments allows the EPC to maintain distinct environments as the gas concentration setpoints are being achieved. The alternative of achieving only one setpoint at a time would temporarily create an unrepresentative difference between the environments of two or more compartments and potentially produce an unwanted physiological response in the test animal.

- *Achieve 95% of all setpoints within 30-90 minutes* – Adjusting the gas concentration in an environment too quickly could influence a test animal not based on the treatment being tested; too slowly would be wasteful of time needed to gather behavioral responses. Ninety minutes was considered a suitable timespan for achieving control setpoints in all four compartments.
- *Able to maintain fresh air environments* – Fresh air environments must have minimal contamination from gases supplied to adjacent compartments. In the case of atmospheric ammonia studies, a fresh air compartment must maintain a NH_3 concentration less than 5 ppm.
- *Self-Correcting* – Test animals will occasionally interact with their environment in ways that can affect system performance. For example, a laying hen may rest or sleep in the acrylic passageway connecting two compartments and prop the doorway partially open, allowing additional air to infiltrate between compartments. It is impractical to directly quantify these system behavior changes when they occur. The gas concentration controller should be designed to observe changes in system behavior and correct its output such that the control setpoints are maintained.

- *Minimal overshoot* – Overshooting a control setpoint may produce an unwanted physiological response in the test animal, influencing behavior not related to the treatment applied.
- *Minimal human input* – Simplification of human inputs allows a more streamlined test procedure and potential for error. The previously implemented gas concentration control scheme required the user, usually a student, to periodically visit the EPC and manually tune the system hardware. Variability in system performance may be reduced by eliminating the needs for this procedure.
- *Easily adaptable for any measurable gas* – The EPC may be used to test animal preferences for several different gases including, Carbon Dioxide, Argon and Ammonia. In this study, the controller is tuned to control ammonia concentrations, but the ability to control other gases should made be a simple process.

A fuzzy logic controller was proposed to control gas concentration in the EPC. This decision was made due to the flexibility and linguistic reasoning of FLC. In future behavior studies, different atmospheric gases such as NH_3, CO_2, or Ar may be used. FLC is quickly adaptable to control any of these gases provided they are measureable by an analyzer with an electronic output. Students who will perform behavioral studies with the EPC may not have a thorough background in controls. The linguistic reasoning of the FLC could allow simplified operation from a non-technical audience without a background in control theory. The FLC receives an input of gas concentration error (computed as the difference between the control setpoint and measured gas concentrations) and outputs an adjustment

to the volumetric flow rate of the control gas, externally supplied from a pressurized cylinder.

Several design criteria were desired in the development of the temperature controller:

- *The ability to achieve uniform thermal environments at thermoneutral and heat-stress conditions* – Temperature must remain uniform in all four compartments of the EPC when it is not a test variable. This may be required at both thermoneutral and heat-stress conditions
- *The ability to achieve distinctly different thermal environments* – Some animal behavior tests may require a distinct temperature differential between compartments.
- *Error no larger than* 1°C *from setpoint* – Large deviations from the temperature setpoint may produce an undesirable behavioral or physiological response in the test animal.

These design criteria were met by controlling the Dry Bulb Temerature of each compartment with electrical resistance convective coils using an ON/OFF controller. Two convective coil axial heaters (200W and 400W) were installed in each compartment with the flexibility to implement a staged heating design if desired. A previous study performed with the EPC by Sales [2012] utilized a similar ON/OFF control design using a single 200W axial heater to maintain thermoneutral conditions for laying hens. Continuing with this design would no longer require the holistic development of a new controller, but an

expansion of the previously used temperature control. No accommodations were proposed for cooling or humidity control.

3. Methodology

3.1 Gas Concentration Control – Fuzzy Logic Controller

System Characterization

An original Fuzzy Logic Controller (FLC) script was written in MATLAB and utilized in tandem with custom software created in a visual-based programming language (Labview 8.2 M63X22281 National Instruments Corporation in Austin, Texas), a LabVIEW Virtual Instrument (VI), for control of gas concentrations. The FLC was tuned and tested to control atmospheric ammonia (NH_3) concentration, though it is applicable to control the concentration of any sensible gas supplied from an exterior source. The MATLAB scripts written for this system are presented in APPENDIX D.

The Fuzzy Logic Controller is an analog, single-input single-output (SISO) control system, accepting a discrete input of gas concentration error ($\varepsilon = C_{setpoint} - C_{measured}$, [ppm]) and outputting an adjustment to the supply gas flow rate ($\Delta\dot{m}$, [mL/min]). The controller is memoryless and causal, meaning the output does not rely on previous inputs or future inputs. The EPC is considered a "black box" during control operations. The current concentration of the air sampled from the compartment is the only input considered in the fuzzy logic controller. This control action is summarized in Figure 3.1.

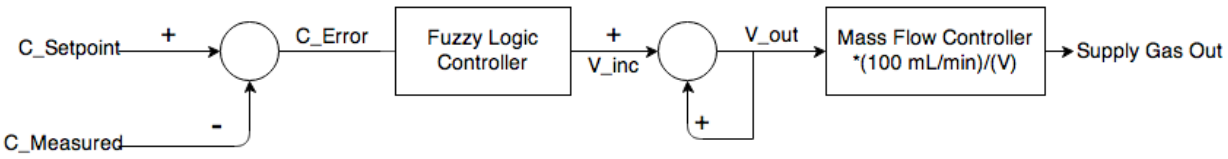

Figure 3.1: Control Strategy of the Fuzzy Logic Control System for Gas Concentration control. The difference between the Setpoint and Measured gas concentrations of a compartment is calculated and input to the Fuzzy Logic Controller ($C_{Error} = C_{Setpoint} - C_{Measured}$) . The Fuzzy Logic Controller outputs an adjustment to the voltage signal controlling the Mass Flow Controllers (V_{inc}), which is added to the pre-existing outgoing voltage signal (V_{out}). This signal voltage is proportional to the volumetric flow rate of the output supply gas to the controlled compartment.

Figure 3.2 summarizes the system operating the fuzzy logic controller. Sample air from each of four EPC compartments is pumped to an Infrared Photo-Acoustic Gas Monitor *(IR-PAS, INNOVA 1412, LumaSense Technologies Inc., Ballerup, Denmark)* at a minimum flow rate of 6L/min. The gas analyzer measures the NH_3 concentration of the sample air and sends the value to the control software (LabVIEW VI). The control software compares the measurement to a user-defined setpoint and inputs the difference to the FLC. The FLC outputs an incremental change, defined by the user, to the voltage signal (0-5V operating range) sent to one of four mass flow controllers *(GFC17, NH3 0-500ml-min^{-1}, Aalborg, Orangeburg, NY, USA)* (one per compartment), analogous to a change in the volumetric flow rate of supplied NH_3 (1.00 V_{DC} = 100 mL/min). For simplification in this study, the FLC was characterized as directly controlling the volumetric flow rate, with the translation from voltage signal to volumetric flow rate performed implicitly.

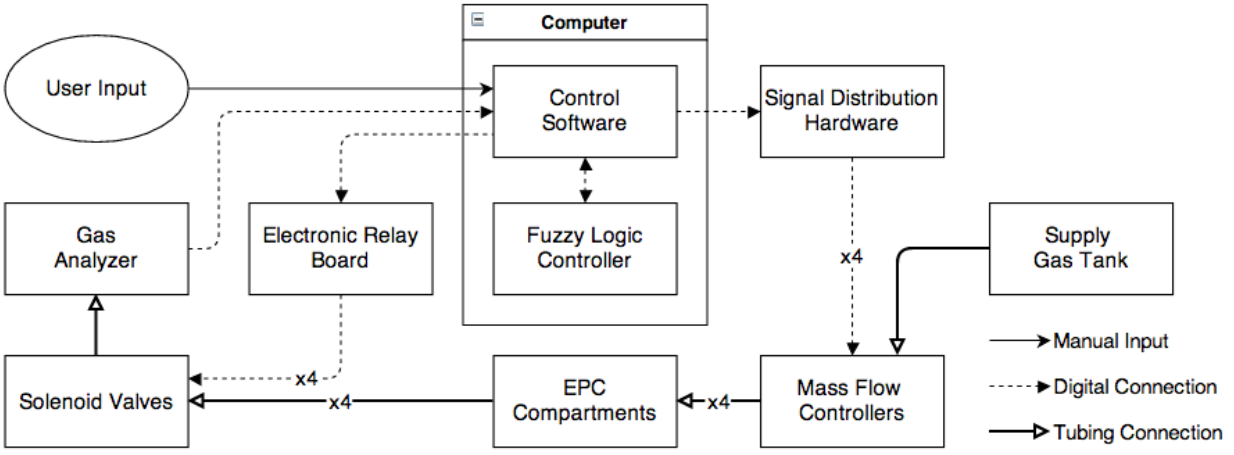

Figure 3.2: System Schematic of the Fuzzy Logic Control System for Gas Concentration control. The user manually inputs the gas concentration setpoint to the control software. The control software sends a signal to the electronic relay board to open one of four solenoid valves to allow air to be sampled from an EPC Compartment to the gas analyzer. The measured gas concentration is digitally communicated to the control software. The control software works in tandem with the fuzzy logic controller, providing a signal voltage through the signal distribution hardware to the mass flow controllers. The mass flow controllers open to allow the passage of an externally supplied gas to the EPC compartment, where it mixes with the supply air.

The control system output utilizes a set of four discrete time signals, that is, the output signal voltage to each of the four mass flow controllers is continuously supplied and incremented in discrete time intervals as the FLC updates the control action. The response time is limited by the gas analyzer, which requires approximately 33 s to return a gas concentration from the sample air, and is only capable of sampling air from one compartment at a time. The control software executes the Fuzzy Logic algorithm and increments the output voltage once every second, meaning the signal voltage is incremented 33 times between gas measurements. Since input to the Fuzzy Controller is unchanged during this 33-second interval, each output signal voltage increment to the mass flow controller is identical until the gas analyzer updates the gas concentration

measurement. These 33 “small” voltage increments are utilized (as opposed to one large voltage increment) to provide a smoother atmospheric transition. For example, if the desired output is +1V over an initial 2V, the voltage increases by 0.03V each second for 33 seconds to achieve a final voltage of 3V.

A sampling manifold consisting of four solenoid valves *(Type 0330, ¼” NPT, Stainless Steel, EPDM seal, Burkert Ingelfingen, Germany)* was installed in parallel to route the sampled air of each compartment to the gas analyzer. The control software determines which solenoid valve to open, allowing the air of a single compartment to flow to the gas analyzer. The control software cycles through all four compartments and the common supply air box on a continuous loop, controlling each for a user-defined sampling period, as summarized in Figure 3.3. During the sampling period that a compartment is being analyzed, the FLC adjusts the volumetric flow rate of supply gas using the real time measurements of the gas analyzer. When a compartment is not being analyzed, the control software holds the last determined volumetric flow rate constant until the next sampling cycle. An initial sampling period of 5 min was selected for the FLC.

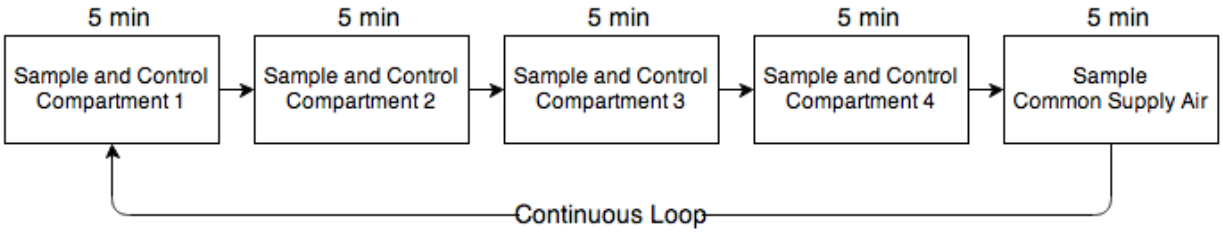

Figure 3.3: Strategy for congruent sample air analysis and control of the EPC.
The atmospheric gas is sampled and controlled in one compartment at a time, each for a 5-min sampling period. The common supply air box is also analyzed for gas concentration. This loop repeats continuously during EPC operations.

When switching from one compartment to the next, the sample line still contains some mixture of air from the previous compartment immediately after the control software activates the next solenoid valve. To avoid any unrepresentative gas concentration measurements, the control software administers a "purge" period immediately after switching solenoid valves. All measurements made by the gas analyzer during this period are ignored. A purge period of 70 s was experimentally determined to be sufficient to ensure representative gas concentration measurements.

Staged Fan Control to Assist Fuzzy Logic Controller

The supply fans for each compartment were programmed to implement four staged increments of fan speed: "Low", "Medium-Low", "Medium-High" and "High", summarized in Table 3.1. These discrete stages were accomplished by conditioning the fan supply voltage through four different sets of resistors. The control software was programmed to trigger an electronic relay board *(USB-ERB24, Measurement Computing, Norton, MA, USA)* to complete the circuit through the desired resistors. Normally, some fraction of air may infiltrate from one compartment to another via the acrylic passageways. These fan stages were designed to ensure that a compartment requiring 0ppm of supply gas concentration ("fresh air") maintains a positive pressure differential with adjacent compartments. This arrangement operates under the principle that it would be easier to add more supply gas to a conditioned compartment receiving additional "fresh air" through infiltration as opposed to removing undesirable gas that is leaking into a fresh air environment.

Table 3.1: Staged Fan Speed Control Logic

The staged fan response for an EPC chamber is given below. Fans always remain "LOW" if the compartment's NH_3 concentration setpoint is above zero.

IF	AND	THEN
$NH_{3,setpoint}$ > 0ppm		Fan Speed = "LOW"
$NH_{3,setpoint}$ = 0ppm	$NH_{3,measured}$ < 1.0ppm	Fan Speed = "LOW"
	1.0ppm < $NH_{3,measured}$ < 1.5ppm	Fan Speed = "MLOW"
	1.5ppm < $NH_{3,measured}$ < 2.0ppm	Fan Speed = "MHIGH"
	$NH_{3,measured}$ > 2.0ppm	Fan Speed = "HIGH"

Changes to the supply fan circuitry were implemented to maintain safe, reliable operation. Power Relays (G8PT Power PCB Relay, Omron Corporation) were installed to bypass the current flow of the supply fans around the EPC's existing instrumentation. This process is explained in greater detail in APPENDIX A.

Fuzzy Parameters

The Fuzzy Logic Controller utilizes five input membership functions to describe the gas concentration status: "Very Negative", "Negative", "Zero", "Positive", and "Very Positive". These parameters describe the difference between the setpoint NH_3 concentration and the actual measured NH_3 concentration ($NH_{3,\,ERROR} = NH_{3,\,SETPOINT} - NH_{3,\,MEASURED}$). Figure 3.4 summarizes the fuzzy set, which defines the rules for assigning the NH_3 concentration membership functions. Interior membership functions are triangular and those at large control errors are truncated. The slopes of the membership functions are created from linearly interpolating from 0 to 100% such that the sum of all truth-values at any value of $NH_{3,\,ERROR}$ is always equal to 100%.

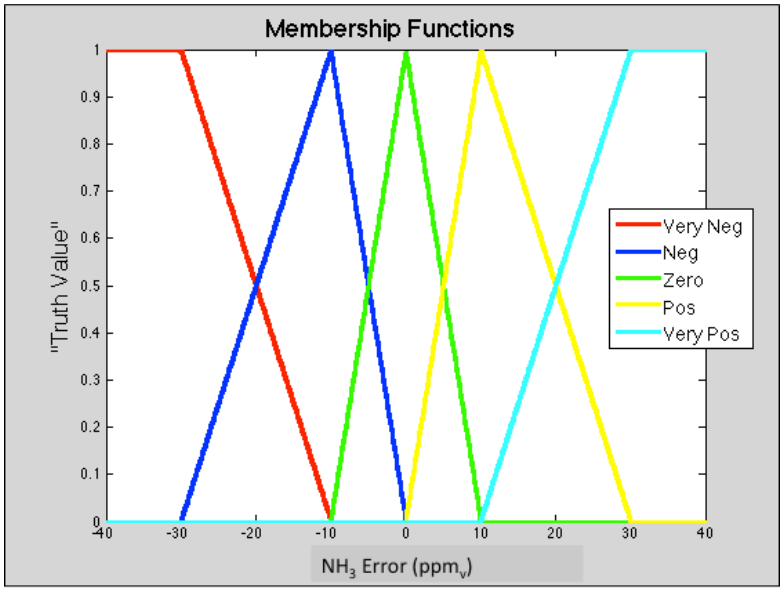

Figure 3.4: Example Fuzzy Set for NH_3 Control.
The "Truth Value" of each membership function is defined as a piece-wise function of NH_3 Error (ppm_v). NH_3 Error = NH_3 Setpoint – NH_3 Measured

The FLC responds to each membership function with proportional control action, using more extreme compensation for more extreme differences from setpoint and more conservative adjustments for smaller differences. This response is summarized in Table 3.2 and visualized with the Control Rule Matrix in Figure 3.5.

Table 3.2: FLC response to membership functions.
When a membership functions is true (Negative, Zero, Positive, etc.), the Fuzzy Logic Controller executes these respective response. The Fuzzy Logic Controller weights a membership function's response by its "Truth Value", defined in Figure 3.3. $\dot{V}$ represents the current volumetric flow rate of the supply gas (mL/min). Inc_High and Inc_low are positive-valued large and small increments to the volumetric flow rate, respectively, defined manually by the user.

IF	Then
Very Negative	$\dot{V} = \dot{V}$ - Inc_High
Negative	$\dot{V} = \dot{V}$ - Inc_Low
Zero	$\dot{V} = \dot{V}$ + 0
Positive	$\dot{V} = \dot{V}$ + Inc_Low
Very Positive	$\dot{V} = \dot{V}$ + Inc_High

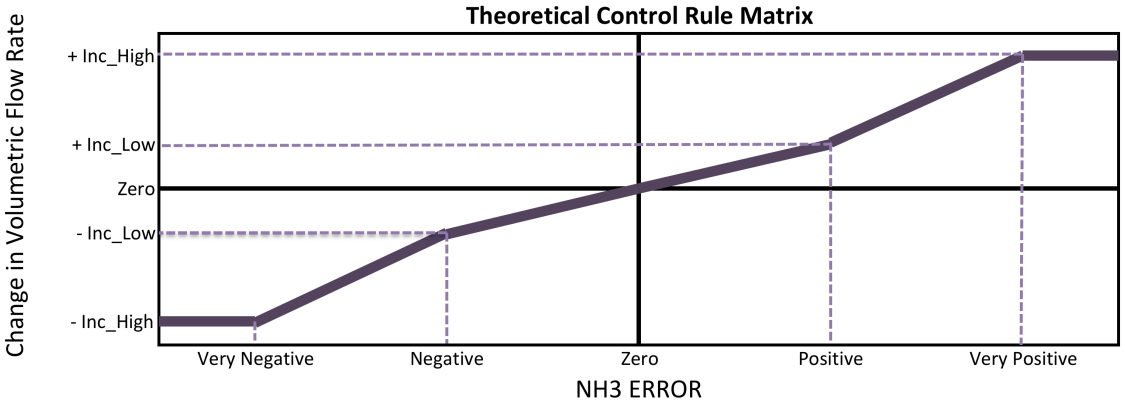

Figure 3.5: Theoretical Control Rule Matrix for Fuzzy Logic Response.
The X-axis represents the input to the fuzzy logic controller which are the membership functions defined by the user. The y-axis is the response output of the fuzzy logic controller.

The control software gives the user control over all system parameters including membership function definitions, the magnitude of incremental responses, gas concentration setpoints, and sampling period via a user interface (Figure 3.6). The user defines an individual gas concentration setpoint for each compartment through the control software.

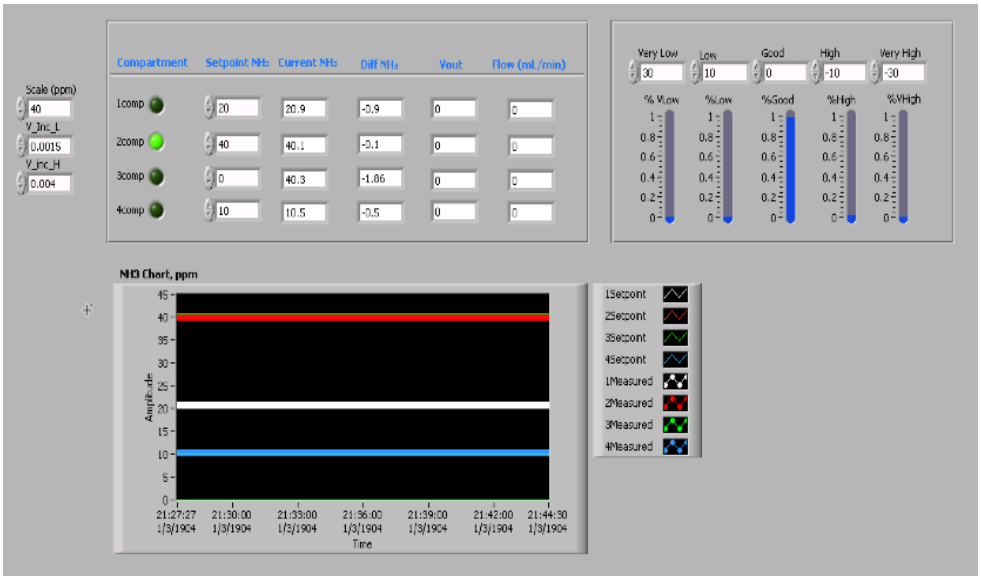

Figure 3.6: User interface of control software.
The control software accepts user inputs for all fuzzy parameters and NH_3 setpoints. Real-time graphs and readings of the current NH_3 concentration, signal voltage and volumetric flow rate of all four compartments are displayed.

Tuning the Fuzzy Logic Controller

The Fuzzy Logic Controller was tuned manually to achieve 30ppm of NH_3 in one compartment over a thirty-min period with minimal overshoot. A thirty-min period was desired so the atmospheric transition would be smoother and appropriate for animal occupants. Likewise, overshoot is undesirable since it would present an unrepresentative and potentially aversive environment for a brief period of time. The parameters Inc_High and Inc_Low, and fuzzy membership functions "Very Negative", "Negative", "Zero", "Positive" and "Very Positive" were manually adjusted for five trials until the desired conditions were achieved. All tuning trials were performed on the same compartment for consistency, and only the settings to the controller varied. The ammoniated compartment air was flushed out before each trial to ensure fresh air starting conditions (<2 ppm NH_3).

For each trial, the FLC's ability to reach and maintain a setpoint of 30ppm was quantified. This setpoint was chosen because it is near expected desired concentrations of future operations. The following values were calculated to quantify the performance of the tuning trials:

t_{95} = The time required to achieve 95% of the setpoint concentration, *min*

t_s = The time required to achieve and maintain 5% of the setpoint concentration, *min*

Max Over = The maximum observed setpoint overshoot, *ppm*

Max Oscillation Amplitude = The largest measured difference in concentration between oscillations, *ppm*

$C_{rms}(T_{95}\text{-}T_s)$ = The root-mean-square of the difference of the measured NH_3 concentration from the setpoint concentration between times T_{95} and T_s, *ppm*

The measured NH_3 concentration data of each tuning trial were normalized on a scale from 0 to 1 using Equation 3.1.

$$C(t) = \frac{C_{measured}(t) - C_{initial}}{C_{setpoint} - C_{initial}} \quad (3.1)$$

where,

C(t) = The normalized NH_3 concentration within the range [0,1]

$C_{measured}$ = The actual NH_3 concentration measured by the gas analyzer, *ppm*

$C_{setpoint}$ = The setpoint NH_3 concentration to be achieved, *ppm*

$C_{initial}$ = The first NH_3 concentration measured by the gas analyzer, *ppm*

The tuning parameters and control block matrices for each trial of tuning are provided below in Table 3.3 and Figure 3.7 respectively:

Table 3.3: Tuning Parameter Trials for NH_3 Control of a Single EPC Compartment. Membership Functions (Negative, Zero, Positive, etc.) were defined as "100% true" in the given parameters. The response variables (Inc_Low, Inc_High) define the magnitude of the Fuzzy Logic Controller's response. The 5th (FINAL) trial met the desired system performance, presented in detail in the Results section.

Trial	Inc_Low	Inc_High	VeryPos	Pos	Zero	Neg	VeryNeg
	mL/min	mL/min	ppm	ppm	ppm	ppm	ppm
1	0.2	1.0	15	5	0	-5	-15
2	0.2	1.0	30	10	0	-10	-30
3	0.2	0.4	15	5	0	-5	-15
4	0.1	0.3	15	5	0	-5	-15
(FINAL) 5	0.1	0.3	30	10	0	-10	-30

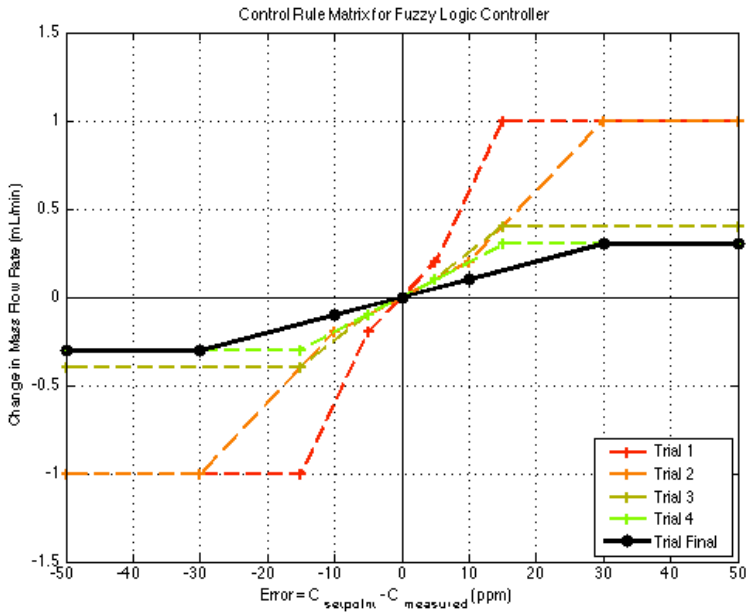

Figure 3.7: Control Block Matrix for Tuning Parameter Trials.
Each line related the output of the Fuzzy Logic Controller (change in volumetric flow rate) as a function of the input (Error in NH_3 concentration).

The control block matrix graphically describes the controller's response (Change in volumetric flow rate), which acts as an integral gain, versus the controller input (Control Error). The control response takes the shape of a piece-wise linear function with joints at the membership function definitions. After tuning the controller, the final values chosen for the incremental parameters Inc_High and Inc_Low were 0.3 mL/min and 0.1 mL/min respectively; the membership functions "Very Negative", "Negative", "Zero", "Positive" and "Very Positive" were -30ppm, -10ppm, 0ppm, 10ppm and 30ppm, respectively (Table 3.3, last row).

NH_3 Control Characterization at Different Setpoints

The Fuzzy Logic Controller was tested for an individual compartment at three different setpoints (10ppm, 30ppm and 50ppm of NH_3) using the final system tuning parameters (Table 3.3, last row). Data were collected for the increase in ammonia concentration for each setpoint with the gas analyzer about once every 33 s. The data were normalized using the same methodology described in Equation 3.1.

Plots were created to compare the results. The same values used for tuning the controller were calculated to quantify the performance between each setpoint: t_{95}, t_s, Max Over, Max Oscillation Amplitude, and $C_{rms}(T_{95}\text{-}T_s)$. This test was performed to gauge the setpoint magnitude's effect on the FLC's performance.

Simultaneous Control of Multiple Unique Ammoniated Environments

New FLC parameters were defined to operate all four of the EPC compartments simultaneously. The 5 locations were monitored in series (C1, C2, C3, C4 and the common supply air mixing box), with a sampling period of 5 min per location. The supply NH_3 volumetric flow rate to each compartment could only be controlled during its respective sampling period. The final NH_3 volumetric flow rate computed by the FLC at the end of a compartment's previous sampling period was held constant until the next sampling period. When the solenoid valve was triggered and sampling began for the next compartment, the sample air immediately entering the gas analyzer would still contain some mixture of the previous compartment's sampled air. As a result, the first two or three measurements at

the start of every sampling period resulted in values near the previous compartment's NH_3 concentration. To fix this issue, the control software was programmed to ignore the first three measurements of every sampling period and instead continue holding the previously measured concentration. Due to these system changes, the response parameters Inc_High and Inc_Low and the membership functions "Very Negative", "Negative", "Zero", "Positive" and "Very Positive" needed to be retuned. The FLC parameters Inc_High and Inc_Low were raised from 0.3 to 0.4 and 0.1 to 0.15 mL/min, respectively (roughly a 50% increase). The membership functions "Very Negative", "Negative", "Zero", "Positive" and "Very Positive" remained the same at -30ppm, -10ppm, 0ppm, 10ppm and 30ppm, respectively.

A test was performed to quantify the EPC's accuracy and precision in simultaneously creating unique ammoniated environments within its four compartments. The system was assigned to maintain approximate set points of 0, 10, 20 and 40ppm of NH_3 for 24 hs. This was performed four times such that each compartment received each NH_3 level once (4x4 Latin Square design, randomly selected arrangement). The NH_3 levels administered were: [40–20–10–0], [20–40–0–10], [0–10–20–40], and [10–0–40–20] ppm for compartments [C1–C2–C3–C4], respectively. The accuracy and precision of controlled concentration for each desired setpoint and each compartment were quantified by taking the mean and standard deviation of the NH_3 concentration of each compartment after 95% of the setpoint had been achieved during the 24h testing period. These performance results were compared to historical performance data of the EPC's pre-existing gas control system, a discretized control scheme that was designed specifically for 0, 10, 20 and 40ppm of NH_3 as discussed in the introduction.

3.2 Temperature Control– Expanded Capacity with Discrete Controller

System Characterization

The EPC interior temperature is controlled using a simple On/Off Controller. The On/Off controller is a discrete SISO control system, accepting a temperature setpoint as an input (one for each compartment), and triggers a set of axial heaters *(AF-20, 200W/400W, 120V, 3.1", Farnam Custom Products, Arden, NC, USA)* when the measured temperature in a compartment is below the user-defined setpoint. These heaters originally totaled 200W of sensible heat output for each compartment but additional 400W axial heaters were installed to expand the sensible heat output to a total of 600W for each compartment. The controller is memoryless and causal, meaning the output does not rely on previous inputs or future inputs. The EPC is considered a "black box" during control operations. No information apart from the current measured temperature is considered. No cooling is utilized in the temperature control scheme. No changes were made to the temperature control logic from the original On/Off temperature control scheme [Sales et al., 2012]. Staged heating was not implemented with the additional axial heater. No hysteresis band was implemented around the setpoint. Temperature is measured from the both the top and bottom tiers of each compartment using commercial Temp/RH sensors *(model HMP50, -40°C to +60°C, 0-98%RH, Vaisala, Helsinki, Finland).* The average of these two measurements is used as the input to the On/Off controller.

One Temp/RH sensor is implemented in each of the eight compartment-levels, for a total of eight sensors. The sixteen measurements made from these sensors (eight each of temperature and relative humidity) are directed through a multiplexer that routes one

input at a time to the control software. Each second, control software signals the multiplexer to collect the next temperature or relative humidity reading and continues to do so such that all readings are refreshed every 16 s.

The installation of the 600W heating capacity required some changes to the system infrastructure. Power Relays (*G8PT Power PCB Relay, 30A, Omron Corporation*) were installed to bypass the 5 amp current flow of the convective coil axial heaters around the EPC's existing instrumentation. This process is explained in greater detail in APPENDIX A.

Performance Check of Temp/Rh Sensors

Verification of sensor calibration was performed on Temp/Rh sensors in the EPC system. The existing Temperature/Relative Humidity sensors within the EPC had been in use for nearly one year since their last calibration. With consistent use, sensors may experience shifts in the accuracy of their measurements and require recalibration. A certified handheld thermo-hygrometer (HP23/HC2-S probe, 0-100% RH [±0.8% RH], -50-100 °C [±0.1 °C], Rotronic Instrument, Inc., Bassersdorf, Switzerland) was used as a standard to confirm the actual temperature and humidity levels in the chamber at nominal temperatures of 20°C, 27°C and 35°C. All of the Temp/Rh sensors were found to be accurate within the manufacturer's claims (±0.5 °C) and no calibration was performed.

Temperature Control Assessment

Two tests were performed to assess the performance of the EPC's temperature control system: 1) A temperature step response test and 2) A maximum temperature rise test. These tests were implemented with the original 200W heating system and the increased 600W capacity in order to quantify changes to the system performance.

Temperature Step Response Test

The EPC temperature control was assessed for four step changes in the setpoint temperature. This included two positive step changes: temperature setpoints of +1°C above ambient and +3°C above ambient, and two negative step changes: -1°C back to ambient, and -3°C back to ambient. Temperature data were logged once every 40 s by the control software. All step changes were conducted over a period of 3 h. Prior to beginning each positive step change, the EPC compartments were operated with no additional heat for 2 h to ensure steady-state baseline conditions. Prior to beginning each negative step change, the temperature control was activated for 2 h to ensure the imposed temperature differential was achieved. The interior temperature was measured in each individual compartment by averaging the measured temperature between the top and bottom tiers.

Both the 600W positive temperature step responses and the negative temperature step responses were first normalized and plotted together to observe differences in response behavior. The time scale was normalized, using the unitless parameter t/τ *on the x-axis*, where t is the elapsed time and τ is a time constant specific to each step response defined as the time required to reach 63% of the setpoint. Temperature for all step responses was

normalized using Equation 3.2. The temperatures and time constants of all four compartments were averaged together.

$$T(t) = \frac{T_{measured}(t) - T_{initial}}{T_{setpoint} - T_{initial}} \quad (3.2)$$

where,

T(t) = The normalized temperature rise within the range [0, *1*]

$T_{measured}$ = The actual temperature measured by the Temp/Rh sensor, °C

$T_{setpoint}$ = The setpoint temperature to be achieved, °C

$T_{initial}$ = The first temperature measured by the Temp/Rh sensor, °C

The positive and negative temperature step responses were quantified differently due to differences in their response behavior. The positive step responses were expected to overshoot the setpoint and could not be described using the same first-order curve used for the negative step response. The temperature profiles for positive temperature step responses (+1°C from ambient and +3°C from ambient) were quantified with the parameters:

t95: The time required to achieve 95% of the setpoint, *min*

τ = A time constant. The time required to achieve 63% of the setpoint. This parameter is used to compare the performance of the positive and negative step responses for first order step response behavior, *min*

Max_Over: Maximum overshoot achieved past the setpoint, *°C*

The measured temperature rise of the positive step responses was plotted for each compartment. Fluctuations in the measured temperature resulted in slight error, require the temperature rise profiles to be standardized to the scale of the step response using Equation 3.3.

$$T(t) = \frac{T_{measured}(t) - T_{initial}}{T_{setpoint} - T_{initial}} * \Delta T \qquad (3.3)$$

where,

T(t) = The standardized temperature rise within the range [0, ΔT], °C

$T_{measured}$ = The actual temperature measured by the Temp/Rh sensor, °C

$T_{setpoint}$ = The setpoint temperature to be achieved, °C

$T_{initial}$ = The first temperature measured by the Temp/Rh sensor, °C

ΔT = The nominal magnitude of the step response, °C

The temperature profiles for the negative temperature step responses (-1°C to ambient and -3°C to ambient) were quantified by fitting a first-order step response curve to the data. This curve is produced using Equation 3.4.

$$T(t) = T_{initial} + \Delta T(1 - e^{-\frac{t}{\tau}}) \quad (3.4)$$

where,

T(t): The observed temperature at time *t, °C*

$T_{initial}$*:* The initial temperature at the beginning of the step response, *°C*

ΔT: The nominal magnitude of the step response, *°C*

τ: Time constant, as determined from nonlinear regression, is the amount of time required to achieve 63% of the setpoint, *min*

t: The elapsed time, *min*

Temperature Rise Test

In the maximum temperature rise test, temperature profiles were obtained for each compartment by continuously supplying the 600W supply heat to each of the four compartments for a period of 8 h. Temperature data were logged once every 40 s by the control software. Prior to beginning this test, the EPC compartments were operated with no additional heat for 2 h to flush out any conditioned air from previous tests and to ensure the changes to the measured temperature were due to the axial heaters alone and not from passive heat sources (lighting, instrumentation, etc.) that the EPC would experience without additional temperature control. The interior temperature was measured in each individual compartment by averaging the measured temperature between the top and bottom tiers. The resultant temperature rise profile was compared to historical data achieved with a 200W supply heating in each compartment, which was acquired using the same methodology.

Two values were obtained from this test: 1) the maximum temperature gain sustained by the EPC, and 2) the time constant of the approximated first order step response to maximum temperature. In reality, many variables in the EPC system such as air mixing, Temp/Rh sensor placement, and heat dissipation prevent the maximum temperature rise from being purely first order, but this approximation is suitable for analysis.

An average ventilation rate of roughly 20 ACH was observed in each compartment for the 600W maximum temperature rise test. The method used to calculate the ventilation rate may be found in Appendix B. A ventilation rate of roughly 13 ACH was observed in the historical data of the 200W heating test [Sales, 2012].

3.3 Simultaneous Control of Gas Concentration and Temperature

The FLC was operated to achieve four unique NH_3 concentrations (0, 10, 20 and 40ppm) in each of the four compartments and the discrete temperature controller set to achieve a temperature setpoint. All data were logged once every 40 s by the control software for duration of 8 h. Prior to beginning this test, the EPC compartments were operated with no additional heat or supply gas for 2 h to flush out any conditioned air from previous tests and to ensure the changes to the measured temperature were due to the axial heaters alone and not from passive heat sources (lighting, instrumentation, etc.) that the EPC would experience without additional temperature control. The interior temperature was measured in each individual compartment by averaging the measured temperature between the top and bottom tiers. Three tests were conducted: 1) achieving maximum temperature rise and the NH_3 setpoints simultaneously, 2) achieving maximum

temperature rise after the FLC had converged to within 95% of the NH_3 setpoints, and 3) achieving a specified setpoint temperature (at +5°C temperature differential) and the NH_3 setpoints simultaneously.

4. Results and Discussion

4.1 Gas Concentration Controller Performance

Tuning the Fuzzy Logic Controller

A normalized plot of the ammonia (NH_3) concentration rise comparing the performance of five different sets of FLC tuning parameters for the case where a single compartment was being controlled is given in Figure 4.1 and summarized in Table 4.1.

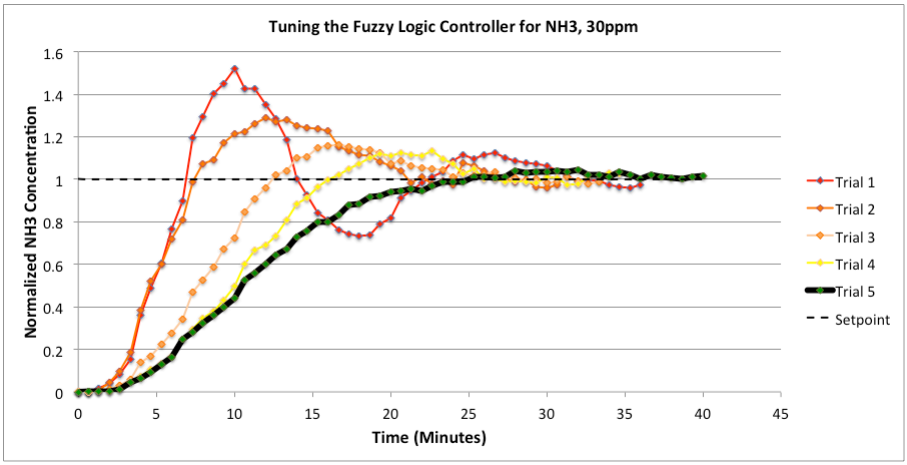

Figure 4.1: Normalized NH_3 Rise Profiles for FLC Tuning Trials On a Single Compartment.
Trial 5 (black line) attained the setpoint NH_3 concentration of 30ppm within 30 min and with minimal overshoot.

Table 4.1: Performance of Fuzzy Logic Controller Tuning Trials.
The Fuzzy Logic Controller's ability to achieve 30ppm of NH_3 in a single compartment was quantified in five tuning trials. The fifth trial was preferred because of the time it required to achieve 95% of the setpoint (21.3 min), its low overshoot (1.3ppm) and stability (concentration never deviated more than 5% from setpoint). The parameter Max_Over is presented in both percent and ppm_v.

Parameter	Tuning Trial Results					Units
Trial	1	2	3	4	**(FINAL) 5**	
t_95	6.7	7.3	11.3	14.7	**21.3**	min
t_s	30.7	26.0	22.7	24.7	**21.3**	min
Max Over	51.4	28.9	16.2	13.6	**4.4**	%
	15.0	8.4	4.7	4.0	**1.3**	ppm
Max Osc. Amp.	23.0	9.1	5.2	4.5	**1.3**	ppm
C_rms	6.6	4.6	3.9	3.2	**0.0**	ppm

Trial 5 was chosen because its performance met the design criteria outlined in the Objectives and Approach regarding overshoot. The overshoot of this trial was minimal (4.4%) and the response never oscillated below the setpoint. All prior trials exhibited an amount of overshoot, which was considered undesirable for animal preference tests. Trial 5 required 21.3 min to achieve 95% of the setpoint, which was also the settling time due to low overshoot. This timespan was far quicker than the imposed design constraint for animal behavior tests, but this constraint was omitted since this tuning was meant to validate the control of a single compartment and would not be used in an actual animal behavior test. The delayed initial concentration rise is due to the FLC adjusting the volumetric flow rate of ammonia because the controller response is based on integral gain response.

NH_3 Control Characterization at Different Setpoints

A normalized plot of the NH_3 concentration rise comparing the performance of three different NH_3 setpoints (10 ppm, 30ppm, and 50ppm) for the case where a single compartment was being controlled is given in Figure 4.2 and summarized in Table 4.2. The FLC tuning parameters from trial 5 in the previous test were used for all three setpoints.

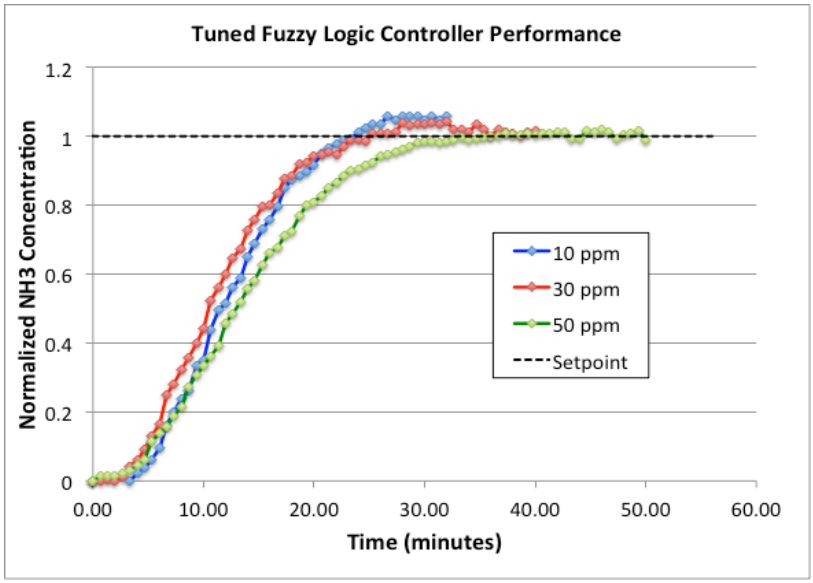

Figure 4.2: Normalized NH_3 Rise Profiles In a Single Compartment at Different Concentration. Setpoints. This plot demonstrates how the Fuzzy Logic Controller's performance changes as the setpoint magnitude is adjusted. Each setpoint was achieved using the same tuning parameters.

Table 4.2: Performance of FLC at Different Concentration Setpoints.
The Fuzzy Logic Controller's ability to achieve 10ppm, 30ppm and 50ppm of NH_3 in a single compartment was quantified. The parameter Max_Over is presented in both percent and ppm_v. Maximum Oscillation Amplitude was equal to Max Over since the controller response did not oscillate below the setpoint. The value for C_{rms} was zero for all three concentrations since the controller response did not overshoot more than 5% of any setpoint.

Parameter	Tuning Trial Results			Units
Setpoint	10 ppm	30 ppm	50 ppm	
t_95	20.7	20.7	27.0	min
t_s	20.7	20.7	27.0	min
Max Over	5.0	4.3	1.4	%
	0.5	1.3	0.7	ppm
Max Osc. Amp.	0.5	1.3	0.7	ppm
C_rms	0.0	0.0	0.0	ppm

The controller performance was nearly identical when reaching concentration setpoints of 10ppm and 30ppm. The FLC required roughly 7 min longer to reach T_{95} at 50ppm, however this came with the benefit of having essentially far less overshoot, by percent. None of the concentrations deviated from their setpoint by more than 5%, setting T_{95} and T_s equal, and

making $C_{rms}(T_{95}-T_s)$ equal to zero These results validate the FLC's ability to acquire and hold different gas concentration setpoints for control of an individual compartment.

Simultaneous Control of Multiple Unique Ammoniated Environments

A few consequences resulted from the multiplexer approach to controlling four compartments. First, the ammonia supply rate of each compartment was held at the last computed value while other compartments were sequentially controlled. The ammonia supply rate would continue unchanged while a compartment was "idle" until the following sampling period. Second, the observed ammonia concentration of each compartment was also held at the last measured value while other compartments were sequentially sampled and controlled. In reality, the actual ammonia concentration continued to change while the compartment was "idle", but the known measurement could not be achieved. Third, at the start of a new sampling period when air began being sampled from the next compartment, the air sampling line connecting the EPC compartments to the gas analyzer would temporarily contain a mixture of air from both compartments. The gas analyzer would consequently measure an unrepresentative ammonia concentration from mixed sample air that did not represent any single compartment. The control software corrected for these transition periods by ignoring the first three measurements after each sampling location change.

Figure 4.3 shows a 3-h sample of NH_3 concentration measurements from the [20-40-0-10] test that would be displayed in real-time by the control software. This includes the constant, assumed NH_3 concentrations held in between sampling periods. Figure 4.4 shows

only the measured NH_3 concentrations from the gas analyzer that initiated a response from the FLC.

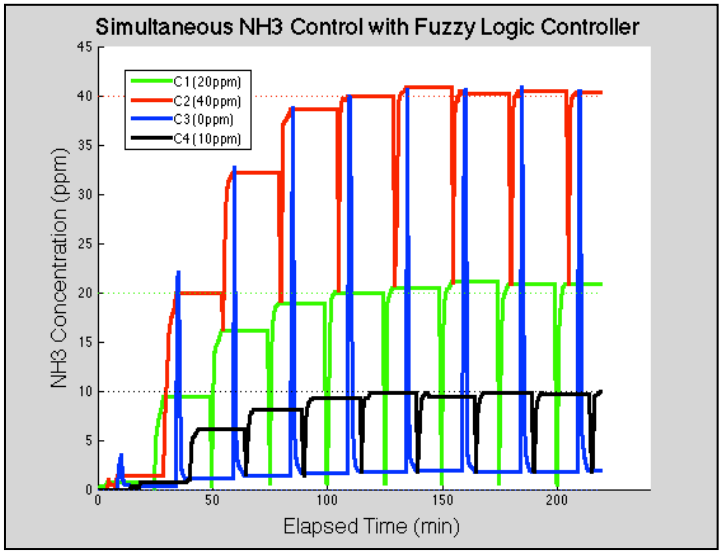

Figure 4.3: Raw data of NH_3 rise of four compartments when controlled simultaneously by FLC. The control software displays these NH_3 concentrations during operation. The large vertical "streaks" occur immediately after the gas analyzer begins reading a different compartment. Time is required before the analyzed sample air is an accurate representation of the monitored compartment's air.

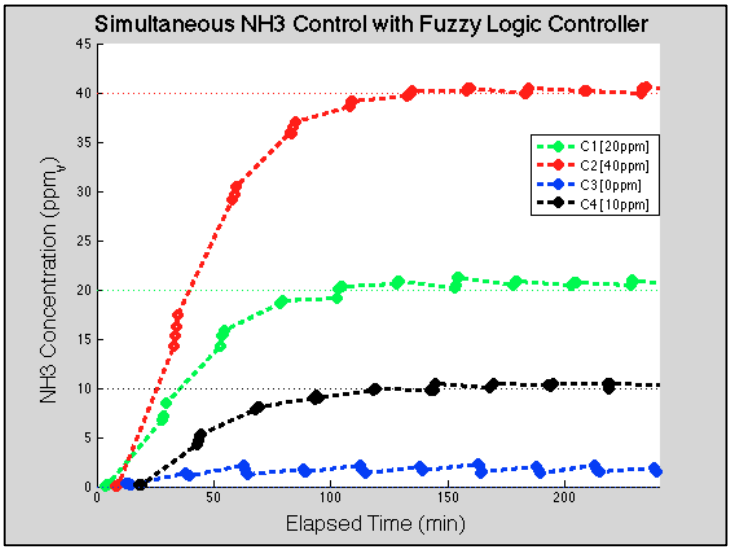

Figure 4.4: Corrected data of NH_3 rise of four compartments controlled simultaneously by FLC. Four unique NH_3 concentration setpoints could be achieved in each of the EPC's four compartments by the Fuzzy Logic Controller. The data presented are the actual gas measurements from the gas analyzer that initiated response from the FLC. This process required roughly 90 min.

The time required to achieve 95% of the setpoint, t_{95}, was within 90 min for all four compartments. None of the compartments displayed major overshoot or undershoot around the setpoint before converging. The desired concentration of 0 ppm could not be maintained due to some infiltration from adjacent compartments. This concentration never rose above 5ppm, which is the maximum allowable NH_3 concentration accepted for fresh air conditions in the planned studies with the chamber. These results were similar for all four NH_3 concentration combinations.

The average (± standard deviation) NH_3 levels among the compartments over 24 h for each setpoint were: 1.8 ± 0.8ppm, 10.2 ± 0.5ppm, 20.1 ± 0.8ppm, and 40.5 ± 1.3ppm for setpoint concentrations of 0, 10, 20, and 40ppm, respectively, across all four arrangements tested in the Latin Square. This demonstrates better accuracy and precision than did the discrete NH_3 control scheme previously implemented with the EPC, which acquired concentrations of 2.5±1.1ppm, 10.4±2.2ppm, 22.2±1.5ppm, and 37.9±1.4ppm for setpoint concentrations of 0, 10, 20, and 40ppm, respectively. These results are seen in Figure 4.5a and 4.5b:

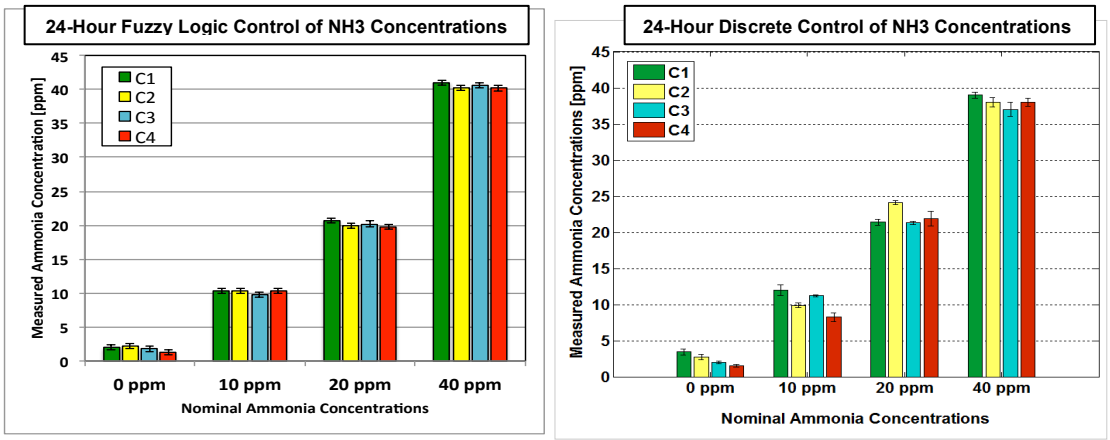

Figure 4.5 a) (Left) Average NH_3 concentrations in compartments using FLC; b) (Right) Historical data of Average NH_3 concentrations in compartments using discrete control system [Sales et al., 2013]. The Fuzzy Logic Control exhibits are greater accuracy and precision than the previous discrete staged control design.

4.2 Temperature Controller Performance
Positive vs. Negative Temperature Responses

The normalized 600W positive temperature step responses and normalized negative temperature step responses are plotted together on Figure 4.6 below.

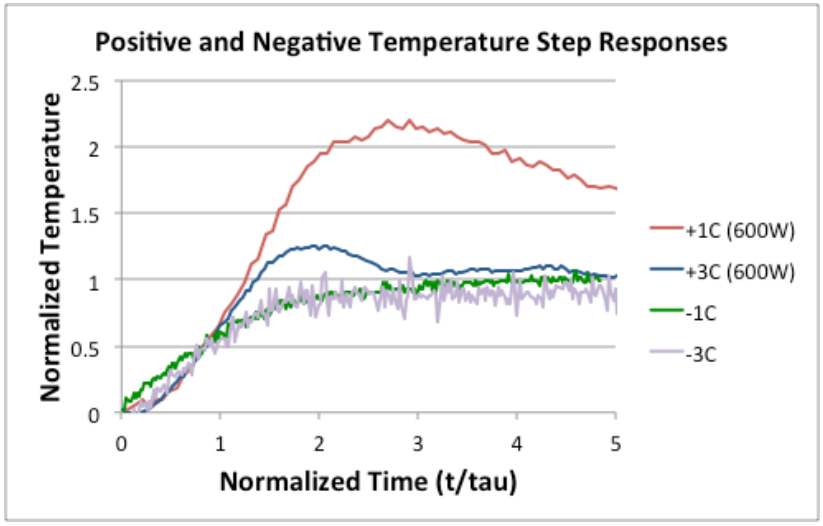

Figure 4.6:Normalized Positive and Negative Temperature Step Responses.
X-axis is normalized time represented by the elapsed time divided by each curve's specific time constant, τ, defined as the time required to achieve 63% of the setpoint. Y-axis is normalized temperature, where the magnitude of the step response is set equal to 1. Negative temperature step responses show first-order behavior, while positive temperature step responses do not.

The positive temperature step responses display large overshoot, which varies by the magnitude of the response. The +1°C step is a small temperature adjustment compared to the capacity of the 600W heat supply, resulting in far greater overshoot on the normalized scale compared to the +3°C step response. Such overshoot results from the time lag between the moment the heat supply is triggered OFF and when the Temp/Rh sensors measure the resultant change in temperature. This time lag is partially dependent on ventilation rate and air distribution, which are unchanged between both step responses. Higher operating temperatures also affect the controller response by introducing greater

heat dissipation to the environment. The +1°C step had a smaller temperature differential with the ambient environment, lowering the rate of heat loss and lengthening the time required to "cool down" on the normalized time scale compared to the +3°C step.

In general, larger positive step responses would appear to show more first-order step response behavior. Higher operating temperatures require a heat load closer to the capacity of the 600W heat supply. More step responses at +2°C, +5°C or +10°C could provide more useful information regarding the performance of the EPC temperature control system.

The negative temperature step responses display first order behavior, showing smooth convergence to the ambient temperature. This is mostly likely because these negative temperature responses cooled to ambient air temperature and did not require action from the temperature controller. It is important to consider that not all negative temperature step responses may be first order. A negative temperature step down to a temperature higher than the ambient air temperature may still result in "overshoot", since heat dissipation to the environment could drop the measured temperature below setpoint before the heat generated from the axial heaters reaches the compartments.

Positive Step Response in Temperature Test

The EPC's ability to make small changes to the interior temperature was observed.

Results of the positive step response temperature tests for the 200W and 600W heating capacities are seen in Table 4.3 and Figures 4.7 and 4.8.

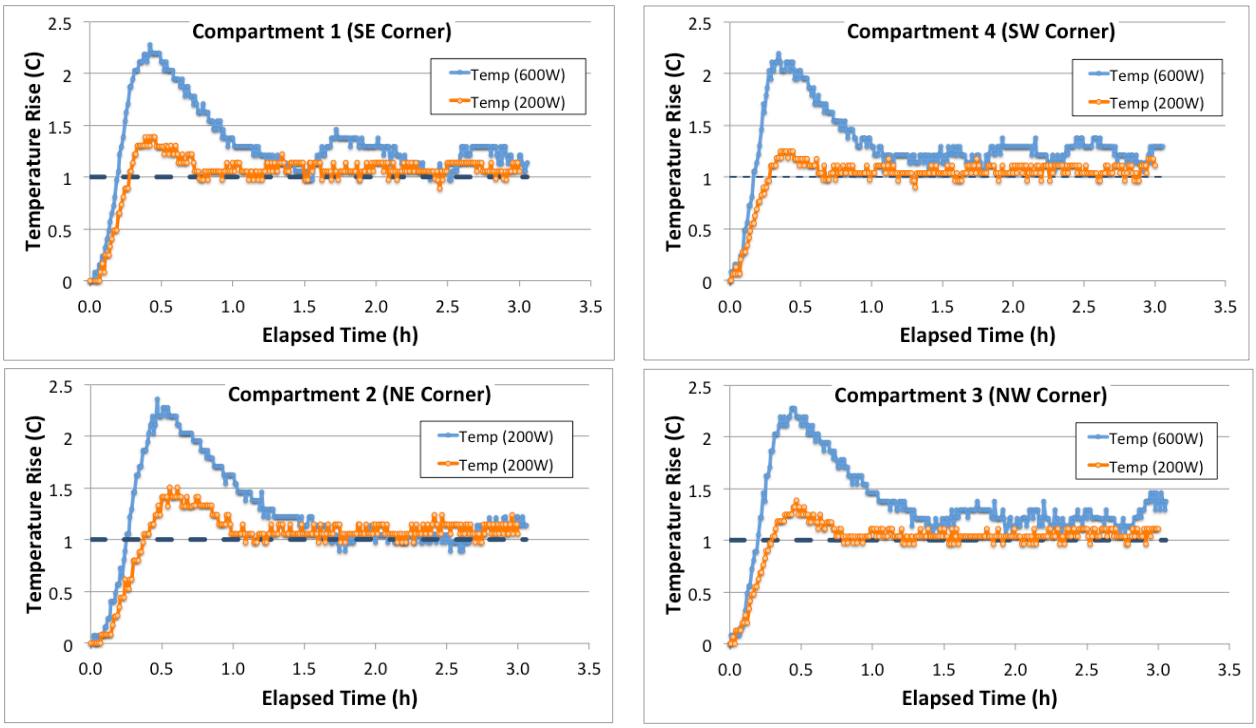

Figure 4.7: 1°C Step Increase Response Test Temperature Profiles for Each Compartment. The 600W heating system overshot the setpoint significantly more than the 200W heating system. The 600W heating system oscillated just above the setpoint after settling.

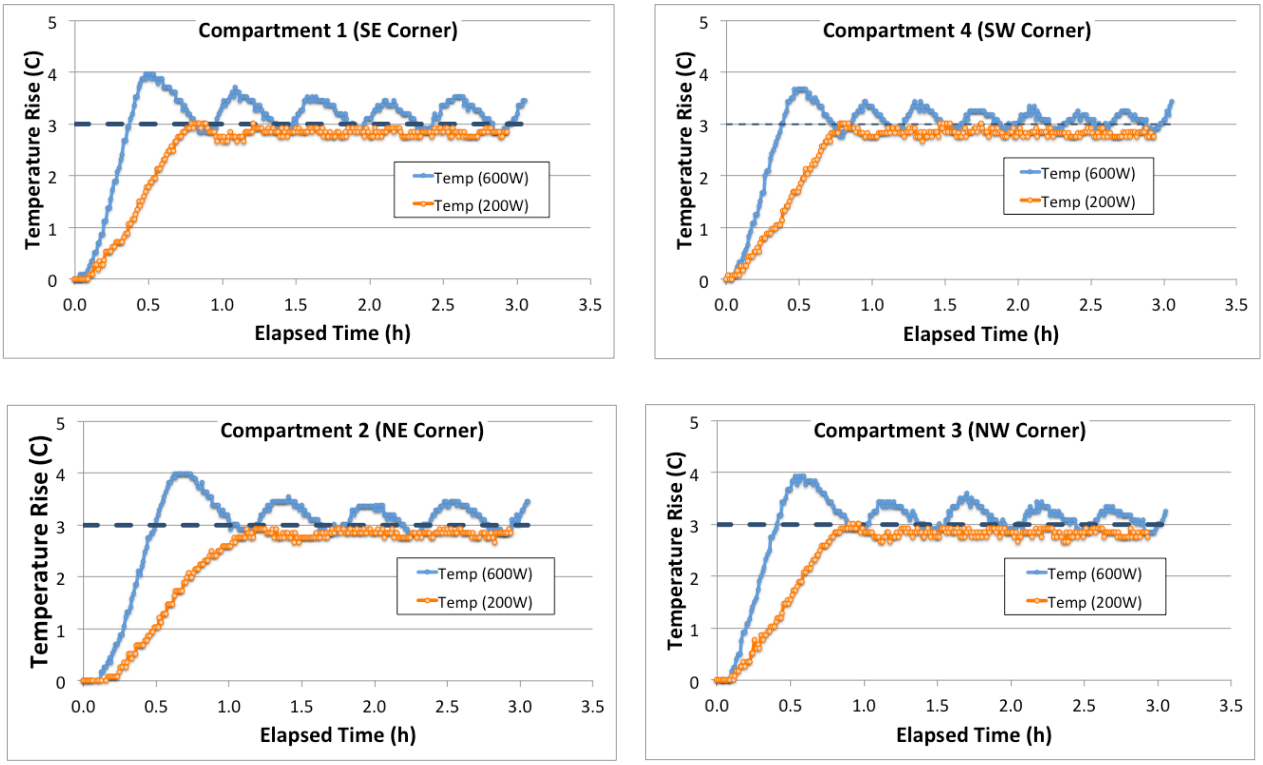

Figure 4.8: 3°C Step Increase Response Test Temperature Profiles for Each Compartment.
The 600W heating system had slight overshoot above the setpoint while the 200W heating system had nearly none. The 600W heating system oscillated above the setpoint with no signs of convergence.

Table 4.3: Positive Step Increase Response Test Results

The 600W heating system achieved each setpoint in roughly half the time as the 200W heating system, but also had a greater overshoot.

Compartment	Heat (W)	Step Response (°C)	τ (min)	t95 (min)	Max Over (°C)
1	200	1.2	12.0	16.8	0.4
	200	3.3	31.8	45.6	0.0
	600	1.2	9.0	11.4	1.3
	600	3.4	16.8	21.6	1.0
2	200	1.1	17.4	22.2	0.5
	200	3.4	41.4	70.8	-0.1
	600	1.2	12.0	15.6	1.4
	600	3.3	22.8	28.8	1.0
3	200	1.4	12.0	16.8	0.4
	200	3.4	33.6	48.0	0.0
	600	1.2	9.6	12.0	1.3
	600	3.5	17.4	23.4	0.9
4	200	1.4	10.8	16.2	0.3
	200	3.3	31.2	43.2	0.0
	600	1.2	7.8	10.2	1.2
	600	3.5	16.2	22.2	0.7

The 600W heating system achieved 95% of the temperature setpoint in 12.3±2.3 min and 24.0±3.3 min for +1°C and +3°C, respectively. This was faster than the 200W heating system, which achieved 95% of the temperature setpoint in 18.0±2.8 min and 51.9±12.8 min for +1°C and +3°C, respectively. The maximum setpoint overshoot of the 600W heating system was 1.5±0.4°C and 0.9±0.1°C for +1°C and +3°C, respectively. The 200W heating system showed a 0.4±0.1°C overshoot for the +1°C step response and a negligibly small overshoot for the 3°C.

These results were anticipated, given the simple design of the discrete ON/OFF controller. The 600W heating system achieves the setpoint much quicker but suffers from large overshoot. The 600W heating system never converged on the setpoint, showing oscillations of roughly 0.5°C above the setpoint. These oscillations appear more pronounced and frequent in the +3°C step response due to the increased temperature differential between the EPC and the ambient air. The 600W of heat would boost the temperature briefly, the heater would turn off, and the heat loss through the compartment envelope would then reduce the temperature below the setpoint. These oscillations are not ideal from a control standpoint, but are within acceptable limits for the planned use of the compartments for animal preference testing. Temperature oscillations of ±0.5°C are not large enough to induce a physiological or behavioral response in any test animals.

If desired in future studies, this behavior could be improved using a discrete proportional control [Chao et al, 2000]. The 600W heating system uses two separate convective coil axial heaters in series (400W and 200W). It would be possible to develop the heating controls to trigger only the 400W or 200W (or both) as needed to achieve different setpoints quickly and accurately.

Negative Temperature Step Response Test

Results of the negative temperature step response tests are given in Table 4.4 and Figures 4.9 and 4.10.

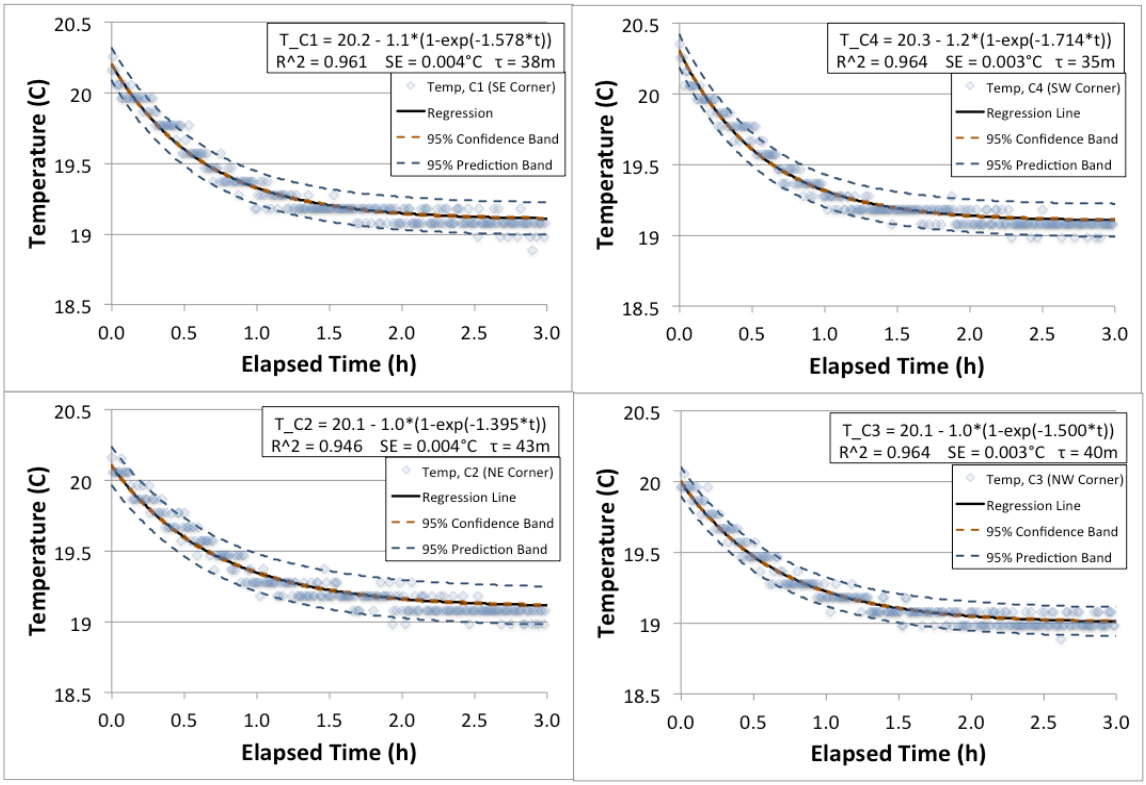

Figure 4.9: 1°C Step Decrease Response Test Temperature Profiles.

The 1°C step decrease to ambient air conditions fit a first-order step response curve. These plots demonstrate the EPC's ability to "cool down" from an imposed 1°C temperature differential.

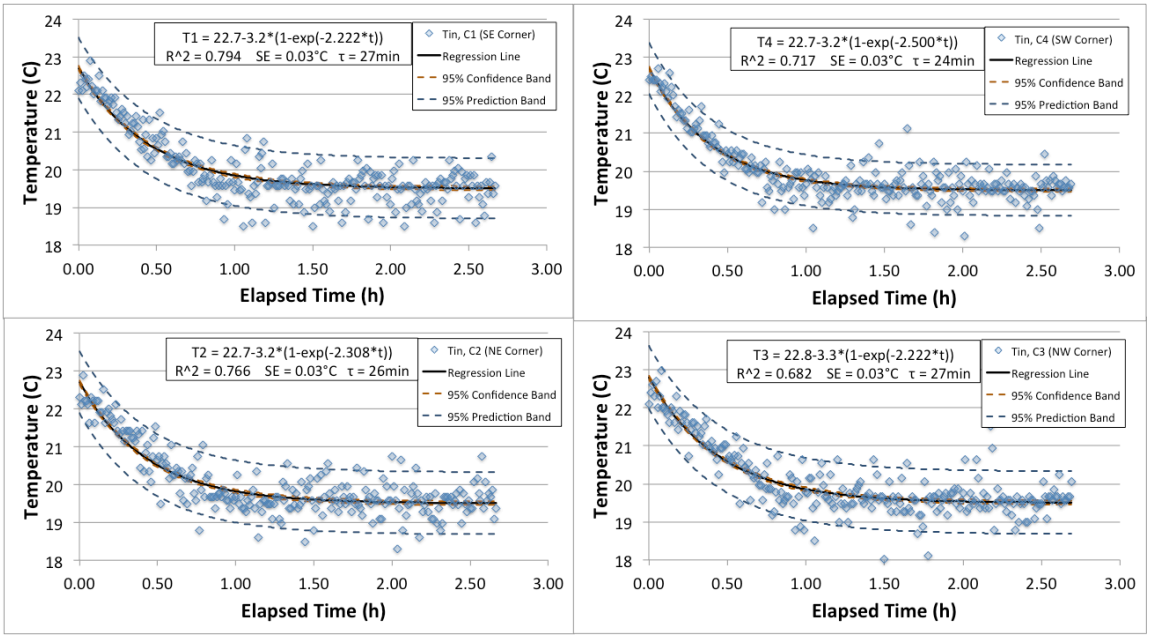

Figure 4.10: 3°C Step Decrease Response Test Temperature Profiles.
The 3°C step decrease to ambient air conditions fit a first-order step response curve. These plots demonstrate the EPC's ability to "cool down" from an imposed 3°C temperature differential. Noise in the data is a result of electronic interference from nearby laboratory equipment.

Table 4.4: Negative Step Response Test Results
The time constant, τ, represents the amount of time required to complete 63% of the temperature step change, ΔT.

Compartment	ΔT (°C)	τ (min)	R^2
1	-1.1	38	0.961
	-3.2	27	0.794
2	-1.0	43	0.946
	-3.2	26	0.766
3	-1.0	40	0.964
	-3.3	27	0.768
4	-1.2	35	0.965
	-3.3	24	0.825

The EPC compartments primarily lose heat from three mechanisms: *Ventilation*, which is a heat loss linearly dependent on the ventilation rate and temperature differential between compartment and room air, *Conduction and Convection*, which is a heat loss linearly dependent on the temperature differential between compartment and room air, and *Radiation*, which is a dependent on the differential between compartment surface

temperature raised to the fourth power and room surface temperature raised to the fourth power. These three mechanisms together form a complex relationship between the time constant, τ, and the interior temperature of an EPC compartment. The first-order step response time constants, τ, were 39.0±3.4 min and 26±1.4 min for the -1°C and -3°C step responses, respectively. It can be inferred that τ will decrease even more as the step response increases in magnitude. This data provides an expectation of how long the system requires to "cool down" to ambient air after a heat-stress test.

Maximum Temperature Rise Test

These results were compared to an identical maximum temperature rise test performed using only the 200W heating system when the EPC was initially commissioned for animal testing [Sales, 2012]. Temperature data were fit to the first-order step response curve as described above for the negative temperature step response tests. Results are provided in Table 4.5 and Figures 4.11 and 4.12.

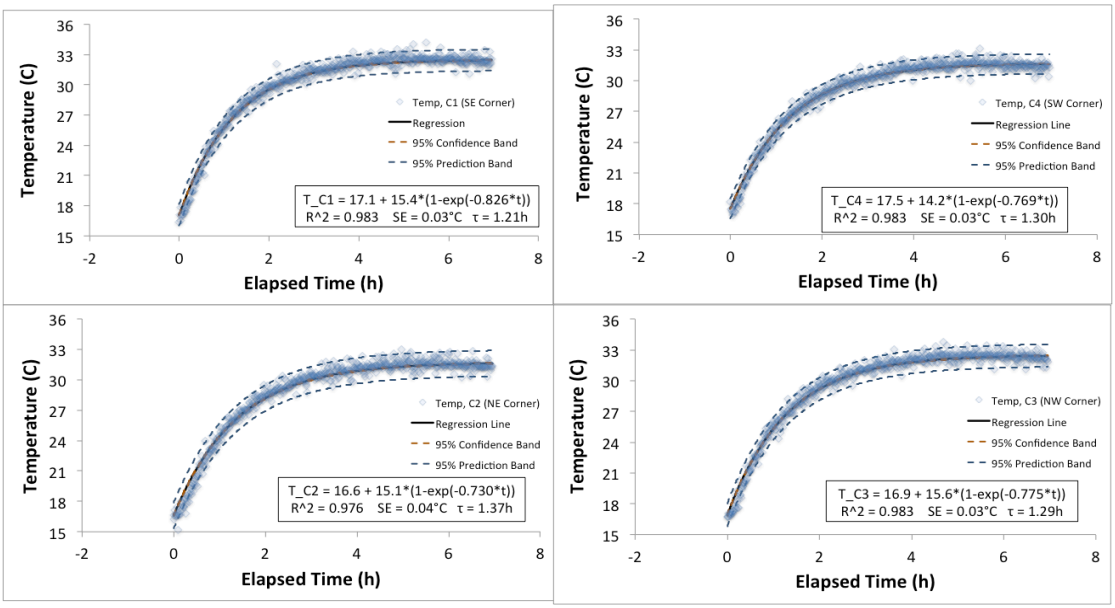

Figure 4.11: Maximum Temperature Rise in each of the EPC compartments (600W heating).

The max temperature rise profiles fit a first-order step response curve. Compartments reached an average temperature increase of 15.1±0.6°C.

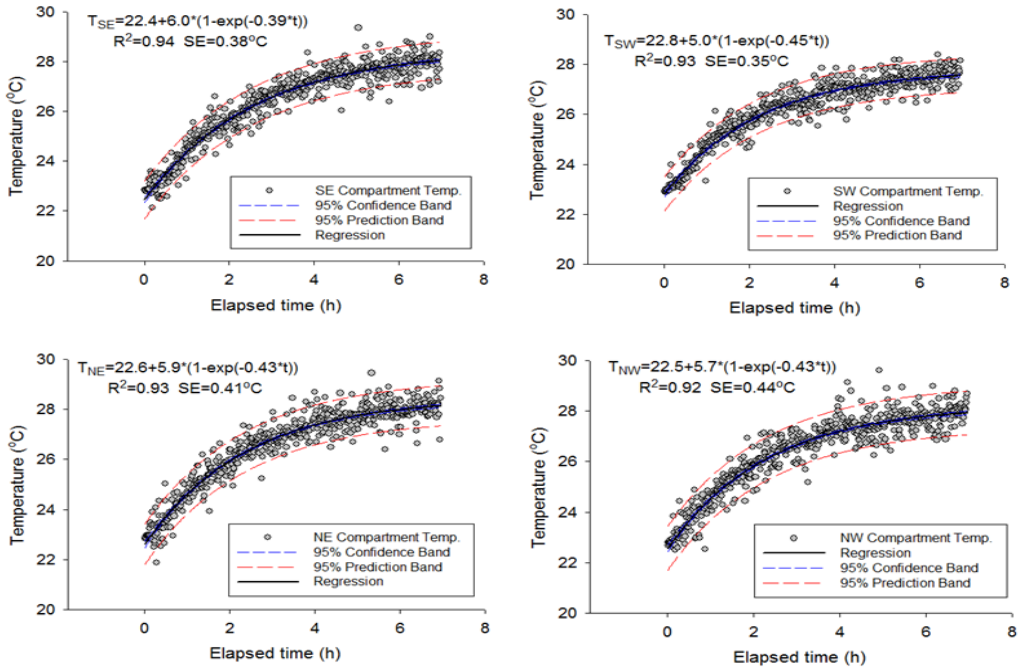

Figure 4.12: Maximum Temperature Rise in each of the EPC compartments (200W heating) [Sales et al., 2013].

The max temperature rise profiles fit a first-order step response curve. Compartments reached an average temperature increase of 5.7±0.5°C.

Table 4.5: Maximum Temperature Rise Results.

The time constant, τ, *represents the amount of time required to complete 63% of the temperature step change,* ΔT. The maximum temperature rise of the 600W heating system was almost triple of the 200W heating system.

Compartment	Heat (W)	ΔT (°C)	τ (hours)	R^2
1	200	6.0	2.56	0.94
	600	15.4	1.21	0.98
2	200	5.9	2.33	0.93
	600	15.6	1.37	0.98
3	200	5.7	2.33	0.92
	600	15.1	1.29	0.98
4	200	5.0	2.22	0.93
	600	14.2	1.30	0.98

The implementation of the 600W heating capactiy increased the maximum achievable temperature of the EPC to 15.1±0.6°C with a time constant, τ, of 1.3±0.1 h. This was a desirable improvement over the original EPC heating capabilities, which used only a 200W heating capacity to achieve 5.7±0.5°C with a time constant of 2.4±0.1 h. The decrease in the time constant may have been due to heat losses from radiation. The heat loss due to radiation increased as a function of the differences between the surface and surrounding temperatures each raised to the fourth power, causing the temperature profile to level out quicker. Differences in ventilation rate may have also caused a change in the time constant, as a higher ventilation rate could introduce dynamic changes to the airflow inside each compartment as well as remove more heat through the exhaust air. The 600W heating test used a higher ventilation rate than the 200W heating test (Roughly 20 ACH compared to 13ACH). Radiation and ventilation may also explain why the maximum temperature gain is not directly proportional to the heat supply. Assuming a linear relationship between heat supply and temperature gain, one would expect a maximum temperature rise of 17.1°C (= 5.7°C * [600W/200W]). Such results may have arisen if heat was lost to the environment

due to convection alone, but ventilation and radiation introduce non-linear attributes to the heat balance.

4.3 Simultaneous Gas Concentration and Temperature Control Performance

In the first simultaneous control test, the Discrete Temperature Controller was tasked to achieve heat-stress conditions while the FLC was converging to four unique NH_3 setpoints in each of the four compartments. The FLC was set to achieve 20, 40, 0, and 10 ppm of NH_3 in compartments 1, 2, 3 and 4, respectively. Compartment began operation at ambient air temperature. Both the FLC gas concentration controller and On/Off temperature controller began operation at the same moment. A Temperature and NH_3 concentration rise profile from this test is given in Figure 4.13.

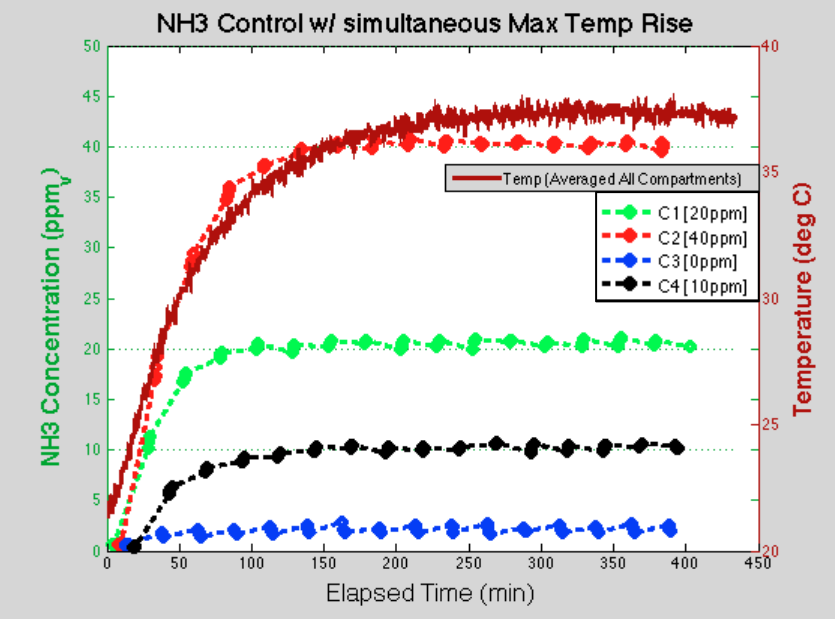

Figure 4.13: Reaching heat- stress conditions while NH_3 setpoints were achieved
The Fuzzy Logic Controller achieved four distinct NH_3 concentration setpoints while the 600W heating system was switched ON continuously. Both systems began operation at baseline conditions. No significant difference can be seen in the NH_3 control. Temperature was averaged for presentation since no significant differences were observed between the compartment temperature rise profiles

In the second simultaneous control test, the Discrete Temperature Controller was tasked to achieve heat-stress conditions after the FLC had converged to four unique NH_3 setpoints in each of the four compartments. A Temperature and NH_3 concentration rise profile from this test is given in Figure 4.14.

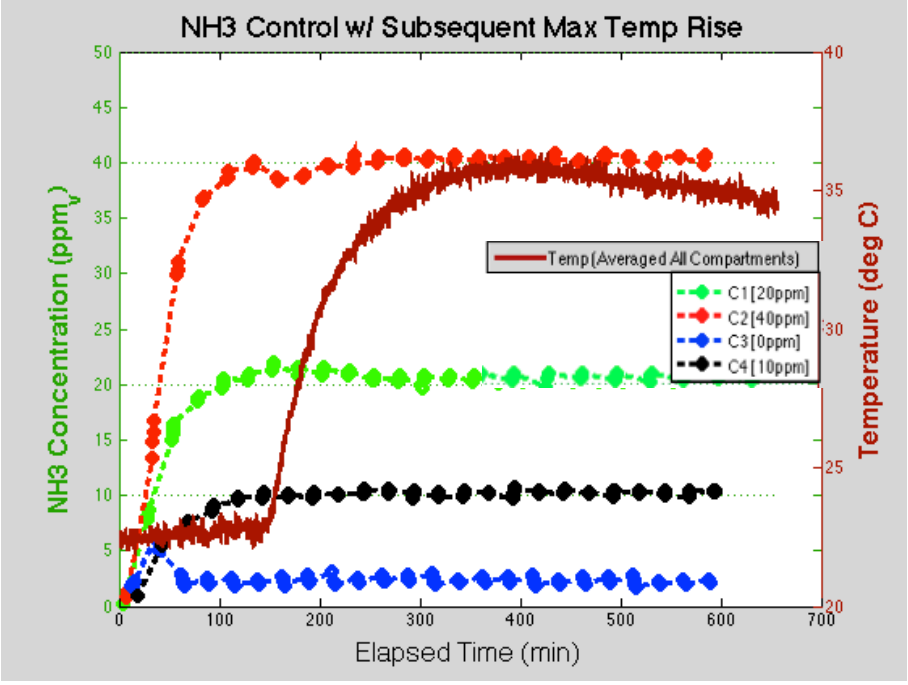

Figure 4.14: Reaching heat-stress conditions after NH_3 setpoints were achieved
The Fuzzy Logic Controller achieved four distinct NH_3 concentration setpoints with the 600W heating system switched OFF. Once all setpoints had been achieved, the heaters were switched ON continuously to reach maximum temperature conditions. Slight perturbations can be seen in the NH_3 control of the 20ppm and 40ppm compartments. Temperature was averaged for presentation since no significant differences were observed between the compartment temperature rise profiles.

A subtle fluctuation in the NH_3 concentration of the 20 and 40ppm compartments can be observed when the temperature initially jumps in the first simultaneous control test (Figure 4.14). The 20ppm compartment briefly rose about 2ppm and the 40ppm compartment dropped about 2ppm. However, the FLC corrected for these fluctuations and

converged back to the proper setpoints. No large differences were observed in the temperature rise profiles of these two compartments at the time of these perturbations. Interaction between the two controllers was otherwise very limited in this test. The FLC achieved 95% of each setpoint in just over 90 min, which was the same performance observed when testing the FLC alone. Likewise, the temperature rise was unhindered by the FLC. In the second simultaneous control test, a maximum temperature rise of 13.5°C was observed, compared to the temperature rise of 15.0°C in the first simultaneous control test. This small change in performance was actually due to a drop in supply air temperature as the laboratory ambient air briefly cooled during testing.

These results aligned with expectations, since the discrete temperature controller and FLC do not directly share any instrumentation or equipment in their implementation. If any compartment is set to maintain 0ppm of gas concentration, the control software is programmed to implement the staged fan control, where the fan speed increases incrementally as the gas concentration strays too far from 0ppm. This increase in fan speed would increase the ventilation rate of the 0ppm compartment and consequently increase the heat loss from exhausted air; however the magnitude of this ventilation rate increase is only enough to impose a positive pressure differential with adjacent compartments and is not expected to be a significant detriment to the maximum achievable temperature.

In the third simultaneous control test, the Discrete Temperature Controller was tasked to achieve a Setpoint of 27°C (+5°C temperature step response) while the FLC converged to

four unique NH_3 concentration setpoints in each of the four compartments. A Temperature and NH_3 concentration rise profile from this test is given in Figure 4.15.

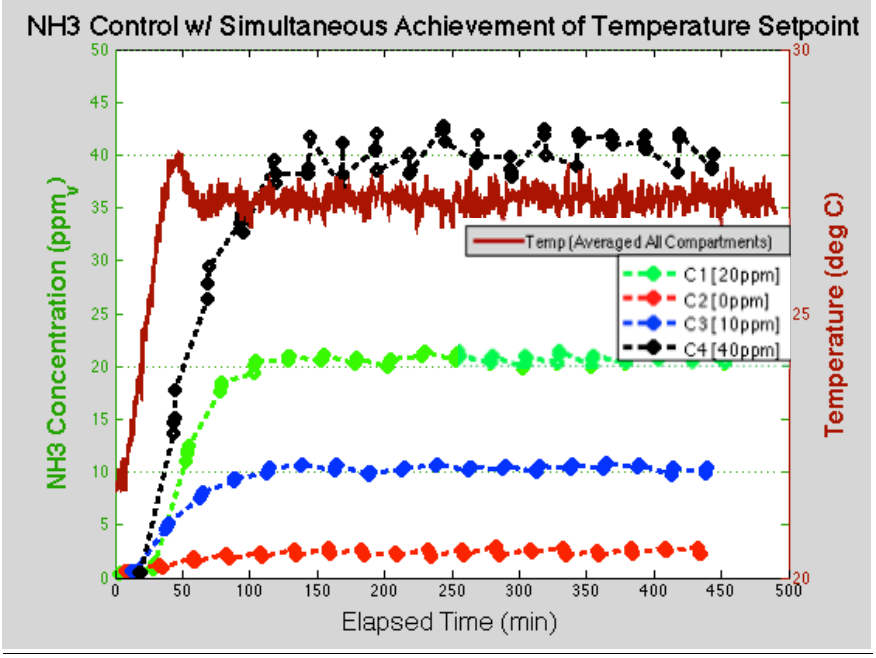

Figure 4.15: Imposing a 27°C temperature setpoint (+5°C Temperature Step Response) while NH_3 setpoints were achieved. The presence of the exhaust fan required for the NH_3 Control created noise in the temperature measurements. The noise had a dampening effect on any oscillations in the temperature control. All NH_3 setpoints were met, but greater fluctuation was present in the 40ppm compartment.

The temperature and NH_3 concentration setpoints were all met but with a slight reduction in precision. Most notably, the large ventilation fan used to exhaust the outgoing ammoniated air from the EPC was found to create noise in the Temp/Rh sensors with a magnitude of roughly 0.5°C. This noise triggered the ON/OFF response of the temperature control at a high frequency since no hysteresis band was implemented around the temperature setpoint. As a result, the noise had a dampening affect on the temperature oscillations and leveled out the measured temperature. The NH_3 concentration setpoints were mostly unaffected by the temperature step response. The 40ppm compartment

appeared to have greater variability, but its observed NH_3 concentration was still centered on the setpoint and was not meaningfully different than the performance of the NH_3 concentration control alone (40.2 ± 1.6 ppm over a 5 h sampling period compared to 40.5 ± 1.3 ppm over four 24 h sampling periods, one in each compartment).

5. Conclusions

5.1 Gas Concentration Controller

The first objective was to develop a control scheme to continuously control distinctly different atmospheric gas concentrations in each compartment simultaneously. A fuzzy logic controller (FLC) was implemented, accepting a discrete input of gas concentration error ($\varepsilon = C_{setpoint} - C_{measured}$, [ppm]) and outputting an adjustment to the volumetric flow rate ($\Delta\dot{V}$, [mL/min]) of an externally supplied gas. The FLC was first tuned to achieve ammonia (NH_3) concentration setpoints in a single compartment without overshoot. A multiplexer approach was successfully implemented to achieve simultaneous control of distinctly different ammoniated environments in each of the four compartments of the Environmental Preference Chamber.

5.2 Temperature Controller

The second objective was to expand the temperature control scheme to attain a higher maximum temperature. The heating capacity of each compartment of the Environmental Preference Chamber was expanded from 200W to 600W. A pre-existing discrete On/Off controller was utilized with this additional heat. No hysteresis band was implemented around the temperature setpoint.

5.3 Gas Concentration and Temperature Control Performance

The third objective was to characterize the performance of the gas concentration and temperature control schemes, independently and simultaneously.

When testing the gas concentration controller alone for simultaneous control of four distinct NH_3 concentrations (0, 10, 20 and 40 ppm, 4x4 Latin Square, randomly assigned) over a 24 h period, the mean (± standard deviation) NH_3 levels of the compartments were: 1.8 ± 0.8ppm, 10.2 ± 0.5ppm, 20.1 ± 0.8ppm, and 40.5 ± 1.3ppm for setpoint concentrations of 0, 10, 20, and 40ppm, respectively. Approximately 90 min were required for all compartments to be with 5% of their setpoint concentration. All design criteria outlined in the approach were fulfilled.

When testing the expanded temperature controller alone, the maximum temperature rise increased from 5.7±0.5°C to 15.1±0.6°C, with a time constant, τ, of 1.3±0.1 h. The 600W heating capacity achieved 95% of a 1°C and 3°C positive temperature step response in 12.3±2.3 min and 24.0±3.3 min, respectively. This was faster than the 200W heating system, which achieved 95% of a 1°C and 3°C positive temperature step response in 18.0±2.8 min and 51.9±12.8 min, respectively. The maximum setpoint overshoot of the 600W heating system was 1.5±0.4°C and 0.9±0.1°C for 1°C and 3°C, respectively. This increased over the 200W heating system, which showed a 0.4±0.1°C overshoot for the 1°C positive step response and a negligibly small overshoot for the 3°C. The first-order step response time constants, τ, for the 1°C and 3°C negative step responses were 39.0±3.4 min and 26±1.4 min, respectively, when dropping to ambient air conditions.

The discrete On/Off temperature controller did not noticeably impact the performance of the fuzzy logic gas concentration controller when operating simultaneously. Four distinct

ammoniated environments were created while the temperature controller was set to maximum temperature rise. The ammonia concentrations experienced minor perturbations during temperature rise, but the gas concentration controller quickly corrected these. The exhaust fan created noise in the Temp/Rh sensors, affecting the temperature control by dampening any oscillations when achieving a temperature setpoint of 27°C.

5.4 Future Work

The discrete temperature controller could benefit from being transitioned from an on/off controller to a discrete proportional controller. The 600W heating capacity is achieved with two convective coil axial heaters (400W and 200W). In the current control scheme, both axial heaters are turned ON or turned OFF simultaneously. The control software is not programmed to operate only the 400W heater or only the 200W heater. In a discrete proportional control design, the controller could switch ON both axial heaters in order to reach a setpoint temperature quickly and then switch OFF either the 200W or 400W axial heater close to the setpoint temperature as needed to reduce overshoot [Chao et al., 2000]. This would allow the benefit of the quick temperature gain of the 600W heating capacity and the minimal overshoot of the 200W (and 400W) heating capacity.

It is also of interest to simultaneously test the FLC's ability to maintain four distinct gas concentrations while the discrete temperature controller is set to maintain a temperature that is not the maximum possible temperature rise. It was observed during the simultaneous NH_3 and temperature control test that the NH_3 concentration fluctuated slightly as the temperature increased. As the temperature leveled out, the FLC converged

back to its assigned concentration setpoints. This infers some relationship between temperature change and the FLC's performance. Since temperature oscillations were observed in the positive temperature step response tests, it is possible that the FLC's performance could be worsened when a small temperature step change is attempted.

References

Alsam, H., & Wathes, C. M. (1991). Thermal preferences of chicks brooded at different air temperatures. *British Poultry Science, 32*(5), 917-927.

Anderson, N., Strader, R., & Davidson, C. (2003). Airborne reduced nitrogen: Ammonia emissions from agriculture and other sources. *Environment International, 29*(2–3), 277-286.

ASHRAE. (2001). Flow measurement in a duct. *2001 ASHRAE fundamentals handbook (SI)* (pp. 14.7-14.21) American Society of Heating, Refrigeration and Air Conditioning Engineers.

ASHRAE. (2001). Psychrometric Analysis*. 2001 ASHRAE fundamentals handbook (SI)* American Society of Heating, Refrigeration and Air Conditioning Engineers.

ASHRAE. (2001). Reflectance and Emittance of Various Surfaces and Effective Emittances of Air Space. *2001 ASHRAE fundamentals handbook (SI)* American Society of Heating, Refrigeration and Air Conditioning Engineers.

Åström, K. J. (2002). PID control. Control system design: Lecture notes for ME 155A (pp. 216-250). Lund Institute of Technology: Department of Automatic Control.

Belohlavek, R., & Klir, G. J. (2011). Fuzzy logic: A tutorial. Concepts and fuzzy logic (pp. 45-88). Cambridge, Massachusetts: The MIT Press.

Bridges, T. C., & Gates, R. S. (2009). Modeling of animal bioenergetics for environmental management applications. In James A. DeShazer (Ed.), Livestock energetics and thermal environmental management (pp. 151-175). St.Joseph, MI: ASABE.

Bruzzone, O. A., & Corley, J. C. (2011). Which is the best experimental design in animal choice tests? Animal Behaviour, *82*(1), 161-169.

Bubier, N. E. (1996). The behavioural priorities of laying hens: The effect of cost/no cost multi-choice tests on time budgets. *Behavioural Processes, 37*(2–3), 225-238.

Bunton, B., O'Shaughnessy, P., Fitzsimmons, S., Gering, J., Hoff, S., Lyngbye, M., et al. (2007). Monitoring and modeling of emissions from concentrated animal feeding operations: Overview of methods. Environmental Health Perspective, 115(February), 303-307.

Chao, K., R.S. Gates, & N.S. Sigrimis. (2000). Fuzzy logic controller design for staged heating and ventilating systems. Transactions of the American Society of Agricultural Engineers, 43(6), 1885-1894.

Charles, D. R., & Payne, C. G. (1966). The influence of graded levels of atmospheric ammonia on chickens. II. effects on the performance of laying hens. *British Poultry Science, 7*(3), 189-198.

Colina, J. J., Lewis, A. J., & Miller, P. S. (2000). *A review of the ammonia issue and pork production* No. 108)Nebraska Swine Report.

Daskalov, P. I., Arvanitis, K. G., Pasgianos, G. D., & Sigrimis, N. A. (2006). Non-linear adaptive temperature and humidity control in animal buildings. *Biosystems Engineering, 93*(1), 1-24.

Dawkins, M. S. (2006). A user's guide to animal welfare science. *Trends in Ecology & Evolution, 21(2), 77-82.*

Deaton, J. W., Reece, F. N., & Lott, B. D. (1982). Effect of atmospheric ammonia on laying hen performance*. Poultry Science, 61(9), 1815-1817.*

DeShazer, J. A., Hahn, G. L., & Xin, H. (2009). Basic principles of the thermal environment and livestock energetics. In James A. DeShazer (Ed.), *Livestock energetics and thermal environment management (pp. 1-20).* St.Joseph, MI: ASABE.

Drummond, J., Curtis, S., Simon, J., & Norton, H. (1980). Effects of aerial ammonia on growth and health of young-pigs. *Journal of Animal Science, 50*(6), 1085-1091.

Duncan, I. J. H. (1978). The interpretation of preference tests in animal behaviour. *Applied Animal Ethology, 4*(2), 197-200.

Gao, Z., Trautzsch, T. A., & Dawson, J. G. (2000)**.** A stable self-tuning fuzzy logic control system for industrial temperature regulation. *Industry Applications Conference, , 2.* pp. 1232-1240.

Gates, R. S., Chao, K., & Sigrimis, N. (2001). Identifying design parameters for fuzzy control of staged ventilation control systems. *Computers and Electronics in Agriculture, 31*(1), 61-74.

Green, A. R., Wesley, I., Trampel, D. W., & Xin, H. (2009). Air quality and bird health status in three types of commercial egg layer houses . Journal of Applied Poultry Research, (18), 605-621.

Green, A. R., & Xin, H. (2008). Development of a novel environmental preference test *system* for laying hens and its initial application to assess hen aversion to atmospheric ammonia. , 8. pp. 4859-4870.

Heber, A. J., Ni, J. -., Lim, T. T., Tao, P. -., Schmidt, A. M., Koziel, J. A., et al. (2006). Quality assured measurements of animal building emissions: Gas concentrations. Journal of the Air and Waste Management Association, 56(10), 1472-1483.

Hughes, B. O. (1976). Preference decisions of domestic hens for wire or litter floors. *Applied Animal Ethology, 2*(2), 155-165.

Jensen, M. B., & Pedersen, L. J. (2008). Using motivation tests to assess ethological needs and preferences. *Applied Animal Behaviour Science, 113*(4), 340-356.

Jones, E. K. M., Wathes, C. M., & Webster, A. J. F. (2005). Avoidance of atmospheric ammonia by domestic fowl and the effect of early experience. *Applied Animal Behaviour Science, 90*(3-4), 293-308.

Jones, J. B., Burgess, L. R., Webster, A. J. F., & Wathes, C. M. (1996). Behavioural responses of pigs to atmospheric ammonia in a chronic choice test. *Animal Science, 63*(3), 437-445.

Kirkden, R. D., & Pajor, E. A. (2006). Using preference, motivation and aversion tests to ask scientific questions about animals' feelings. *Applied Animal Behaviour Science, 100*(1–2), 29-47.

Kolokotsa, D., Pouliezos, A., Stavrakakis, G., & Lazos, C. (2009). Predictive control techniques for energy and indoor environmental quality management in buildings. *Building and Environment, 44*(9), 1850-1863.

Kristensen, H. H., Burgess, L. R., Demmers, T. G. H., & Wathes, C. M. (2000). The preferences of laying hens for different concentrations of atmospheric ammonia. *Applied Animal Behaviour Science, 68*(4), 307-318.

Lindberg, A. C., & Nicol, C. J. (1996). Effects of social and environmental familiarity on group preferences and spacing behaviour in laying hens. *Applied Animal Behaviour Science, 49*(2), 109-123.

Lute, P., & Paassen, D. v. (Aug, 1995). Optimal indoor temperature control using a predictor. *Ieeecss,*

Mattson, J. (2011). *Swirling pipe flow laboratory*. Oral Roberts University:

McQuiston, F. C., Parker, J. D., & Spitler, J. D. (2005). In Hayton J., Vargas V. A., Power J., Kulesa T. and Nolan H. (Eds.), *Heating, ventilationg, and air conditioning analysis and design* (6th ed.). Danvers, MA: John Wiley & Sons, Inc.

Mitroy, J. (2009). *Laminar and turblent flows in pipes - lecture*. Charles Darwin University:

Ni, J., & Heber, A. J. (2001). Sampling and measurement of ammonia concentration at animal facilities – A review. , *ASAE Annual International Meeting.* (Paper Number: 01-4090)

Nicol, C. J. (1986). Non-exclusive spatial preference in the laying hen. *Applied Animal Behaviour Science,* (15), 337-350.

NIOSH. (2011). *NIOSH pocket guide to chemical hazards: Ammonia*National Institute for Occupational Safety and Healthy.

Petriu (2001), E. M. *Fuzzy systems for control applications - sensing and modeling research laboratory* University of Ottawa - School of Information Technology.

Popescu, S., Stefan, R., Borda, C., Lazar, E. A., Sandru, C. D., & Spinu, M. (2010). The ammonia concentration in growing-finishing pig houses . *Lucrări Ştiinłifice Medicină Veterinară, XLIII*, 320-326.

Sales, G. T. (2012). *An investigation of laying hen interactions with ammoniated environments by means of preference testing* (PhD Disseration. University of Illinois at Urbana-Champaign: Department of Agricultural and Biological Engineering.

Sales, G. T., Green, A. R., & Gates, R. S. (2013). Commissioning results of an environmentally controlled animal preference chamber for testing behavioral responses to atmospheric ammonia. *Computers and Electronics in Agriculture, In press.*

Soyguder, S., Karakose, M., & Alli, H. (2009). Design and simulation of self-tuning PID-type fuzzy adaptive control for an expert HVAC system. *Expert Systems with Applications, 36*(3, Part 1), 4566-4573.

UEP. (2010). *Animal husbandry guidelines for US egg laying flocks*United Egg Producers.

Wathes, C. M., Jones, J. B., Kristensen, H. H., Jones, E. K. M., & Webster, A. J. F. (2002). Aversion of pigs and domestic fowl to atmospheric ammonia. *Transactions of the American Society of Agricultural Engineers, 45*(5), 1605-1610.

Wescott, T. (2000, PID without a PHD. *EE Times-India,* , 1-7.

Zhang, Y., & Barber, E. M. (1995). An evaluation of heating and ventilation control strategies for livestock buildings. *Journal of Agricultural Engineering Research, 60*(4), 217-225.

Zhang, Y. (1995). Air quality in production animal facilities: Updates and research needs. *Indoor and Built Environment, 4*(2), 80-86.

Zhong, J. (2006). *PID controller tuning: A short tutorial*. Department of Mechanical Enginering: Purdue University.

APPENDIX A: System Component Redesigns

A.1 Redesign of the Fan Circuit

The electrical circuit powering the EPC's ventilation supply fans was redesigned to maintain proper operations. The original circuit design implemented a 12V power supply wired through a PC-Controlled Electro-Mechanical Relay Board *(USB-ERB24, Measurement Computing, Norton, MA, USA)*, a group of resistors designed to limit the fan's power, and then directly to the inductive load of the fan itself *(12V, 3.3A, Delta Electronics, Inc., Bangwua, Thailand)* (Figure A.1). When a new ventilation rate would be desired, the relay board would complete the circuit to a different set of resistors to alter the fan's supply voltage. The fan ran at a maximum rated current of 3.3A but could occasionally experience even greater surges of current upon the switching of relays. The relay board was rated for up to 8A of current, but may not have been designed to handle the quantity of current surges. Whenever a relay switched, the high amperage of the supply fans would create a spark between the relay contacts. After several months of operating the EPC (and thus hundreds of relay switches) one of the relay channels welded together, creating a permanent closed loop. In order to prevent future damage and to maintain reliable ventilation, a new circuit design was implemented.

The new circuit was designed to bypass the high fan current around the electro-mechanical relay. This was accomplished by introducing sets of 30A power relays (G8PT Power PCB Relay, Omron Corporation) in series with the relay contacts on the electro-mechanical relay board. When the PC would command a new fan speed, the relay board would complete the circuit to the 127Ω power relay coil, closing a circuit leading directly from the power

supply to the resistors and supply fan. A diode was also placed in parallel with the inductive load of the fan, opposing the direction of flow. This was implemented to bypass any current backflow that occurs when the power is switched on and off (Figure A.2).

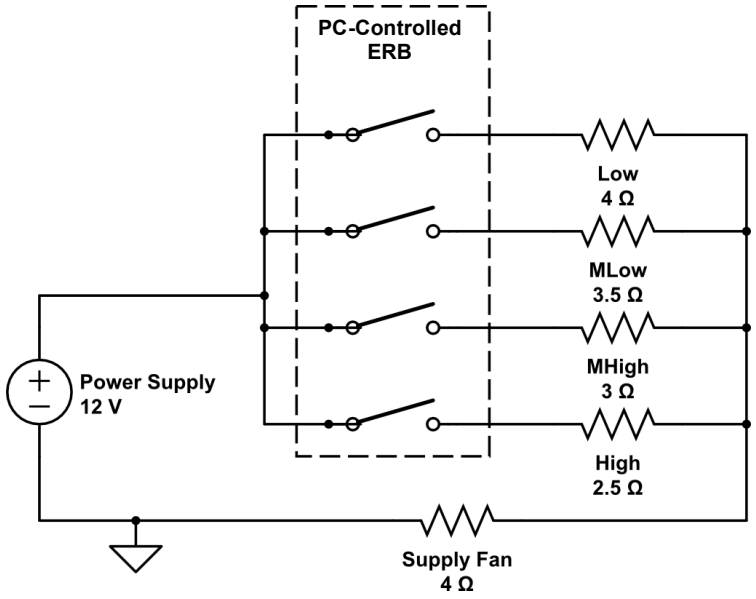

Figure A.1: Original circuit design for a single supply fan to an EPC compartment. The four fan stages (Low, Medium-Low, Medium-High, and High) are implemented by adjusting the Supply Fan's voltage using resistors of varying resistance. Fan stages are triggered by the PC-Controlled Electronic Relay Board (ERB). Fan power runs directly through the PC-Controlled ERB, sometimes causing relay contacts to weld together.

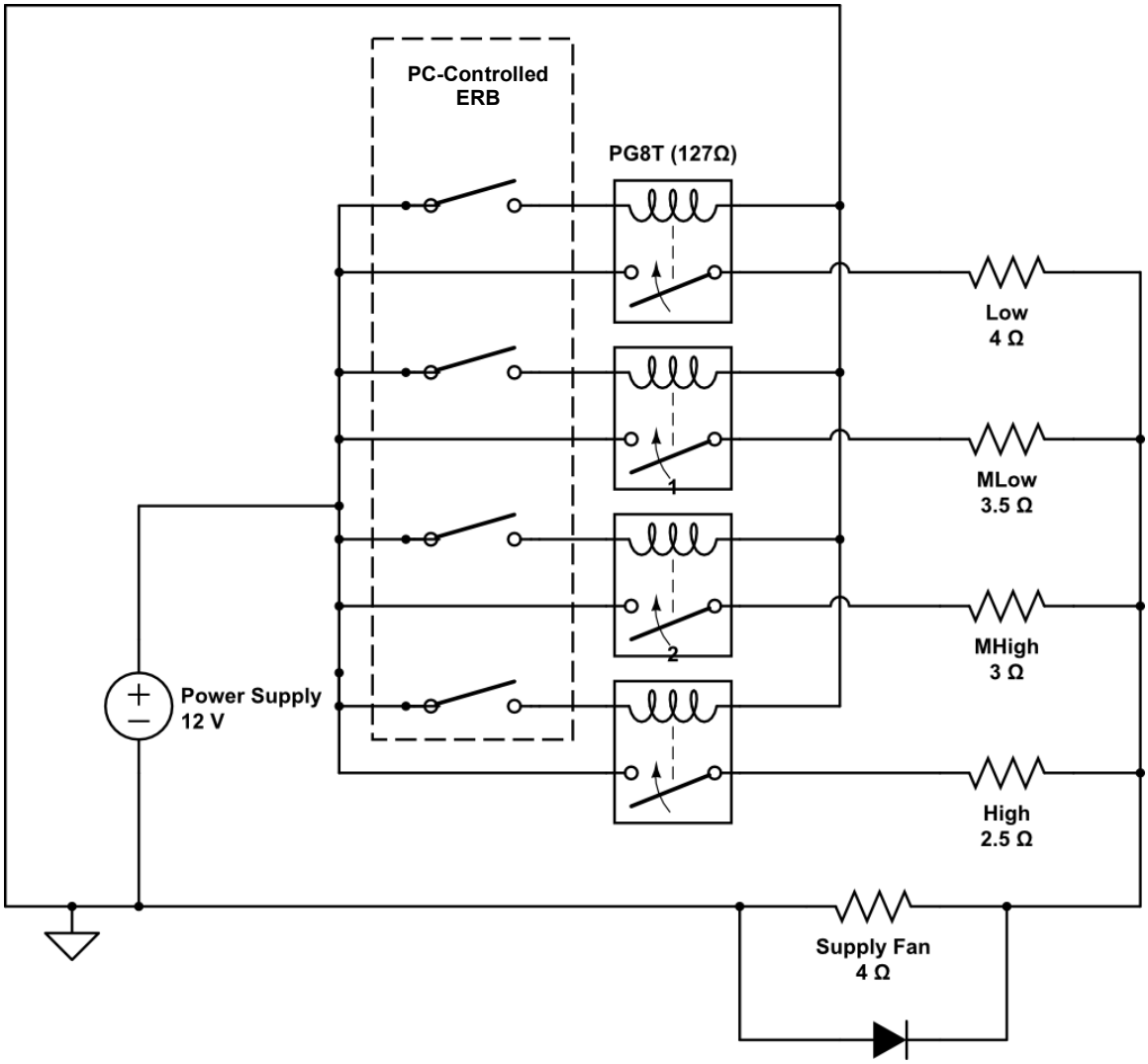

Figure A.2: New circuit design for a single supply fan to an EPC compartment.
The four fan stages (Low, Medium-Low, Medium-High, and High) are implemented by adjusting the Supply Fan's voltage using resistors of varying resistance. Fan stages are triggered by the 30A Power Relays (PG8T), which are directly controlled by the PC-Controlled Electronic Relay Board (ERB). Fan power bypasses the PC-Controlled ERB. A diode is installed around the supply fan to prevent current backflow.

A.2 Redesign of Axial Heater Circuit

The electrical circuit powering the axial heaters for each compartment required a redesign to handle the expanded heating load. The original circuit design connected 120 V_{AC} directly through the electro-mechanical relay board to a 200W convective coil axial heater *(200W, 120V, Farnam Custom Products, Arden, NC, USA)* in each compartment's ventilation shaft (Figure A.3). The control software operated the relay switches using the discrete ON/OFF control scheme to complete the circuit to any the four axial heaters as needed. This control scheme was sufficient for the original EPC design, requiring only 1.7A at 120V_{AC} to travel through the relay board rated for 6A at 120V_{AC}. The new heating load required an additional 400W convective coil axial heater to be placed in series with the previous 200W heater, tripling the amperage. The resultant current (5.1A) was within the relay board's performance rating but a new circuit design was preferred for safety. This new design split the original circuit in two. The relay board triggered a signal to close an added 30A power relay, which completed the circuit between the 120V_{AC} and the two axial heaters (Figure A.4).

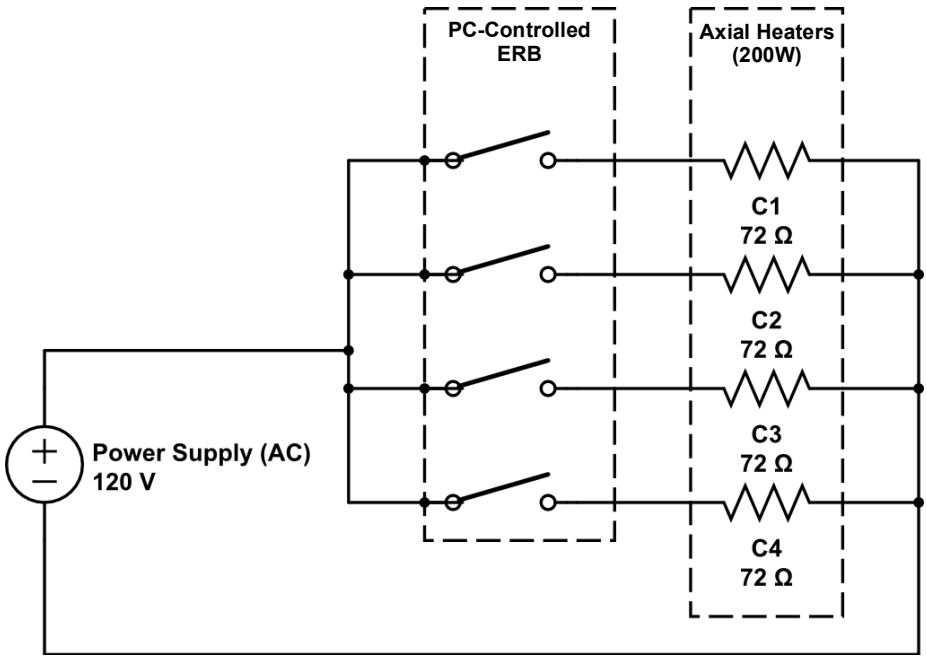

Figure A.3: Original circuit design for the 200W axial heaters for all compartment.
The PC-Controlled Electronic Relay Board (ERB) completes the circuit, allowing $120V_{AC}$ to travel to any of the four 200W convective coil axial heaters, one for each compartment (C1, C2, C3, C4).

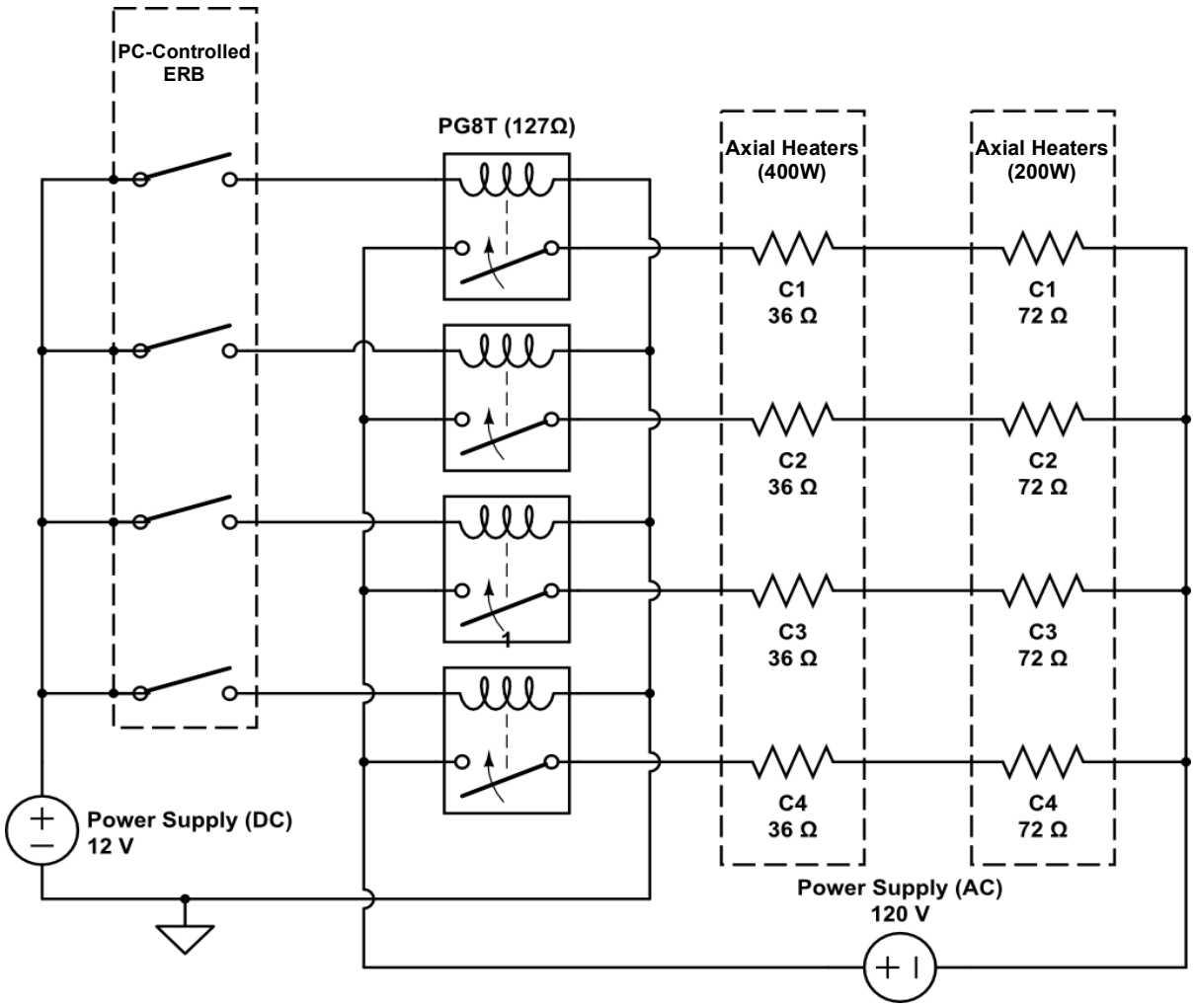

Figure A.4: New circuit design for the 200W and 400W axial heaters for all compartments. The PC-Controlled Electronic Relay Board (ERB) triggers any of four 30A Power Relays (PG8T). These power relays complete a second circuit, allowing $120V_{AC}$ to run through a 400W and 200W convective coil axial heater placed in series. There are four sets of axial heaters, one for each compartment (C1, C2, C3, C4). Axial Heater power bypasses the PC-Controlled ERB

APPENDIX B: Analysis of Environmental Preference Chamber Ventilation System

B.1 Introduction

In order to design new equipment and controllers for the EPC's environmental control, a thorough understanding of the ventilation was needed. This required quantifying the volumetric flow rate of the air and understanding mechanics of its flow in the ventilation system. This analysis was an exploration of the EPC's ventilation system with goals to understand how much air is flowing through the system and why the air flows the way it does. In this chapter, the airflow within the ventilation system of the EPC was characterized. Velocity profiles of the ventilation pipe flow were created by point measurements from a hot-wire anemometer. Analysis was completed to assess how velocity profiles developed along each pipe length, if they were radially symmetrical, and how they differed between pipes.

B.2 Theory

Flow development in a pipe is often characterized by the convergence of the flow boundary layer. When the flow enters through the pipe opening, a boundary layer begins to develop from the outer radius at a rate proportional Equation B.1

$$\delta(x) \sim \sqrt{\frac{\nu x}{U}} \quad \text{(B.1)}$$

Where,

δ = height of the boundary layer

ν = kinematic viscosity

x = distance from the boundary layer origin

U = planar velocity of the fluid

The boundary layer will expand inwards from the outer perimeter of the pipe until converging at the centerline. The flow within the boundary layer, closer to the pipe wall, is considered *developed* and the flow not yet within the boundary layer, closer to the centerline, is considered *undeveloped*. As fluid flows down the pipe, the boundary layer continues growing until the entirety of the flow is developed.

When pipe flow is undeveloped, the flow is turbulent and its velocity profile usually appears to have a flatted "plateau" shape. Within this turbulent region, viscous effects of the flow are negligible. In the developed regions, the flow is laminar and the velocity profile becomes more and more parabolic. This pattern is illustrated in Figure B.1, as provided by Mitroy, 2009.

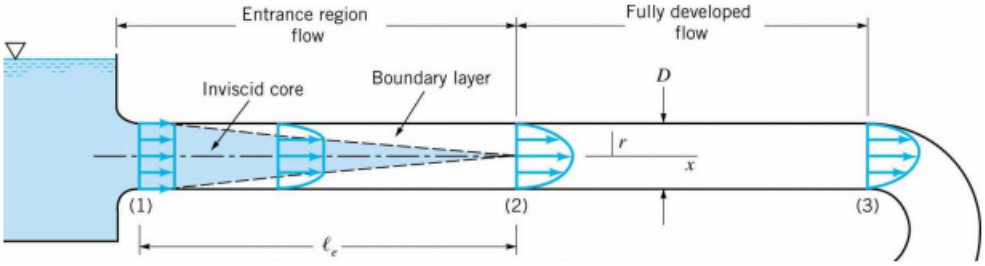

Figure B.1: Development of fluid flow in a pipe [Mitroy, 2009].
The airflow develops through a pipe as the radial boundary layer converges to the pipe centerline.

The characterization of a pipe flow as either laminar or turbulent may be quantified using the non-dimensional Reynolds Number, calculated in Equation B.2.

$$Re = \frac{\rho v D}{\mu} \tag{B.2}$$

Where,

ρ = fluid density

v = fluid velocity

D = diameter of the pipe

μ = dynamic viscosity

In SI units:

The flow is considered LAMINAR for Re < 2000.

The flow is considered TRANSITIONAL between 2000 < Re < 4000.

The flow is considered TURBULENT for Re > 4000.

These limits are considered "soft" guidelines as the actual values for flow transition vary depending on the shape of the pipe, surface roughness and the shape of the pipe inlet [Mitroy, 2009]. Under carefully controlled conditions, some researchers have been able to maintain laminar flow at much higher Reynolds numbers, even up to 100,000 [Mattson, 2011]. However, in this analysis only the previously defined range will be considered.

Mitroy describes the *entrance length* of a flow as the distance from the pipe opening where the flow fully develops. Past this length, the flow would be laminar. Entrance length is calculated in Equation B.3.

$$l_e = 0.06 * Re * D \quad \text{(B.3)}$$

B.3 Objectives

In this analysis, four goals were addressed:

(1) Visualize the development of the airflow along a single pipe

(2) Check for radial symmetry of airflow

(3) Compare the velocity profiles between the EPC's four ventilation pipes

(4) Solve for each pipe's ventilation rate.

B.4 Methodology

The EPC's ventilation system consists of four PVC pipes, 3" Diameter, one for each compartment. The pipes begin at a common "mixing box" where they extend 6-10 feet before turning at a 30° elbow and entering the animal housing compartments. A supply fan *(12V, 3.3A, Delta Electronics, Inc., Bangwua, Thailand)* located at the head of each compartment pulls air inwards through the pipes. The fan is equipped with an air-straightening grid to reduce torsional effects due to the swirling nature of the fan. A pictures and schematic of this setup are visible in Figures B.2 and B.3, respectively.

Figure B.2: Environmental Preference Chamber Ventilation System.
Four 3" Inner Diameter PVC pipes carry the supply air to each of the four animal housing compartments.

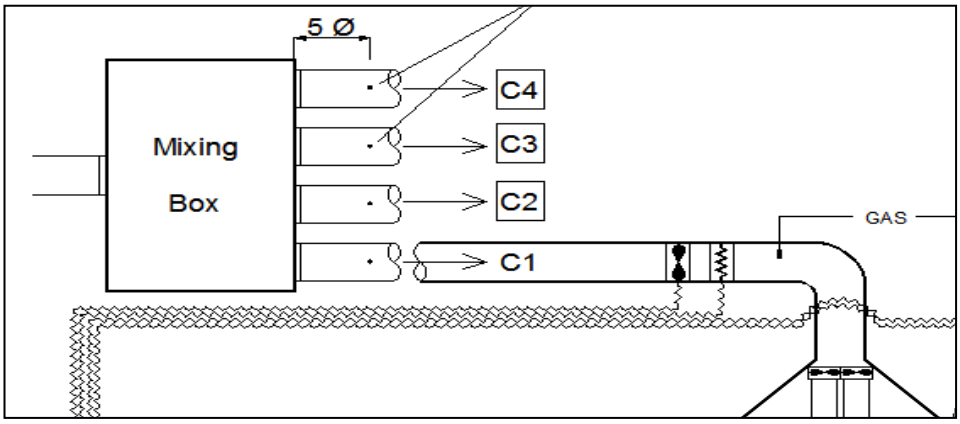

Figure B.3: 2-D Schematic of a Ventilation Pipe provided by Sales [2013].
A supply fan is located near the cap of the compartment and pulls in air from the common mixing box.

The mixing box is implemented to minimize any differences in the supply air between each compartment. Air enters each ventilation pipe through a plexiglass orifice plate. The shapes of each opening of the orifice plate are all slightly different. Two are single, circular openings and two are "dotted", more resistive openings. These were created in a previous experiment to compensate for differences in fan power, pipe friction, and air leakage between each compartment of the system, with the intent of normalizing air flow rate. The orifice plate is visible in Figure B.4.

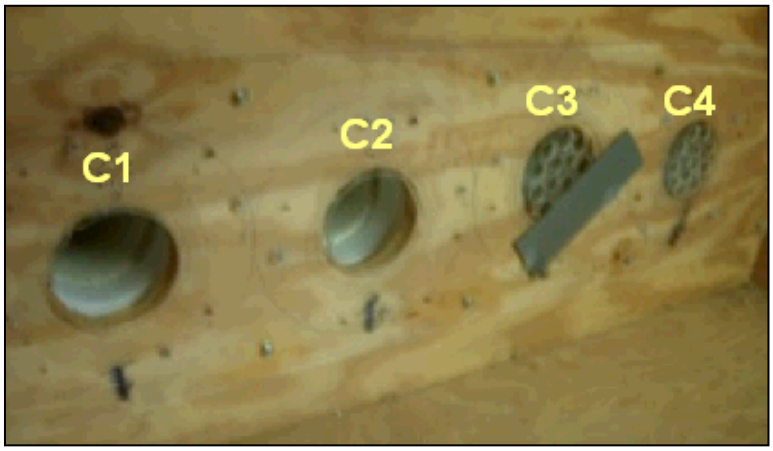

Figure B.4: Opening orifices to each ventilation pipe.
Different orifices were created in previous experiments to equalize volumetric airflow between the four ventilation pipes.

Creating velocity profiles required making point measurements of velocity. This was performed with a commercially available hot-wire anemometer (VelociCalc Air Velocity Meter 9515). A hot-wire anemometer was chosen for this experiment due to its: (1) simple, single-point application, (2) quick response time and (3) wide measurement range (some ranging up to 300 m/s). Due to the physical sensitivity of the sensor, recalibration is required on a regular basis.

There was no previously known calibration curve available for the anemometer used in this experiment. Because of this, the anemometer was first calibrated using a wind tunnel (Model 8390 Bench Top Wind Tunnel, TSI). Calibration was ensured for velocities between 300-1500fpm. The maximum velocity in the EPC ventilation pipes was expected to be near 900fpm. A picture of the calibration setup is visible in Figure B.5.

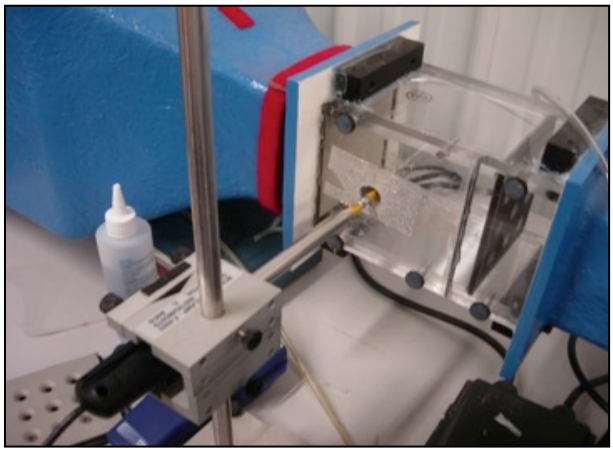

Figure B.5: Calibration of the hot-wire anemometer in a wind tunnel.
A calibration curve was created to compare the readings of the anemometer with the known air velocity produced in the wind tunnel.

The American Society of Heating, Refrigeration and Air Conditioning Engineers (ASHRAE) has a defined standard for measuring average velocity in a pipe or duct with a point-measurement device. This standard was adapted for this experiment. They recommend using the "Log-Linear" Rule for circular ducts, where 6, 8 or 10 point-measurements should be made at specific distances from the pipe wall along a traverse of the pipe diameter. These measurements should be made along three axes, but two axes of measurement are allowed when access to the pipe is limited. The locations of these points are derived experimentally, taking into account factors such as geometry, friction and reduction of velocity at wall surfaces, such that simply taking the average of the measurements will approximate the duct's average velocity [ASHRAE, 2001]. The points of measurement for the "Log-Linear" Rule may be seen in Figure B.6.

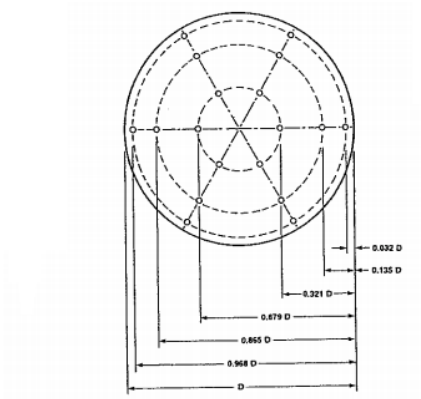

No. of Measuring Points per Diameter	Position Relative to Inner Wall
6	0.032, 0.135, 0.321, 0.679, 0.865, 0.968
8	0.021, 0.117, 0.184, 0.345, 0.655, 0.816, 0.883, 0.981
10	0.019, 0.077, 0.153, 0.217, 0.361, 0.639, 0.783, 0.847, 0.923, 0.981

Log-linear rule for circular ducts

Figure B.6: "Log-Linear" points of measurement across a ventilation pipe.
Air velocity measurements are made at six points along three different axes of a ventilation pipe. The average of these velocity measurements can be considered equivalent to the pipe's net average air velocity. Diagram produced by ASHRAE [2001].

Measurements in this experiment were taken similarly to the "Log-Linear" method. Six point measurements were taken across the 3" diameter ventilation pipes (at 0.35", 0.85", 1.35", 1.65", 2.15", and 2.65" respectively). These point measurements were taken three times each to compensate for fluctuations due to turbulence. The velocities at the pipe walls were considered to be 0 feet-per-minute, using the assumption of no-slip. These observed distances were chosen for ease of measurement. Distance references were marked on the anemometer probe as seen in Figure B.7.

Figure B.7: Pre-labeled distances on hot-wire anemometer probe.
A velocity profile could be quickly constructed by recording the velocity measured inside the pipe at each pre-labeled distance.

To observe the development of the airflow along a single pipe, five 5/8" holes were drilled into one of the PVC ventilation pipes at distances of 7.5", 15", 22.5", 30" and 45" (2.5D, 5D. 7.5D, 10D and 15D, respectively) from the opening orifice. The six point measurements were made at each distance, each three times. All measurements were made across the same pipe axis. The ventilation pipe leading to compartment 4 was used in this stage of analysis, seen in Figure B.8.

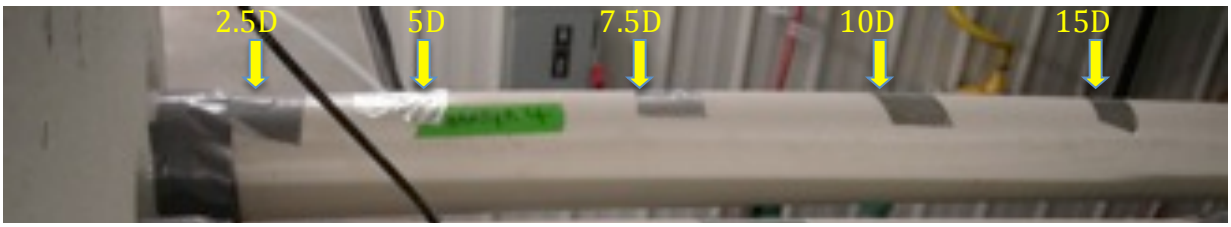

Figure B.8: First 15D of the analyzed ventilation pipe.
Holes were drilled at 2.5D, 5.0D, 7.5D, 10.0D and 15D away from the pipe opening.

To check for radial symmetry in the airflow, an additional 5/8" hole was drilled into the same PVC ventilation pipe at 15D from the opening orifice, at the axis perpendicular to the previous hole. The six point measurements were made through this hole, each three times.

To compare the velocity profiles of all four ventilation pipes, an additional 5/8" hole was drilled into each of the other three PVC ventilation pipes at 15D from the opening orifice, on the same axis as the initial set of holes (Objective 1). The six point measurements were made through each hole, three times. The length scales of these profiles were plotted around the centerline of the pipe as opposed to originating from the pipe wall and each velocity profile was fit to a sixth-order polynomial. This was to simplify volumetric flow rate calculations later in the study.

Every velocity profile location in this analysis is observed in Figure B.9.

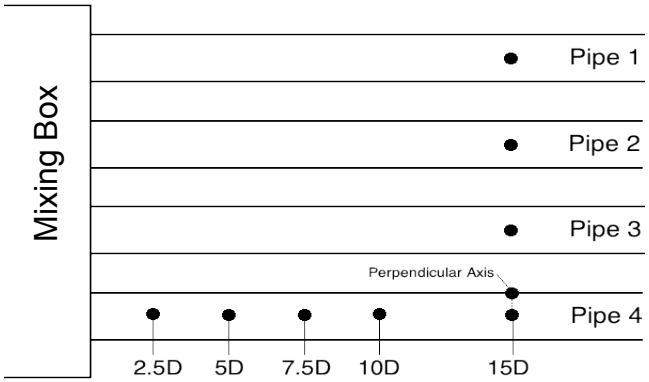

Figure B.9: Schematic of measurement locations of ventilation pipes.
A velocity profile was created at each measurement location. Five measurement locations were used along Pipe 4 to observe the velocity profile development. A perpendicular measurement was made on Pipe 4 at 15D from the opening to check for radial symmetry. Measurements were made at 15D from the opening in all pipes to compare airflow.

B.5 Results

1) Visualize the development of the airflow along a single pipe

The velocity profiles along the length of one ventilation pipe are demonstrated in Figure B.10.

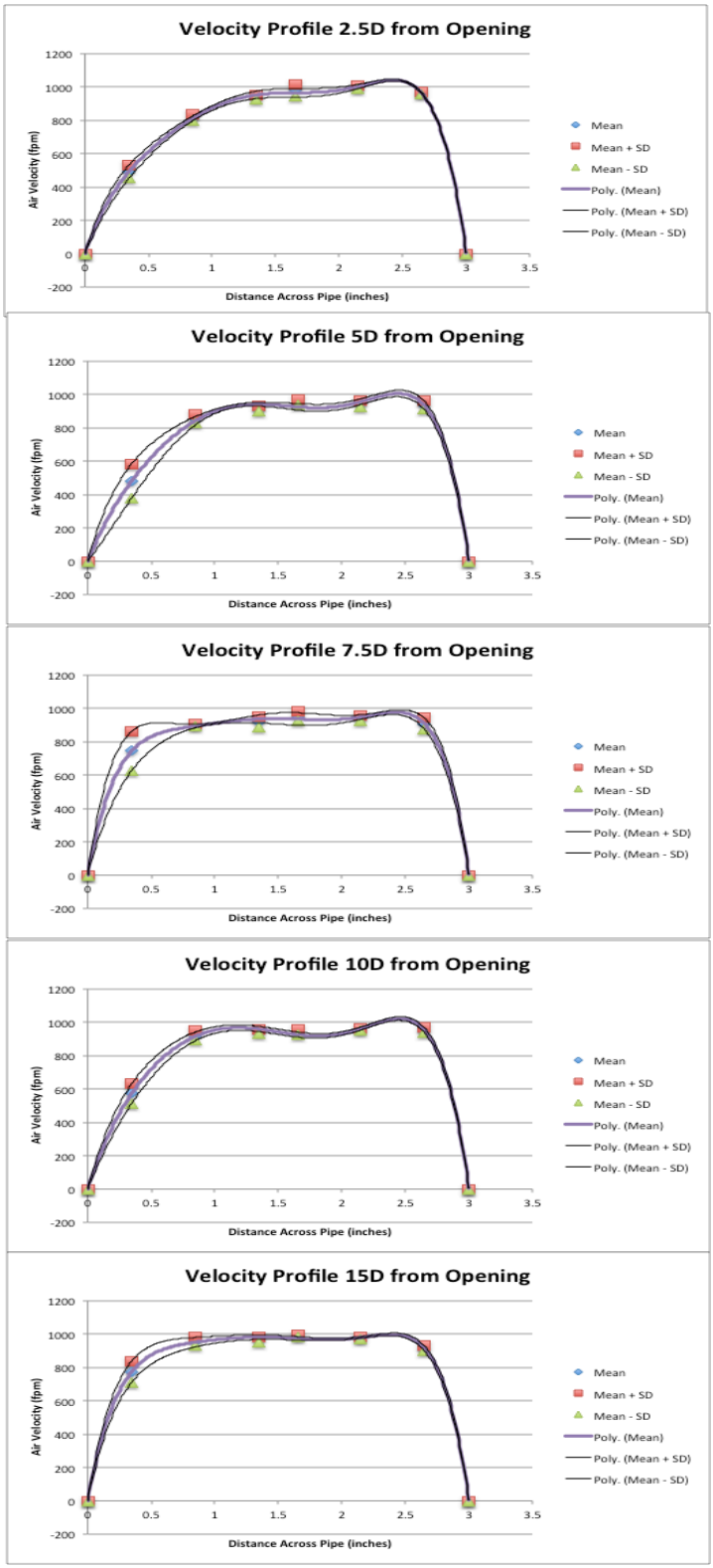

Figures B.10: Development of a velocity profile along a single ventilation pipe.
The velocity profile appeared to gain symmetry along the pipe length, but very little flow development was observed.

The purple polynomial trend-line characterized the mean velocity reading in each profile. The thin black trend-lines characterized the standard deviation of the measurements in each profile. Wider gaps around the mean line indicated a larger standard deviation, which correlates to greater inconsistency in the flow at that point.

The flow appeared to "stabilize" as it traveled away from the opening orifice but never fully developed. The opening orifice was most likely to blame for the oblong profile shape found at 2.5 diameters. The profile's "flat" shape indicated that a majority of the flow may still be turbulent at 15 diameters.

2) Check for radial symmetry of airflow

The resulting velocity profile at 15D measured on a perpendicular axis is visible in Figure B.11.

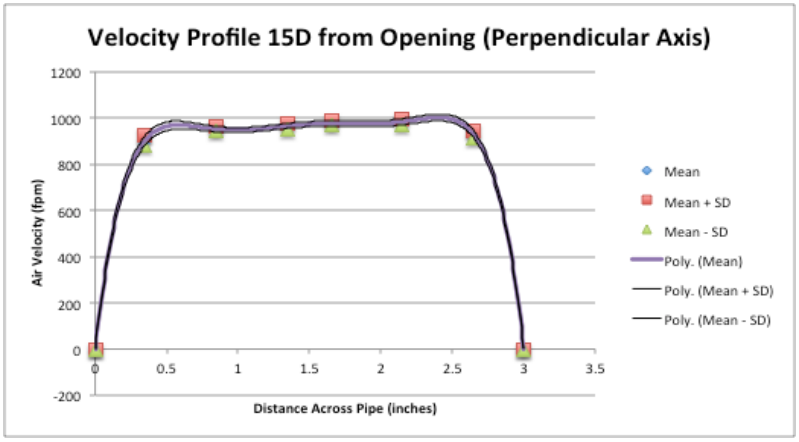

Figure B.11: Velocity profile in the perpendicular axis at 15D from the pipe opening. Minimal profile shape difference is observed when compared to the 15D velocity profile in Figure B.10. This allows the assumption that the pipe airflow may be assumed radially symmetric.

The two-axis measurement provided a check for radial consistency. Little difference was observed between the shape of the velocity profiles on the X or Y axes. This observation allowed the assumption of radial symmetry in the airflow.

3) Comparison of velocity profiles between the EPC's four ventilation pipes

The resulting velocity profiles measured at 15D from the opening of all four pipes are visible in Figures B.12.

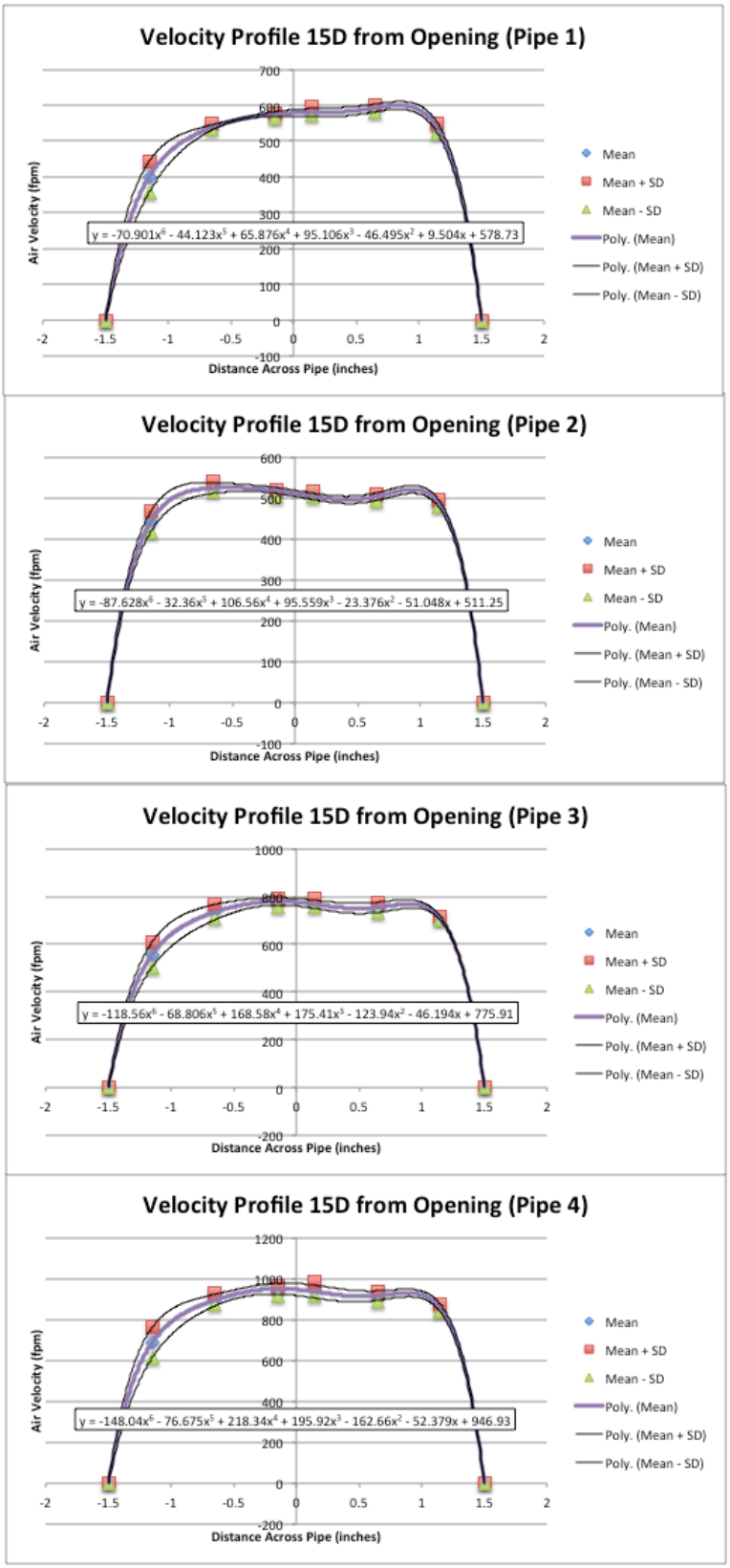

Figures B.12: Velocity profiles at 15D for each of the four ventilation pipes. Sixth-order polynomials were fit to the velocity profile data

Different magnitudes of air velocity were observed between the compartments, ranging from 500fpm to 1000fpm (discussed in section A.5). This was expected to be due to the differences in the opening orifice geometries, pipe geometries and possibly the fan speeds. It is clearly evident in Figure 4 that flow was restricted to pipes 3 and 4 in comparison to pipes 1 and 2. Through this testing it became apparent that the original logic behind creating the different opening orifices (to equalize ventilation rate) was ill informed or the flowrates changed over time. This difference in velocity magnitude was noted for future studies.

Regardless of the difference in velocity magnitudes, all four of the velocity profiles had very similar shapes. By normalizing each velocity profile such that centerline velocity was "1" and then superimposing them on top of one another, their similarity is visualized in Figure B.13.

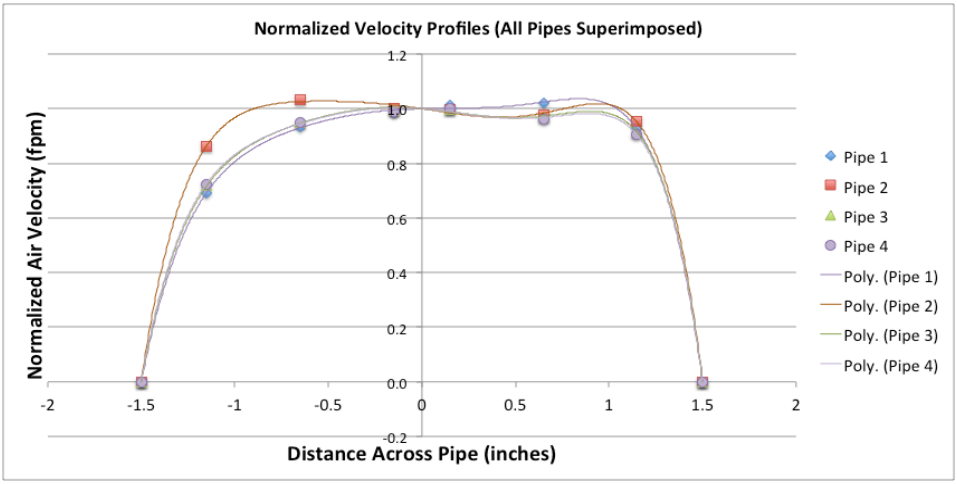

Figure B.13: Normalized velocity profiles for all ventilation pipes.
The velocity profiles at 15D into each pipe were normalized such that their centerline velocity would equal "1". All four profiles were superimposed on top of one another.

The normalized profiles of Pipes 1, 3 and 4 had nearly identical structures. The similarity between profiles was most likely due to the fact that 15D from the opening is not far enough to notice any significant boundary layer development for any of the flows. The velocity profile should develop nearer the pipe entrance for slower flows, since boundary layer development is inversely proportional to fluid velocity. The pipe velocities differed by up to a factor of 2, which implies the boundary layers will develop at different distances along the pipe. This means that velocity is not arbitrary in velocity profile development.

By making a quick calculation of the Reynolds number, the entrance length required for a fully developed boundary layer in Pipe 4, l_e, was calculated as:

$$Re = \frac{\rho v D}{\mu}$$

$$Re = \frac{(0.075192\frac{lbf}{ft^3})(14.56\frac{ft}{s})(0.25ft)}{(3.5 * 10^{-7}\ \frac{lbm - s}{ft^2})}$$

$$\underline{Re = \ 24306\ (Turbulent)}$$

$$l_e = 0.06 * Re * D$$

$$l_e = 0.06 * 24306 * 0.25ft$$

$$\underline{l_e = 365ft}$$

where, the values for air density, ρ, and kinematic viscosity, μ, assume standard atmospheric conditions and are denoted in IP units. The air velocity is centerline velocity

measured in Pipe 4 at 15D from the opening. Though this value appears very large, it is consistent with the experimental results. An entrance length of 365 feet is far longer than the 5ft (15D) of pipe length used in this analysis. This implies that velocity profiles at 15D are all turbulent and similarities in their shapes are not significant.

4) Solve for each pipe's ventilation rate

For the velocity profile at 15D for each pipe, a least squares fit 6th order polynomial trend-line was fit to the mean velocity data. Symmetry was imposed around the pipe centerline on each of these 6th order polynomials by dropping the odd terms. The ventilation rate was then calculated by integrating the velocity profile around the pipe flow. A sample calculation for flow in Pipe 4 is provided:

The least squares fit 6th order polynomial trend-line of velocity (fpm) for C1 was:

$$u_1(x) = -70.90x^6 - 44.12x^5 + 65.88x^4 + 95.11x^3 - 46.50x^2 - 9.50x + 578.73$$

Impose symmetry around the pipe centerline by dropping the odd terms:

$$u_1(x) = -70.90x^6 + 65.88x^4 - 46.50x^2 + 578.73$$

Integrate around the pipe area:

$$V_1 = \int_0^{2\pi} \int_0^r (u_1(x) * x) dx d\theta$$

$$V_1 = \int_0^{2\pi} \int_0^r \left((-70.90x^6 + 65.88x^4 - 46.50x^2 + 578.73) * x\right) dx\, d\theta$$

where, r = 0.125ft

$$\underline{V_1 = 21.4\ cfm}$$

Using the same procedure, the ventilation rates of the other three compartments were found:

$\underline{V_2 = 20.4\ cfm}$

$\underline{V_3 = 28.6\ cfm}$

$\underline{V_4 = 34.9\ cfm}$

These values were equated from the mean velocities profiles. They did not take into account measurement error or instrument accuracy and precision. Also, since symmetry was assumed, any asymmetric effects in the velocity profile were omitted.

By quantifying the ventilation rate, it was now possible to better understand atmospheric differences between compartments and size equipment for future studies. For example, by knowing the volumetric flow rates it would be possible to calculate mass flow rate, pressure differentials and pollutant concentration production within the EPC. This information would be very useful when trying to maintain a fresh-air environment in compartment adjacent to two ammoniated environments. If such a compartment was prone to having lower airflow, polluted air from the adjacent compartments would infiltrate and contaminate the fresh-air environment.

B.6 Conclusions

1) The air "stabilized" within the ventilation pipe but flow never fully developed. It remained turbulent along 15D of pipe.
2) The flow showed radial symmetry when velocity profiles were constructed across two perpendicular axes.
3) Velocity profiles in each pipe showed similar geometries but different velocity magnitudes.
4) Ventilation rates were successfully calculated by integrating over the pipe area. These rates differed between compartments by up to 70%. This may have been due to resistance caused by the orifice plates and decreased performance of some of the supply fans.

APPENDIX C: Environmental Preference Chamber Thermal Model

C.1 Introduction

A thermal analysis was performed on the EPC to better understand heat exchange for the chamber with the surrounding environment. These heat losses were considered through each compartment stainless steel structure. Analysis considered: 1) heat loss "problem areas" with a thermal imaging camera, and 2) a model to calculate the heat loads required to maintain a desired steady-state dry-bulb temperature and humidity.

The need for this information became evident after testing the maximum temperature gain of the EPC's original design. The original design implemented a 200W axial heater and could maintain a maximum temperature gain of 5°C at steady-state. By observation, this temperature gain was lower than expected and inferred significant heat losses to the environment. Analyzing the EPC as a thermal system could help identify how this heat was lost, how to possibly mitigate these losses, and understand additional heating required to compensate for these losses.

C.2 Heat Loss/Gain Analysis

Air flows through the axial heater immediately before entering the cap at the top of each EPC compartment, as seen in Figure C.1. At this point in the flow, the heated air has not touched any of the envelope surfaces and has thus experienced minimal heat loss via conduction, convection or radiation. Consequently, when the airflow reaches the cap

surface the air should be at its local maximum temperature and thus experience heightened conductive heat loss in comparison to other locations in the EPC. The high air velocity in the cap could also contribute greater heat loss as more heated air is available to replace the cooled air near the surface.

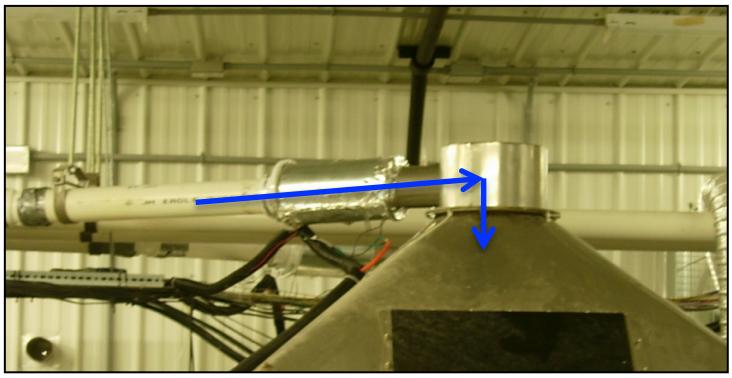

Figure C.1: Cap section of EPC Compartment.
The blue lines denote the direction of airflow. The air supply fan and axial heater are located inside the cylindrical shaft preceding the compartment cap.

After flowing through the cap, air immediately travels into the main compartment. A pair of mixing fans near the top of the compartment pushes air through two tubes to a pair of air diffusers, fabricated from acrylic with an array of holes, that evenly distributed the newly supplied air over the occupant test area. After leaving the air diffusers, the supply air is free to mix inside the compartment but eventually escapes through the exhaust port at the bottom of the compartment due to the imposed pressure gradient. A schematic of this construction is seen in Figure C.2. The temperature measured inside the compartment was much lower than the initial temperature of the heated air. The majority of the conductive/convective heat loss is assumed to take place through the compartment structure due to its large surface area.

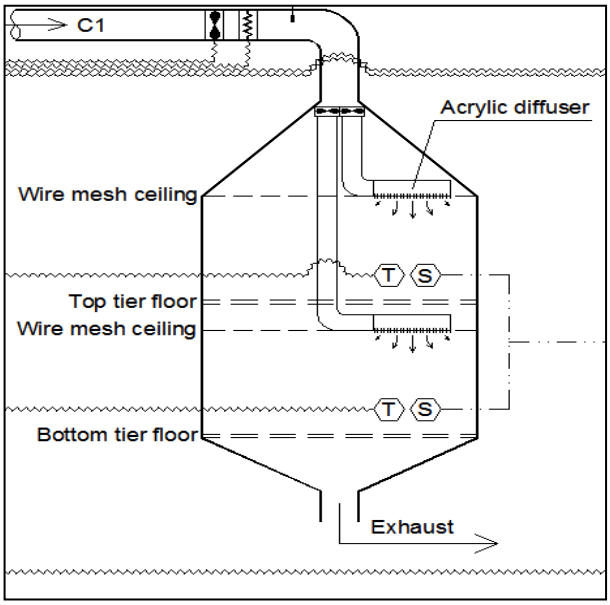

Figure C.2: Schematic of EPC compartment body.
Mixing fans push the supply air through hoses where it is then diffused to each tier. Heat is progressively lost through the surface envelope until the air is eventually exhausted out the bottom of the compartment.

Thermal images of the EPC were taken to visualize the relative heat losses of the cap and compartment. Each compartment received a constant 200W heating load and reached steady-state thermal conditions before the thermal images were taken. At steady-state, the cap and upper-half of the compartment had a surface temperature roughly 8°C greater than the surrounding environment. It was observed that the lower half of the compartment had a surface temperature roughly 2-3°C greater than the surrounding environment. Specific hot spots such as the cap flange and the supply gas orifice, seen as the hot white surfaces in the thermal image, had a surface temperature roughly 11°C greater than the surrounding environment. Thermal images are displayed in Figures C.3 and C.4.

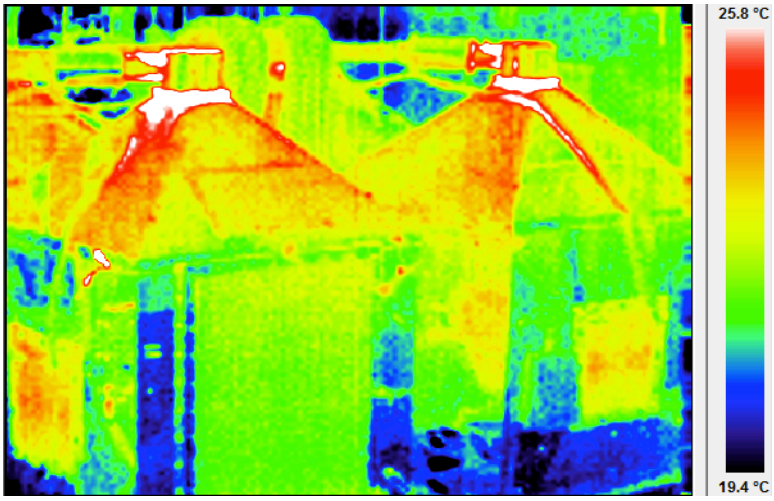

Figure C.3: Thermal Image of EPC compartment surfaces.

Each compartment attained steady-state conditions with a 200W heating load. The compartment surface temperature was highest near the cap and gradually decreased down the compartment body.

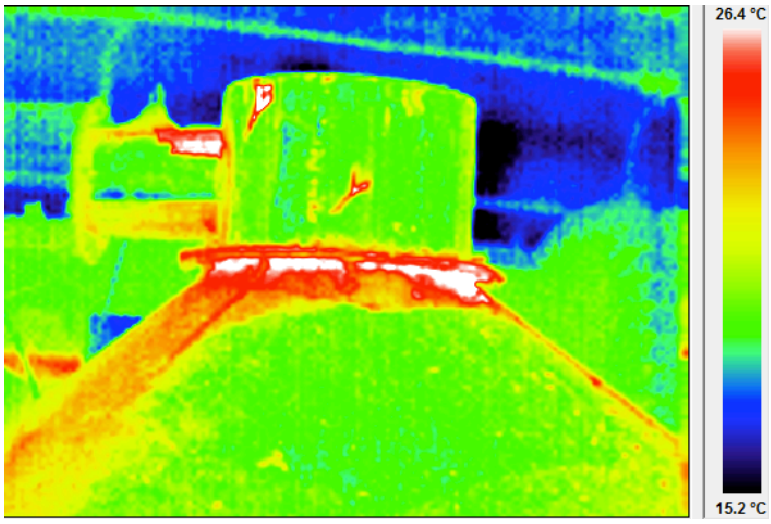

Figure C.4: Thermal Image of EPC compartment cap "hot spot".

A significantly higher surface temperature was observed along the cap flange and supply gas orifice.

The temperature differential between the EPC surface and the exterior environment was highest near the cap and gradually decreased downward towards the exhaust. With the exception of a few hot spots, all EPC surfaces generally retained a temperature differential between 3 and 8°C from the exterior environment at steady state.

C.3 Thermal Model

A thermal model was created empirically using results of the maximum temperature rise test and the calculated heat loss to the environment. This model accepts inputs of: the desired temperature and humidity of the laboratory ambient air, mixing box, and each of the compartments; the centerline air velocities in each compartment's ventilation pipe; and the number of laying hens in each compartment. The model outputs: the sensible and latent heat loads; the predicted sensible and latent heat added to the air itself; the predicted sensible and latent heat added by laying hens; and the predicted sensible heat lost to the environment. All calculations are performed using SI units. Inputs and Outputs are summarized in Figure C.5.

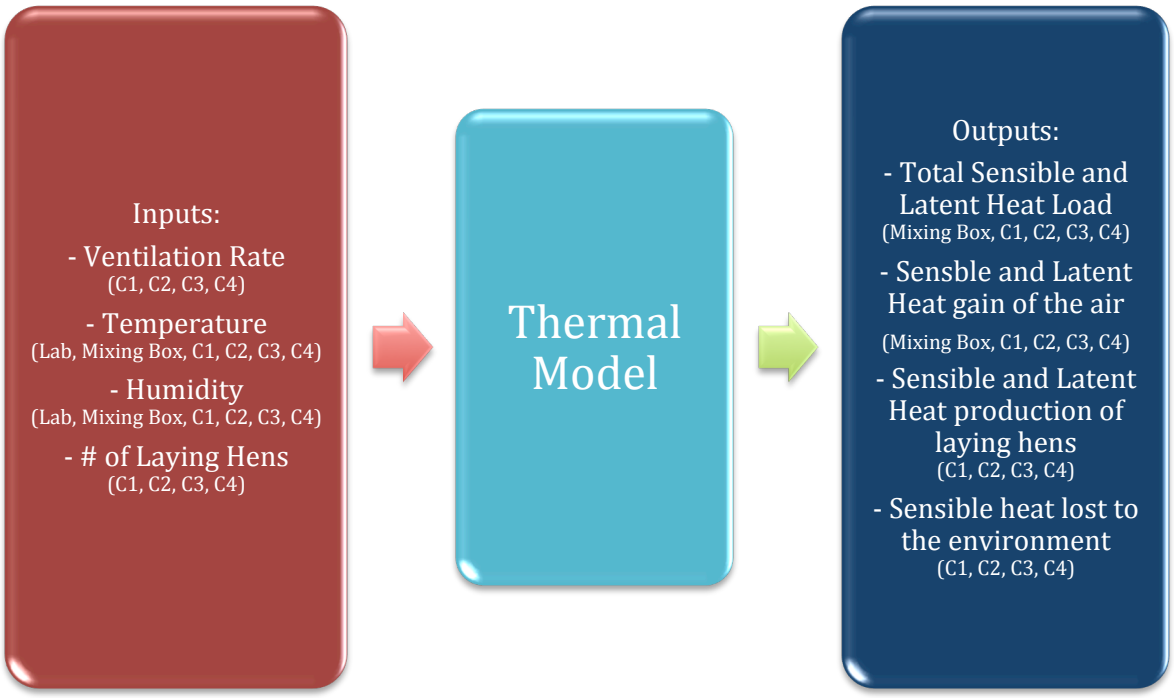

Figure C.5: Inputs and Outputs of the Environmental Preference Chamber Thermal Model. The thermal model calculates the outputs using a mixture of empirical data observed from system performance and theoretically derived psychrometric relationships.

Heat Balance Equation

Quantification of the heat flow through the EPC surface envelope was performed by fitting empirically derived inputs to a theoretical model. The theoretical model was derived from standard psychrometric equations (Appendix D). Accurately quantifying the thermal radiation and thermal conductivity of the compartment wall by theory alone was not practical due to the complex geometry, surface temperature gradient, and combination of materials that comprise the EPC. Instead, two known values for heat load and their respective inside temperatures at steady-state were used to fit a fourth-order polynomial. According to the "Maximum Temperature Rise" test results, applying a 200W sensible heat load to each compartment resulted in a steady state temperature gain of about **5.5°**C, and applying a 600W sensible heat load resulted in a steady-state temperature gain of **15.0°C.**

The model would only be able to make reliable calculations within the boundaries of these temperature inputs, but "ball-park" approximations of the heat flow could still be made outside of this range. Since only a single temperature input was used to quantify the total heat loss for the entire compartment, this model assumed a constant surface temperature across the compartment envelope. By observation of the thermal images, this assumption will yield some error to the model. A more comprehensive model that better represents the compartment heat loss gradient behavior could be implemented with more temperature point measurements, but a simpler model design was ultimately decided upon.

The total sensible and latent heat loads required for each compartment were calculated using the relationships:

$$Q_{s,load} = \Delta Q_{s,air\_in} + Q_{loss\_conduction} + Q_{loss\_radiation} - Q_{s,gained\_hens} \quad \text{(C.1a)}$$

$$Q_{l,load} = \Delta Q_{l,air\_in} - Q_{l,gained\_hens} \quad \text{(C.2)}$$

Where,

$\mathbf{Q_{load}}$ = the imposed supplemental heating/cooling required to maintain the interior temperature

$\mathbf{\Delta Q_{air\_in}}$ = the change in sensible/latent heat between the conditioned air and ambient air

$\mathbf{Q_{loss\_convection}}$ = the sensible heat loss to the environment via convection

$\mathbf{Q_{loss\_radiation}}$ = the sensible heat loss to the environment via radiation

$\mathbf{Q_{gained\_hens}}$ = the sensible/latent heat gained from laying hen occupants

Sensible and Latent Heat Change of the Supply Air

The sensible and latent heat gains required to achieve the desired air temperature and relative humidity in a compartment using the outer ambient air are calculated using the relationships:

$$\Delta Q_{s,air\_in} = \rho_{inside} * \dot{V} * c_{pa} * (T_{inside} - T_{ambient}) \quad \text{(C.3)}$$

$$\Delta Q_{l,air\_in} = \rho_{inside} * \dot{V} * W_{inside} * c_{pv} * (T_{inside} - T_{ambient}) \quad \text{(C.4)}$$

Where,

$\boldsymbol{c_{pa}}$ = Specific heat of dry air, 1.006 kJ/($kg_{dry\ air}$*K)

$\boldsymbol{c_{pv}}$ = Specific of water vapor, 1.805 kJ/(kg_{H20}*K)

$\boldsymbol{W_{inside}}$ = Humidity ratio, calculated using standard psychrometric equations, ($kg_{H20}/kg_{dry\ air}$)

$\boldsymbol{\rho_{inside}}$ = Air density, likewise calculated using standard psychrometric equations, kg/m^3

$\boldsymbol{\dot{V}}$ = Volumetric flow rate, calculated from the ventilation pipe's centerline velocity using the characterization derived in APPENDIX B, m^3/s

Sensible Heat Loss from Convection

Heat loss due to thermal convection, was modeled with the equation:

$$Q_{convection} = \alpha * (T_{inside} - T_{ambient}) * A_{compartment} \quad \text{(C.5)}$$

Where,

$A_{compartment}$ = 9.42 m^2, the surface area of a single compartment

T_{inside} = the average measured interior temperature of an EPC compartment

$T_{ambient}$ = the measured ambient air temperature in the laboratory

The value α is analogous to a thermal convection film coefficient of an EPC compartment, having units of $W/(m^2K)$. In reality, the temperature of the compartment surface should be used to calculate the heat loss from convection, not the temperature of the interior air. As observed by the thermal imaging camera, the surface temperature of the compartments varied across the surface area of the EPC compartments nonlinearly. The surface temperature was a few degrees warmer than the measured interior temperature near the cap and a few degrees cooler than measured interior temperature near the bottom of compartment. Since comprehensive surface temperature data is not acquired during regular EPC operations, α is also implemented to linearly relate the measured interior temperature to the average compartment surface temperature.

Sensible Heat Loss from Radiation

Heat loss due to thermal radiation, was observed with the equation:

$$Q_{radiation} = \sigma * \beta * \left({T_{inside}}^4 - {T_{ambient}}^4\right) * A_{compartment} \quad \text{(C.6)}$$

where,

$\boldsymbol{\sigma}$ = 5.67 * 10^{-8} W/(m^2K^4), Stefan-Boltzmann Constant

The value β is analogous to the emissivity of an EPC compartment surface, is unitless, and acts as a correction for the complex geometry of the EPC. In reality, the temperature of the compartment surface should be used to calculate the heat loss from radiation, not the temperature of the interior air. This choice was made for the same reasons given for calculating the heat loss due to convection. The EPC geometry also introduces some complex radiation behavior. Two walls of any given compartment are open to the laboratory environment and the other two walls hug closely to adjacent compartments. Given the high reflectance of the stainless steel compartment walls, precisely quantifying the actual thermal radiation at this location would require more in-depth modeling. This complex relationship between the measured interior temperature and the actual emitted heat due to radiation at the surface was thus simplified in the given linear relationship using the constant, β.

Sensible and Latent Heat Gain from Laying Hens

The EPC was previously used to test environmental preference in laying hens. These occupant hens would consume feed and convert it into energy through metabolism. Some of this energy would be output as sensible and latent heat into the atmosphere via

respiration, convection and radiation. Quantification of this heat output is often difficult to perform outside of a controlled experiment; however, Chepete et al. [2011] provides an approximation of 4W/kg and 2.5W/kg of sensible heat and latent heat output respectively for laying hens at thermoneutral conditions (24-27°C). Using this knowledge, and the assumed weight of 1.80kg per hen, the sensible and latent heat gain from the occupant laying hens was calculated as:

$$Q_{s,gained\_hens} = (\#\ of\ hens) * (1.80\frac{kg}{hen}) * \left(4\frac{W}{kg}\right) \quad \text{(C.7)}$$

$$Q_{l,gained\_hens} = (\#\ of\ hens) * (1.80\frac{kg}{hen}) * \left(2.5\frac{W}{kg}\right) \quad \text{(C.8)}$$

Solving the Heat Balance Equation for Sensible Heat Load

The previously defined heat balance equation for calculating sensible heat load (Equation C.1a) may be expanded using equations C.3, C.5, C.6 and C.7:

$$\begin{aligned} Q_{s,load} = \quad & \left[\rho * \dot{V} * \left(h_{s,in} - h_{s,out}\right)\right] \\ & + \left[\boldsymbol{\alpha} * (T_{inside} - T_{ambient}) * A_{compartment}\right] \\ & + \left[\sigma * \beta * \left({T_{inside}}^4 - {T_{ambient}}^4\right) * A_{compartment}\right] \\ & - \left[(\#\ of\ hens) * (1.80\frac{kg}{hen}) * \left(4\frac{W}{kg}\right)\right] \end{aligned} \quad \text{(C.1b)}$$

Using the two known inputs:

1) <($Q_{s,load}$ = 200W),(T_{inside}= 25.5°C), ($T_{ambient}$= 20°C),(# of hens = 0),
   ($\dot{V}$ = 0.006 m^3/s)>
2) <($Q_{s,load}$ = 600W),(T_{inside}= 35.0°C), ($T_{ambient}$= 20°C),(# of hens = 0),
   ($\dot{V}$ = 0.01 m^3/s)>

the two unknown constants, α and β, were found to approximately equal:

$$\alpha = \mathbf{1.1}\frac{W}{m^2-K}$$

$$\beta = \mathbf{0.33}$$

In reality, other values α and β would fit the polynomial, but these two appeared to be the best representation of the actual physical behavior of the system. These parameter values were checked with similar parameters provided by ASHRAE [2001]. Stainless steel, which much of the EPC outer surface consists of, has a very low thermal conductance (< $0.1\frac{W}{m^2-K}$, by approximation), but the flow of air contributes to the convective film coefficient depending on air velocity at the surface (potentially $10\frac{W}{m^2-K}$ or greater). A value of $\alpha = \mathbf{1.1}\frac{W}{m^2-K}$ is a conservative estimate when fully considering contributions from flowing air, but seems an adequate compromise when also taking into account heat lost to leakage and exhaust. Stainless steels have an emissivity ranging from 0.1 to 0.5 depending on the style of manufacturing and surrounding environment [ASHRAE, 2001]. This range matches the theoretical emissivity of the value β.

Application of the Thermal Model

This thermal model was implemented in Microsoft EXCEL to allow the calculation of the expected sensible heat and latent loads required to maintain a desired thermal environment in each compartment of the EPC. In the case where a staged heating design is desired, this model could calculate the achievable temperature range of any heating or ventilation stage. The model can also extrapolate to calculate heating/cooling requirements outside of the current operating range (+0°C to +15°C). Each compartment is calculated separately, taking into account the differences in their ventilation behavior (Appendix B). Examples of the thermal model's calculations are given in Figure C.6.

	Lab Ambient Air		M-Box Air		Compartment 1		Compartment 2		Compartment 3		Compartment 4	
Temperature	20	C	20	C	35	C	20		45	C	20	C
Absolute Temp	293.15	K	293.15	K	308.15	K	293.15	K	318.15	K	293.15	K
Relative Humidity	30	%	30	%	20	%	75	%	20	%	30	%
Pressure	101.63	kPa	101.63	kPa	101.63	kPa	101.63	kPa	101.63	kPa	101.63	kPa
Vapor Saturation Partial Pressure	2.34	kPa	2.34	kPa	5.63	kPa	2.34	kPa	9.59	kPa	2.34	kPa
Vapor Partial Pressure	0.70	kPa	0.70	kPa	1.13	kPa	1.75	kPa	1.92	kPa	0.70	kPa
Humidity Ratio	0.00432	kg H20 / kg Air	0.00432	kg H20 / kg Air	0.00697	kg H20 / kg Air	0.01092	kg H20 / kg Air	0.01197	kg H20 / kg Air	0.00432	kg H20 / kg Air
Dry Enthalpy	20.12	kJ/kg	20.12	kJ/kg	35.21	kJ/kg	20.12	kJ/kg	45.27	kJ/kg	20.12	kJ/kg
Moisture Enthalpy	10.97	kJ/kg	10.97	kJ/kg	17.86	kJ/kg	27.72	kJ/kg	30.91	kJ/kg	10.97	kJ/kg
Total Enthalpy	31.09	kJ/kg	31.09	kJ/kg	53.07	kJ/kg	47.84	kJ/kg	76.18	kJ/kg	31.09	kJ/kg
Specfic Volume	0.83	m^3/kg	0.83	m^3/kg	0.87	m^3/kg	0.83	m^3/kg	0.91	m^3/kg	0.83	m^3/kg
Mass Flow Rate	0.051	kg/s	0.051	kg/s	0.011	kg/s	0.011	kg/s	0.014	kg/s	0.014	kg/s
# of Birds					0	Birds	0	Birds	8	Birds	4	Birds
Sensible Heat Gain from Birds					0	W	0	W	55	W	27	W
Latent Heat Gain from Birds					0	W	0	W	36	W	18	W
Cond./Conv. Sens. Heat Loss					-155	W	0	W	-259	W	0	W
Sensible Heat Change in Air					163	W	0	W	294	W	-27	W
Latent Heat Change in Air					74	W	182	W	276	W	0	W
Heat Loss from Radiation					-288	W	0	W	-111	W	0	W
Specific Heat Load (SI)	0	0	W		606	W	0	W	664	W	-27	W
Latent Heat Load (SI)	0	0	W		74	W	182	W	240	W	-18	W
Specific Heat Load (IP)	0	0	Btu/		2067	Btu/Hr	0	Btu/Hr	2265	Btu/Hr	-93	Btu/Hr
Latent Heat Load (IP)	0	0	Btu/		254	Btu/Hr	620	Btu/Hr	820	Btu/Hr	-61	Btu/Hr

Figure C.6: Results of Thermal Model for four unique thermal environments.

C.4 Psychrometric Equations

Some psychrometric relationships were inferred in the explanation of this model. These were observed from those provided by ASHRAE (2001). All additional equations that were utilized in this model are provided in SI units as follows:

Constants

Gas Constant for dry air
$Ra = 287.055 \frac{J}{kg-K}$

Atmospheric Pressure (Standard)
$P_{atm} = 101.625\ kPa$

Equations

Absolute Temperature
$K = °C + 273.15$

Vapor Saturation Partial Pressure (Only applicable from 0°C to 200°C)
$p_{sat} = \exp(\mathrm{A1}/T_{db,K}, + \mathrm{A2} + \mathrm{A3} * T_{db,K} + \mathrm{A4} * {T_{db,K}}^2 + \mathrm{A5} * {T_{db,K}}^3 + \mathrm{A6} * {T_{db,K}}^4 + \mathrm{A7} * \ln(T_{db,K}))$

Where,

$T_{db,K}$ = Dry Bulb Temperature (K)
A1 =-5.8002206*10^3
A2 = 1.3914993*10^0
A3 =-48.640239*10^-3
A4 = 41.764768*10^-6
A5 =-14.452093*10^-9
A6 = 0.0
A7 = 6.5459673*10^0

Vapor Partial Pressure
$p_{vap} = p_{sat} * Rh$

Where,

Rh = Relative Humidity

Humidity Ratio

$$W = 0.62198 * \frac{p_{vap}}{P_{atm} - p_{vap}}$$

Enthalpy of Dry Air

$$h_a = c_p * t_{db,C}$$

Where,

$t_{db,C}$ = Dry Bulb Temperature ($°C$)

c_p = Specific Heat of Air ($= 1.006 \frac{kJ}{kg-K}$)

Enthalpy of Vapor

$$h_v = W * (h_g + c_{pv} * t_{db,C})$$

Where,

h_g = Enthalpy of Saturated Water Vapor ($= 2501.3 \frac{kJ}{kg}$, at $0°C$)

c_{pv} = Specific Heat of Water Vapor ($= 1.805 \frac{kJ}{kg-K}$)

Total Enthalpy

$$h = h_a + h_v$$

Specific Volume

$$v = \frac{R_a * T_{db,K} * (1 + 1.6078 * W)}{P_{atm} * (1 + W)}$$

Density

$$\rho = {}^{1}/_{v}$$

Mass Flow Rate

$$\dot{m} = \rho * \dot{V}$$

Where,

$\dot{V}$ = Volumetric Flow Rate

APPENDIX D: Programming Scripts

D.1 Fuzzy Logic Controller: "Fuzzy Membership Function"

The following code was written in MATLAB and utilized by the LabVIEW Virtual Instrument control software. This code performs the "fuzzification" process explained in Chapter 2.1. This code iterates once every second and updates the fuzzy membership functions as defined by the user.

```
%Fuzzy Logic LabVIEW Script
%Fuzzification Model Code
%
%Ryan Johnson
%Graduate Student
%University of Illinois: Urbana-Champaign
%Department of Agricultural and Biological Engineering

%LABVIEW INPUT CHANGES
%%%%%%%%%%%%%%%%%%%%%
%This code has been altered from the file "Fuzzify_ManualInput" to be used
%directly in LabVIEW software. For this reason, all manual input prompts
%have been removed from the code. The parameters [Par], [min], [max], and
%[val] have been commented out as they are automatically input through the
%LabVIEW VI.
%
%Par = 'NH3 Content';  %The name of the parameter to be fuzzified
n = 5;                %The number of membership functions
state1 = 'Very Neg';  %(string) The name of the first membership function
state2 = 'Neg';       %(string) The name of the second membership function
state3 = 'Zero';      %(string) The name of the third membership function
state4 = 'Pos';      %(string) The name of the fourth membership function
state5 = 'Very Pos'; %(string) The name of the fifth membership function


%min = -40;            %(integer) Minimum expected value of variable
%max =  40;            %(integer) Maximum expected value of variable
%val =  [-15, -5, 0, 5, 15]; % (1x5 vector) Each value corresponds to the
                            %state value of each membership function. That
                            %is, at each value in this vector the
                            %corresponding membership function is 100%
                            %true. If there are only 3 or 4 membership
                            %functions for the fuzzified parameter, leave
                            %the final values in this vector equal to 0.
                            %They will not be used.



%PURPOSE%
%%%%%%%%%
%The aim of this MATLAB script is to automatically construct a
%"Fuzzification" model based on user inputs.
%
%Fuzzy Logic systems operate by utilizing multiple "truth" states. That is,
```

```
%they logically assume multiple states simultaneously. This creates a more
%subjective interpretation by the computer program that is not unlike
%natural human interaction with a system.
%
%The design of this code is to create discretized fuzzification models for
%the sake of environmental control. Ideally, this would be used to create
%temperature, humidity, and gas models; however, since the output is
%strictly numerical it may be used for any application.
%
%For example, for use in the Environmental Preference Chamber with the
%University of Illinois in Urbana-Champaign, four gas levels are to be
%controlled (one for each preference chamber). Since controlled gasses
%have varying potencies, the fuzzification model must be variable. For
%example, 20ppm of NH3 is very noticable to human smell whereas 400ppm of
%CO2 can barely be sensed. Thus, the range of the what is considered
%"High", "Medium" and "Low" gas levels is different depending on the gas
%being used for the study.
%
%Likewise, fuzzification models for "Cold", "Warm" and "Hot" temperatures
%or "Dry", "Normal" and "Moist" humidity levels may be created.


%RESOLUTION
%Here, the resolution of the Fuzzification System is set. The value of 1000
%is chosen for this program, though the number is arbitrary.
R=1000;

%RANGE
%Here, the range of the values expected to be interpreted by the Fuzzy
%system is calculated.
range = max-min; %Total range of system
r = range/R;     %Size of one "pixel" of fuzzification system



%CONSTRUCTION OF FUZZIFICATION MODEL
%The remaining code will use the user inputs to create the fuzzification
%model. This model will use "triangle" shaped fuzzy shapes. That is, a
%state will be considered 100% true and the defined state value, but will
%linearly decrease to 0% true at the point where the adjacent state value
%is 100% true. This creates a series of "triangles" that intersect at the
%average state value between the two. A plot will be produced to show this
%to be true.
F = zeros(5,R); %F is a matrix where each row is a vector describing a Fuzzy
State
for i = 1:n
    p1 = round((val(i)-min)/r); %p1 is equal to the current state value, as
%position on the defined scale
    F(i, p1) = 1.0;
    if i==1              %The code under this 'if' statement ONLY applies to
%the first state value
        for j = 1:p1     %For the first state, all values lower than the
%state value are set equal to 1
            k = 1.0;
            F(i,j) = k;
        end
    end
```

```
    if i==n              %The code under this 'if' statement ONLY applies to
%the last state value
        for j = p1:R     %For the final state, all values higher than the
%state value for set equal to 1
            k =1.0;
            F(i,j) = k;
        end
    end
    if i<n               %the code under this 'if' statement applies to all
%state values EXCEPT the final one
        p2 = round((val(i+1)-min)/r);  %p2 is equal to the next adjacent
%state value.
        pr2 = p2-p1+1;   %pr2 is equal to the range value between
%adjacentstate values
        for j = p1:p2
            F(i,j) = 1.0 - (j-p1)/pr2;
        end
        for j = p2:R
            k = 0.0;
            F(i,j) = k;
        end
    end
    if i>1
        p0 = round((val(i-1)-min)/r);
        pr0 = p1-p0+1;
        for j = p0:p1
            F(i,j) = 0.0 + (j-p0)/pr0;
        end
        for j = 1:p0
            k = 0.0;
            F(i,j) = k;
        end
    end
end
%FUZZY SYSTEM GRAPH
%%%%%%%%%%%%%%%%%%
%The following code produces a plot of the Fuzzy System created in this
%code.
%s1 = F(1,:);
%s2 = F(2,:);
%s3 = F(3,:);
%s4 = F(4,:);
%s5 = F(5,:);
%y = [(min+r):r:max];
%plot(y,s1,'r-', y,s2,'b-', y,s3,'g-', y,s4,'y-', y,s5,'c-');
%xlabel(Par);
%if n==2
%legend(state1,state2);
%end
%if n==3
%legend(state1,state2,state3);
%end
%if n==4
%legend(state1,state2,state3,state4);
%end
%if n==5
%legend(state1,state2,state3,state4,state5);
%end
```

D.2 Fuzzy Logic Controller: "Defuzzification"

The following code was written in MATLAB and utilized by the LabVIEW Virtual Instrument control software. This code performs the "defuzzification" process explained in Chapter 2.1. This code iterates once every second and outputs an adjustment to the voltage signal each iteration.

```
%Fuzzy Logic LabVIEW Script
%Defuzzification Code
%
%Ryan Johnson
%Graduate Student
%University of Illinois: Urbana-Champaign
%Department of Agricultural and Biological Engineering


%DEFUZZIFICATION FOR LABVIEW
%%%%%%%%%%%%%%%%%%%%%%%%%%%%%
%The following code is designed specifically to "defuzzify" the fuzzified
%membership functions of the EPC  control. This code requires six
%inputs:
%
%The following variables must be directly input from LabVIEW:
%tin:  (integer or double float) value of current NH3 content in ppm
%tset: (integer or double float) value of setpoint NH3 content in ppm
%v1:   (double float) Current voltage output to Mass Flow Controller

%The following variables are created by the function "Fuzzify_LabVIEW.m":
%F:    (5x1000 matrix) Matrix representing fuzzification system being analyzed.
%r:    (double float) Size of one "pixel" of fuzzification system
%min:  (double float) Minimum expected value of the fuzzified parameter.

%This code uses the reqiores function to create a series of
%vectors in 5x1000 matrix F that correspond to a fuzzy system.
%For this LABVIEW version of the code, the parameters "F", "r", and "min"
%are automatically input from the code "Fuzzify_LabVIEW.m". However, the


%INPUT
%The following code requests input value that corresponds to the parameter
%of the created fuzzy sets. This is then transformed into "pixelated" form,
%on a scale of 1-1000 corresponding to the input value's position in the parameter
range.
dt = tset-tin;
n = round((dt-min)/r);

%The following code draws out the values of the fuzzy set in matrix "F" and
%writes them into a single 5x1 vector "J"

for j = 1:5
      J(j) = F(j,n);
end


%DEFUZZIFICATION
%%%%%%%%%%%%%%%%
%The following code creates the Deffuzification model used to create output
%data. This program will assume one output, although multiple outputs are possible.
%
%For now, the code is written with NH3 control in mind. The
```

```
%Deffuzification process will generate output voltage to a Mass Flow Controller,
%an output between 0-5V.
%
%The following code assumes a single Fuzzification model that controls
%NH3 CONTENT with 5 states: Very Low, Low, Good, High, Very High.
%
%The following code controls the output voltage change for each state. The
%Mass Flow Controllers operate between 0-5V, where 0V correlates to 0ml/min
%and 5V correlates to around 550ml/min. These values must be fine-tuned to
%create an optimal control scheme. This can be done with observation:

VLOW =  V_Inc_High;   %"Very Low" NH3 content. Will increase the output %voltage by
the user input for "V_Inc_High" when 100% true.

LOW  =  V_Inc_Low;   %"Low" NH3 content. Will increase the output voltage by  %the
user input for "V_Inc_Low" when 100% true.

GOOD =   0;   %"Good" NH3 content. Will not change the output voltage at all
              %when 100% true.

HI   = - V_Inc_Low;   %"High" NH3 content. Will decrease the output voltage by  %the
user input for "V_Inc_Low" when 100% true.

VHI  = -V_Inc_High;   %"Very High" NH3 content. Will decrease the output voltage %by
the user input for "V_Inc_High" when 100% true


%TRUTH VALUE INITIALIZATION
%The Truth Vales for VERY LOW, LOW, MEDIUM, HIGH and VERY HIGH are initialized here.
%These are analogous to the terms “Very Negative”, “Negative”, “Zero”, “Positive”, and
%“Very Positive”, used in the literature. These values will generally range between 0-
%1.00, %but are capable of growing higher
%depending on how the RULE BLOCK is decided upon. Every time LabVIEW loops the code,
%the truth values will be recalculated, starting from zero.
vlow = 0;
low  = 0;
good = 0;
hi   = 0;
vhi  = 0;
%
%RULE BLOCK
%The following code creates the Deffuzification rules that create the
%output voltage values:
%
%1) IF ..NH3 CONTENT is ..VERY LOW, then Voltage increase is .... + V_Inc_High
vlow = vlow + J(5);
%
%2) IF ..NH3 CONTENT is .......LOW, then Voltage increase is .... + V_Inc_Low
low  = low  + J(4);
%
%3) IF ..NH3 CONTENT is ......GOOD, then Voltage increase is .... + 0
good = good + J(3);
%
%4) IF ..NH3 CONTENT is ......HIGH, then Voltage increase is .... - V_Inc_Low
hi   =   hi + J(2);
%
%5) IF ..NH3 CONTENT is .VERY HIGH, then Voltage increase is .... - V_Inc_High
vhi  =  vhi + J(1);


%VOLTAGE OUTPUT
vout = v1 + vlow*VLOW + low*LOW + good*GOOD + hi*HI + vhi*VHI;
```

```
if vout > 5
    vout = 5;
end
if vout < 0
    vout = 0;
end
```

D.3 NH_3 Analysis

The following code was written in MATLAB and utilized for data analysis. This code analyzes the raw NH_3 and Temperature data of each compartment from the output data file produced by the LabVIEW VI control software.

```
%RYAN JOHNSON
%MASTER'S STUDENT
%AGRICULTURAL AND BIOLOGICAL ENGINEERING
%UNIVERSITY OF ILLINOIS: URBANA-CHAMPAIGN

%SIMULTANEOUS NH3 AND TEMP CONTROL IN FOUR COMPARTMENTS
%
%This code reads the .txt file that the EPC's LabVIEW program writes during
%testing. Several columns of data are retrieved from the data:
%
%SOL  = Solenoid Location (# of compartment being monitored)
%NH3  = NH3 Concetration
%Temp = Dry-Bulb Temperature of both tiers of all 4 compartments. These
%       values are averaged together for analysis
%
%This code outputs:
%
%SETPOINTS = The setpoint of each compartment. Must be manually input
%
%MEAN = Mean NH3 concentration of each compartment after 95% of the
%setpoint has been achieved. Only measurements taken when the respective
%Solenoid Location is active is considered.
%
%STDEV = Standard Deviation NH3 concentration of each compartment after 95% of the
%setpoint has been achieved.
%
%T95 = Time elapsed until 95% of the setpoint was achieved.
%
%PLOT - Plots the "unabridged data without transition lines". This is the
%data as observed in real-time during operation, omitting unrepresentative
%concentrations.
%
%Import Data from Raw Output Text File
filename = 'NH3_rise_Temp_rise_May5';
delimiterIn = '\t';
headerlinesIn = 3;
A = importdata(filename,delimiterIn,headerlinesIn);

%Grab NH3 and Solenoid Data
```

```
NH3 = A.data(:,19);
SOL = A.data(:,18);

%Initialize timescale for analysis
%To fit known data:
len = length(NH3);
%To fit for plots:
%len = 750;
%"lenshort" used for abridged data
lenshort = round((len/5))+2;
t = zeros(1,len);
ts = zeros(1,lenshort);
for i = 2:len
    t(i) = t(i-1) + 0.666667;
end
for i = 2:lenshort
    ts(i) = ts(i-1) + 0.666667;
end

%Grab Temperature Data
Temp = zeros(8,len);
Tr = zeros(1,len);
k = [2,3,6,7,10,11,14,15];
for i = 1:len
    for j = 1:8
        l = k(j);
        Temp(j,i) = A.data(i,l);
    end
    Tr(i) = mean(Temp(:,i));
end

%Setpoints for each compartment (ppm)
SET1 = 20;
SET2 = 40;
SET3 = 0;
SET4 = 10;
Setpoints = [SET1, SET2, SET3, SET4]'

%Initialize parameters for "abridged" data
%
%Actual Measured Concentrations of each compartment. No Assumed
%concentrations or "transition" measurements
C1 = zeros(1,lenshort);
C2 = zeros(1,lenshort);
C3 = zeros(1,lenshort);
C4 = zeros(1,lenshort);
%Arbitrary counters
j1 = 1;
j2 = 1;
j3 = 1;
j4 = 1;
count = zeros(4,1);
%# of measurements until 95% of Setpoint concentration met. Not 'real' time
t95_1 = 0;
t95_2 = 0;
t95_3 = 0;
t95_4 = 0;
%Total # of measurements
t0_1 = 0;
t0_2 = 0;
t0_3 = 0;
t0_4 = 0;
```

```
%Initialize parameters for "unabridged" data w/o transition lines
%
%Measured/Assumed Concentrations of each compartment
C1fv = zeros(1,len);
C2fv = zeros(1,len);
C3fv = zeros(1,len);
C4fv = zeros(1,len);
countv = zeros(4,1);

%Initialize parameters for "unabridged" data
%
%Measured/Assumed Concentrations of each compartment
C1f = zeros(1,len);
C2f = zeros(1,len);
C3f = zeros(1,len);
C4f = zeros(1,len);
%Real Time to achieve 95% of Setpoint concentration
t95f_1 = 0;
t95f_2 = 0;
t95f_3 = 0;
t95f_4 = 0;

%Distribute Abridged Data
for i = 1:len

    if SOL(i) == 1
        if count(1) > 3
            C1(j1) = NH3(i);
            j1 = j1 + 1;
        end
        count(1) = count(1) + 1;
        count(2:4) = 0;

    elseif SOL(i) == 2
        if count(2) > 3
            C2(j2) = NH3(i);
            j2 = j2 + 1;
        end
        count(2) = count(2) + 1;
        count(1) = 0;
        count(3:4) = 0;

    elseif SOL(i) == 3
        if count(3) > 3
            C3(j3) = NH3(i);
            j3 = j3 + 1;
        end
        count(3) = count(3) + 1;
        count(1:2) = 0;
        count(4) = 0;

    elseif SOL(i) == 4
        if count(4) > 3
            C4(j4) = NH3(i);
            j4 = j4 + 1;
        end
        count(4) = count(4) + 1;
        count(1:3) = 0;

    else
    end
end
```

```
%Distribute Unabridged Data w/o transition lines
for k = 2:len

    if SOL(k) == 1
        if countv(1) > 3
            C1fv(k) = NH3(k);
            C2fv(k) = C2fv(k-1);
            C3fv(k) = C3fv(k-1);
            C4fv(k) = C4fv(k-1);
        else
            C1fv(k) = C1fv(k-1);
            C2fv(k) = C2fv(k-1);
            C3fv(k) = C3fv(k-1);
            C4fv(k) = C4fv(k-1);
        end
        countv(1) = countv(1) + 1;
        countv(2:4) = 0;

    elseif SOL(k) == 2
        if countv(2) > 3
            C1fv(k) = C1fv(k-1);
            C2fv(k) = NH3(k);
            C3fv(k) = C3fv(k-1);
            C4fv(k) = C4fv(k-1);
        else
            C1fv(k) = C1fv(k-1);
            C2fv(k) = C2fv(k-1);
            C3fv(k) = C3fv(k-1);
            C4fv(k) = C4fv(k-1);
        end
        countv(2) = countv(2) + 1;
        countv(1) = 0;
        countv(3:4) = 0;

    elseif SOL(k) == 3
        if countv(3) > 3
            C1fv(k) = C1fv(k-1);
            C2fv(k) = C2fv(k-1);
            C3fv(k) = NH3(k);
            C4fv(k) = C4fv(k-1);
        else
            C1fv(k) = C1fv(k-1);
            C2fv(k) = C2fv(k-1);
            C3fv(k) = C3fv(k-1);
            C4fv(k) = C4fv(k-1);
        end
        countv(3) = countv(3) + 1;
        countv(4) = 0;
        countv(1:2) = 0;

    elseif SOL(k) == 4
        if countv(4) > 3
            C1fv(k) = C1fv(k-1);
            C2fv(k) = C2fv(k-1);
            C3fv(k) = C3fv(k-1);
            C4fv(k) = NH3(k);
        else
            C1fv(k) = C1fv(k-1);
            C2fv(k) = C2fv(k-1);
            C3fv(k) = C3fv(k-1);
            C4fv(k) = C4fv(k-1);
        end
        countv(4) = countv(4) + 1;
```

```
        countv(1:3) = 0;

    elseif SOL(k) == 5
        C1fv(k) = C1fv(k-1);
        C2fv(k) = C2fv(k-1);
        C3fv(k) = C3fv(k-1);
        C4fv(k) = C4fv(k-1);
    else
    end
end
%Append Data for plot
Cfv = [C1fv;C2fv;C3fv;C4fv];

%Distribute Unabridged Data w/ transition lines
for i = 2:len
    if SOL(i) == 1
        C1f(i) = NH3(i);
        C2f(i) = C2f(i-1);
        C3f(i) = C3f(i-1);
        C4f(i) = C4f(i-1);
    elseif SOL(i) == 2
        C1f(i) = C1f(i-1);
        C2f(i) = NH3(i);
        C3f(i) = C3f(i-1);
        C4f(i) = C4f(i-1);
    elseif SOL(i) == 3
        C1f(i) = C1f(i-1);
        C2f(i) = C2f(i-1);
        C3f(i) = NH3(i);
        C4f(i) = C4f(i-1);
    elseif SOL(i) == 4
        C1f(i) = C1f(i-1);
        C2f(i) = C2f(i-1);
        C3f(i) = C3f(i-1);
        C4f(i) = NH3(i);
    elseif SOL(i) == 5
        C1f(i) = C1f(i-1);
        C2f(i) = C2f(i-1);
        C3f(i) = C3f(i-1);
        C4f(i) = C4f(i-1);

    else
    end
end


%Calculate MEAN and STDEV of measured concentrations once C95 has been met:
for i = 1:lenshort
    if C1(i) > 0.95*SET1
        if t95_1 == 0
            t95_1 = i;
        end
    end
    if C1(i) == 0
        if t0_1 == 0
            t0_1 = i-1;
        end
    end
    if C2(i) > 0.95*SET2
        if t95_2 == 0
            t95_2 = i;
        end
    end
    if C2(i) == 0
```

```
        if t0_2 == 0
            t0_2 = i-1;
        end
    end
    if C3(i) > 0.95*SET3
        if t95_3 == 0
            t95_3 = i;
        end
    end
    if C3(i) == 0
        if t0_3 == 0
            t0_3 = i-1;
        end
    end
    if C4(i) > 0.95*SET4
        if t95_4 == 0
            t95_4 = i;
        end
    end
    if C4(i) == 0
        if t0_4 == 0
            t0_4 = i-1;
        end
    end
end

Mean = zeros(4,1);
Stdev = zeros(4,1);
N = 8; % # of Samples used to calculate mean and stdev
Mean(1) = mean(C1(t95_1:t0_1));
Stdev(1) = std(C1(t95_1:t0_1));
Mean(2) = mean(C2(t95_2:t0_2));
Stdev(2) = std(C2(t95_2:t0_2));
Mean(3) = mean(C3(t95_3:t0_3));
Stdev(3) = std(C3(t95_3:t0_3));
Mean(4) = mean(C4(t95_4:t0_4));
Stdev(4) = std(C4(t95_4:t0_4));
Mean
Stdev

%Calculate real time to achieve C95 in Unabridged data:
for i = 1:len
    if C1f(i) > 0.95*SET1
        if t95f_1 == 0
            t95f_1 = i;
        end
    end
    if C2f(i) > 0.95*SET2
        if t95f_2 == 0
            t95f_2 = i;
        end
    end
    if C3f(i) > 0.95*SET3
        if t95f_3 == 0
            t95f_3 = i;
        end
    end
    if C4f(i) > 0.95*SET4
        if t95f_4 == 0
            t95f_4 = i;
        end
    end
end
t95f_1 = t95f_1*0.66667; %minutes
```

```
t95f_2 = t95f_2*0.66667; %minutes
t95f_3 = t95f_3*0.66667; %minutes
t95f_4 = t95f_4*0.66667; %minutes
t95f = [t95f_1, t95f_2, t95f_3, t95f_4]'


%Create Setpoint Lines for plot
SL =  Cfv;
for i = 1:len
    SL(1,i) = SET1;
    SL(2,i) = SET2;
    SL(3,i) = SET3;
    SL(4,i) = SET4;
end

%Plot NH3 Data only
%hold on
%figure(1)
%plot(t,C1f,'g-', t,C2f,'r-', t,C3f,'b-', t,C4f,'k-', 'LineWidth', 2)
%plot(t,C1fv,'g-', t,C2fv,'r-', t,C3fv,'b-', t,C4fv,'k-', 'LineWidth', 2)
%plot(ts,C1,'g-', ts,C2,'r-', ts,C3,'b-', ts,C4,'k-', 'LineWidth', 2)
%plot(tset,SL1,'g:', tset,SL2,'r:', tset,SL3,'b:', tset,SL4,'k:')
%axis([0 600 0 45]);
%xlabel('Elapsed Time (min)', 'FontSize', 16);
%ylabel('NH3 Concentration (ppm_v)', 'FontSize', 16)
%title('NH3 Concentration over time', 'FontSize', 18)

%Plot NH3 and Temp Data Together
hold on
figure(1)
[AX,H1,H2] = plotyy(t,Cfv,t,Tr);
plot(t,SL(1,:),'g:', t,SL(2,:),'g:', t,SL(3,:),'g:', t,SL(4,:),'g:')
xlabel('Elapsed Time (min)', 'FontSize', 16);
set(get(AX(1),'Ylabel'),'String','NH3 Concentration (ppm_v)', 'FontSize',16,
'FontWeight', 'Bold','Color', [0 .6 0])
set(get(AX(2),'Ylabel'),'String','Temperature (deg C)', 'FontSize',16, 'FontWeight',
'Bold','Color', [.6 0 0])
set(AX(1),'YTick',[0:5:50],'YColor', [0 .6 0])
set(AX(2),'YTick',[20:5:40],'YColor', [.6 0 0])
set(H1,'Color',[0 .6 0],'LineStyle','-', 'LineWidth', 1.5)
set(H2,'Color',[.6 0 0],'LineStyle','-', 'LineWidth', 1.5)
title('Simultaneous NH3 and Temp Control', 'FontSize', 18)
legend(H1,'NH3 (Individual Compartments)')
legend(H2,'Temp (Averaged All Compartments)')
```